Development and Characterization of Targeted Green Nanotechnology Based Delivery System(s) for Cancer Therapy

THESIS
SUBMITTED IN FULFILLMENT FOR THE AWARD OF THE DEGREE OF

Doctor of Philosophy

IN
PHARMACEUTICAL SCIENCES

Submitted By

Malti
Enrollment no. 251/13

Supervisor
Prof. (Dr.) Shubhini A. Saraf
Head
Dept. of Pharmaceutical Sciences
BBAU Lucknow, U.P. India

Co-Supervisor
Dr. Krishna P. Gupta
Ex- Senior Principal Scientist
Carcinogenesis Division
CSIR-IITR Lucknow, U.P. India

DEPARTMENT OF PHARMACEUTICAL SCIENCES
SCHOOL FOR BIOSCIENCES AND BIOTECHNOLOGY
BABASAHEB BHIMRAO AMBEDKAR UNIVERSITY
(A CENTRAL UNIVERSITY)
VIDYA VIHAR, RAIBARELI ROAD, LUCKNOW-226025, U.P., INDIA
(2018)

DECLARATION

I hereby declare that the thesis entitled **"Development and Characterization of Targeted Green Nanotechnology Based Delivery System(s) for Cancer Therapy"** has been prepared by me under the supervision of **Prof. (Dr.) Shubhini A. Saraf**, Head, Dept. of Pharmaceutical Sciences, Babasaheb Bhimrao Ambedkar University, Lucknow, U.P. India and co-supervision of **Dr. Krishna P. Gupta,** Ex-Senior Principal Scientist, Carcinogenesis Division, CSIR- Indian Institute of Toxicology Research, Lucknow, U.P. India, at Department of Pharmaceutical Sciences, School for Biosciences and Biotechnology, Babasaheb Bhimrao Ambedkar University, Lucknow (U.P.).

No part of this thesis has formed the basis for the award of any degree, diploma or fellowship previously. I further declare that the material embodied in the present work is based on original research work and indebtedness to others has been duly acknowledged at relevant places. I hereby also declare that the thesis is essentially free from all kind of plagiarism.

Malti

CERTIFICATE

This is to certify that the thesis titled **"Development and Characterization of Targeted Green Nanotechnology Based Delivery System(s) for Cancer Therapy"** submitted by **Ms. Malti** is an original research work and has not been previously submitted in part or full for the award of any other degree or diploma to this or any other university.

The thesis submitted to Babasaheb Bhimrao Ambedkar University Lucknow satisfies all the requirements as stipulated in the *Doctor of Philosophy (Ph.D.) regulations -1999 as amended in 2008/2010/2013* and it is fit for submission and evaluation for the award of the degree of Doctor of Philosophy of the University.

Date 30th Aug 2018

Supervisor
(Krishna Giri) (Shubhini A. Saraf)

Head of the Department

Acknowledgements

My thesis is the culmination of my Ph.D. journey which was just like mountaineering a high peak step by step. Although only my name appears on the cover page, many people are there whose unconditional help was mandatory for the accomplishment of this thesis. While I write this acknowledgement, I look back and feel my gratitude towards this university and all these people.

I am short of words while articulating my honest regards to my worthy supervisor, ***Prof. (Dr.) Shubhini A. Saraf,*** *Head, Department of Pharmaceutical Sciences, Babasaheb Bhimrao Ambedkar University, Lucknow. I am very fortunate to get her adroit guidance right from the beginning till date. This work would not have been possible without her superior indulgence, encouragement, meticulous efforts, constructive criticism and valued suggestions. Her own pursuit of brilliance, the mission for doing only high-quality research, unflinching courage and conviction has always inspired me to do better. She made me a believer, a hard worker and a better human being. She has guided and supported me not only professionally but personally, as well. I sincerely thank her for everything and I will be truly indebted to her throughout my life. I could never imagine having a better supervisor and a mentor for my Ph.D.*

Also, I am incredibly thankful to my co-supervisor, ***Dr. Krishna P. Gupta,*** *Ex- Senior Principal Scientist, Environmental Carcinogenesis Division, CSIR-Indian Institute of Toxicology Research, Lucknow for her immense help, lab facilities and approval for conducting animal studies. Even though it was a short duration but I was graced with her patronage and pearls of wisdom during my work in her laboratory.*

I am very much grateful to ***Prof. R.C. Sobti****, honourable vice-chancellor of Babasaheb Bhimrao Ambedkar University, Lucknow, for providing infrastructure, facilities and encouraging words of wisdom for accomplishing this project.*

Besides my supervisor and other faculty members, I am very grateful to my Departmental Research Committee (DRC) members: ***Dr. Gaurav Kaithwas, Dr. Sudipta Saha, Dr. R. Venkatesh Kumar, Dr. N.K.S. More*** *and* ***Dr. V. Elangovan*** *for their encouragement, insightful comments, meaningful queries, suggestions, support and guidance during my sojourn in the department.*

My sincere thanks also extend to the office and non-teaching staff i.e. ***Mr. Anand, Mr. Bhandari, Ms. Seema*** *and* ***Mr. Amar*** *for their respective capacity and extended support in carrying out my work on time.*

I am also very thankful to my seniors, ***Dr. Pooja, Dr. Mahendra Singh*** *and* ***Dr. Jovita Kanoujia*** *for their friendly support and enlightening discussions. I also express my exult and genuine appreciation to my cherished friends* ***Chandra Bhushan, Poonam Parashar, Heena*** *and* ***many more****. I am also indebted to* ***my juniors*** *who were always with me whenever I asked for their help.*

My heartfelt gratitude to my senior cum closest friend ***Ms. Niharika, Mr. & Mrs. Bharat Lal*** *(Jija Ji & Di) and* ***Mr. & Mrs. Manjeet Vohra*** *(Uncle & Aunt) for the joy, love and parental care that they provided me, during my stay in Lucknow. They were always with me whenever I needed them.*

I wish to extend my warmest and cordial thanks to my new family, ***in-laws****. They not only motivated me but also supported in all aspects of life.*

The chain of my gratitude would be incomplete without thanking the first cause of this chain, viz. ***my late grandparents****,* ***my parents****,* ***my naanu****,* ***my uncles*** *and* ***aunts*** *for their unconditional support and encouragement. They always showed blind faith in me and gave me the liberty to choose what I wished for. I owe a lot to all of them for the selfless love, care and the sacrifice they made to shape my life and career. I would never be able to pay back the love and affection they showered on me. I would like to extend my special thanks and love to my younger siblings (****Rohit, Rahul*** *and* ***Romi)*** *and* ***cousins*** *for their love, prayers and joyous moments which always kept me energetic and full of enthusiasm throughout.*

Saving the most important for the last, I owe my warmest thanks to a very special person, my husband, ***Aditya*** *who is my friend first and then a life partner. His understanding regarding my pursuit of Ph.D. degree and my career has made it worthwhile. He was always around at times whenever I needed him to be. I thank God for enlightening my life with his presence.*

Finally, I would like to express my whole hearted appreciation to all of those, whom I may not be able to name individually, for helping directly or indirectly and I also apologize for not mentioning them individually.

Malti

Malti

CONTENTS

List of figures

List of tables

Abbreviations

ACF	Aberrant crypt foci
AgNPs	Silver nanoparticles
APC	Adenomatous polyposis coli
BMRB	Biological Magnetic Resonance Data Bank
BSCs	Basal cell skin carcinomas
CEA	Carcinoembryonic antigen
COX-2	Cyclooxygenase-2
CT	Computed tomography
DCP	Dicetylphosphate
DEC	Dual extrusion cell
DLS	Dynamic light scattering
DMBA	Dimethylbenz(a)anthracene
DMEM	Dulbecco's modified eagle medium
DMH	Dimethylhydrazine
DNA	Deoxyribonucleic acid
ECG	Electrocardiogram
EE	Entrapment efficiency
EPR	Enhanced permeability and retention
FDA	Food and Drug Administration
FID	Free induction decay
FTIR	Fourier transforms infrared spectrum
GNPs	Gold nanoparticles
$HAuCl_4$	Chloroauric acid
HET-CAM	Hen's Egg Test on the Chorioallantoic Membrane
HMDB	Human Metabolome Database

HRV	Heart rate variability
IAEC	Institutional Animal Ethics committee
IC50	Inhibitory concentration 50
ICMR	Indian Council of Medical Research
IITR	Indian Institute of Toxicology Research
IJP-GNPs	IP6 loaded jacalin-pectin-gold nanoparticles
IP6	Inositol hexaphosphate
mAb	Monoclonal antibodies
MRI	Magnetic resonance imaging
MTT	3-(4,5-dimethylthiazol-2-yl)-2,5-diphenyltetrazolium bromide
$NaBH_4$	Sodium borohydride
NK-cell	Natural killer cell
NMR	Nuclear magnetic resonance
NMSCs	Non-melanoma skin cancers
OD	Optical density
ODC	Ornithine decarboxylase
PBS	Phosphate-buffered saline
PCA	Principal Component Analysis
PCL	Polycaprolactone
PCNA	Proliferating cell nuclear antigen
PDI	Poly dispersity index
PEG	Polyethylene glycol
PET	Positron emission tomography
P-GNPs	Pectin-gold nanoparticles
PLA	Poly (lactic acid)
PLS-DA	Partial Least Squares Discriminant Analysis
PMSA	Prostate-specific membrane antigen

PVDF	Polyvinylidene fluoride
RNA	Ribonucleic acid
RT-PCR	Reverse transcription polymerase chain reaction
SEM	Scanning electron microscopy
SLNs	Solid Lipid Nanoparticles
SRB	Sulforhodamine-B
SSCs	Squamous cell skin carcinomas
TCA	Trichloroacetic acid
TEM	Transmission electron microscopy
TOABr	Tetraoctylammonium bromide
US FDA	United States Food and Drug Administration
VEGF	Vascular endothelial growth factor
VIP	Variable importance on projection
WHO	World Health Organization
Wnt	Wingless/Integrated

Chapter 1

Introduction and review of literature

1. Introduction

1.1. Background

Cancer is among the most devastating diseases globally regardless of huge government funding as well as heroic attempts on cancer research to diminish mortality and improve survival. At present, cancer is a much familiar word. Most of us know at least one relative/ friend/ neighbour/ colleague or one associated to them, who have been diagnosed with cancer. There is a rising perception that cancer incidence is on a significant increase [1], owing to increased toxicants in the environment.

Cancer is a multifaceted disease which is the result of abnormal/ uncontrolled growth and division of atypical cells as a result of gene mutations. Due to mutation, cancer cells display certain characters like proliferation, resistance to the signals which restrain their growth and resistance to signals of apoptosis which causes cell death. These characteristics make it difficult to treat this disease [2, 3].

Cancer is linked with a group of diseases that shares analogous characteristics and cells grow abnormally/ uncontrollably while disregarding the normal cell division rules. External factors (such as tobacco, infectious organisms, chemicals and radiation) as well as internal factors (inherited mutations, hormones, immune conditions and mutations that occur from metabolism) are mostly responsible for cancer. These causal factors may act together or in sequence to initiate or promote the development of cancer [4].

Cancer can influence all living cells of the body and can affect at any age and in both the genders [5]. Diagnosis of cancer often tends to shatter personal health expenditures. Such expenditures may lead the entire family to a financial condition below the poverty line [6].

1.2. Current situation

Globally, one out of six deaths occurs due to cancer and it is the second most common reason for deaths, superseded only by heart diseases. The World Health Organization (WHO) projected that the number of new cases of cancer is expected to rise by nearly 70% within the two next decades, with wide occurrence in low/ middle-income countries [7]. The Indian Council of Medical Research (ICMR) has recently projected

that India would possibly report over 17 lakh new cases of cancer and over 8 lakh deaths due to the disease by the year 2020 [8].

1.3. Cancer biology

Carcinogenesis or cancer biology is a multi-stage process which conventionally involves initiation, promotion and progression. Generally, carcinogenic agents are initiators and promoters which may be similar to vital environmental factors for cancer development [9]. According to researchers, the agents that promote the cells to develop tumours are known as initiators and the agents that stimulate the development of tumours are known as promoters. Compounds that behave as both initiators as well as promoters are called 'complete carcinogens' [10]. There are significant developments in the count of models for studying the stepwise investigation of carcinogenesis. Foci of the studies today are on the carcinogenic agents and immediate effects of these agents on cells and tissues i.e. identifying the rising number of carcinogens, initiators as well as promoters. Technological developments have enabled studies of the multistep nature of carcinogenic processes *in-vivo* [11].

1.4. Steps in cancer development

1.4.1. Initiation

Initiation is the prior step in the development of cancer. It is contemplated as the result of a genetic alteration that leads to the abnormal proliferation of a cell [12]. Initiators, react with deoxyribonucleic acid (DNA) leading to its alteration. Also, drug-metabolizing enzymes present inside the body may cause DNA damage. Effects of these initiators are generally irreversible. Once a cell gets affected by an initiator it will be disposed to the promotion of carcinogenesis till its death. Thus, initiation is considered as a permanent genetic change and further daughter cells producing these mutated cells would also bear these mutations [10, 13].

1.4.2. Promotion

Once initiation by a carcinogen occurs in a cell, then the cell becomes susceptible to the effect of promoters. These promoter agents promote the proliferation of these cells and result in the production of a large number of daughter cells containing the mutation which was created by the initiator agent [14]. Promoters generally show no effect when the organism has not been affected previously with an initiator [13]. In contrast with initiators, promoters do not react with DNA or macromolecules present

inside the cell. Usually, promoters bind to receptors present on the cell surface to affect intracellular pathways leading to cell proliferation [10]. Promoters may be of two categories including, specific promoters (interact with receptors or target cells of particular tissues) and non-specific promoters (alter gene expression in absence of a known receptor). Effect of the promoter in tumour development is dose-dependent. There is a minimum as well as a maximum effect of promoters. A very low dose is not capable of developing a tumour. An extremely high dose also would not lead to a higher risk beyond a specific level of exposure [13].

1.4.3. Progression

The term progression was coined by Leslie Foulds and it refers to the step-wise transformation of the benign tumour to neoplasm and neoplasm to malignancy. Progression is coupled with karyotypic changes as nearly all tumours are aneuploid. The karyotypic changes get associated with increased invasiveness, growth and metastasis [13]. Tumour progression persists in the form of additional mutations that arise within tumour cells. These mutations many times lead to rapid production of the descendant cells bearing mutation and consequently become dominant in that tumour population. This process is known as clonal selection. Clonal selections go on through all the stages of tumour development leading to the rapid tumour progression [12, 15].

1.5. Symptoms of Cancer

General symptoms linked with cancers are not specific and may include:

- Thickening or lump that may be felt under the skin
- Unintended weight changes
- Fatigue
- Changes in bowel or bladder habits
- A constant cough
- Persistent discomfort after the meal
- Inexplicable muscle/ joint pain
- Inexplicable sweat or fever at night [16]

1.6. Stages of tumour development

The development of a tumour from a genetically altered cell is basically a step-wise progression. Stages involved are hyperplasia, dysplasia, carcinoma *in-situ* and cancer.

1.6.1. Hyperplasia- Genetically altered cell starts dividing in an uncontrolled manner and leads to the production of excess numbers of cells in that region. The cells usually have the normal appearance but they become too many in number.

1.6.2. Dysplasia- It is referred as additional genetic changes occurring in the hyperplastic cells that lead to a rise in abnormal growth. At this stage, the cells/ tissue remain no longer normal and may become disorganized.

1.6.3. Carcinoma *in-situ*- Further alterations make the cells/ tissues appear all the more abnormal. At this stage, the abnormal cells form a larger area. A key aspect of *in-situ* development is that the cells are restricted to the initial location and have not yet started to invade other tissues. These types of cancers are curable through surgery as all the abnormal cells are present in one location and have not yet invaded the neighbouring tissue.

1.6.4. Cancer (malignant tumours)- Malignant tumours have the capability of invading neighbouring tissues or metastasize to the areas outside the local tissue. The most dangerous form of cancer is the metastatic tumour and it accounts for the largest percentage of deaths due to cancer. The tumours which do not progress to invade distant tissues are said to be the benign tumours. As they do not move from their initial location, they are not considered to be dangerous. Benign tumours are often less lethal than malignant, but may still lead to severe health problems. Larger benign tumours may put pressure over organs and may cause other health issues. As in the case of brain tumours, there is limited space within the skull and thus a larger growth in the brain cavity may be mortal [9, 12, 17-21].

1.7. Skin cancer

Skin cancers are basically of two types including melanoma and non-melanoma skin cancers (NMSCs). The NMSCs include basal and squamous cell skin carcinomas (BSCs and SSCs respectively). Melanoma is the one which is most responsible for cancer-related deaths among skin cancers. Worldwide, NMSCs occurrence is estimated to be about 2-3 million every year [22-24]. NMSCs normally have a benign course with locally affecting characteristics [25]. Nearly 3 to 8% augmentation has been recorded in skin cancer each year. Exact percentage of incidence of skin cancer in India is not known statistically, but NMSCs is quite uncommon among Asians [26]. SSCs are common in dark-skinned individuals than BSCs. Various studies in India

have constantly reported SSCs as the most prevalent skin malignancy [27]. SSCs generally occur in sites which are not exposed to the sun and are often more aggressive [28]. The occurrence of SSCs increases rapidly with increasing age [29].

1.7.1. Reasons for increasing incidence of skin cancer

The pragmatic increase in the incidence of skin cancers is linked with numerous factors including:

- The shift towards considerably older age which is associated with the higher risk of NMSCs [30].
- Increased recreational or occupational UV light exposure [31].
- Indoor tanning is also associated significantly with increased risk of BSCs and SSCs [31].
- Exposure to the excess of radiations like X-rays.
- Impairment of the immune system, which is meant to protect the skin from allergic substances and harmful reactions.
- Skin type (white skin more prone).
- Contact with carcinogenic chemicals like hydrocarbons in tar and soot [25, 32, 33].

1.7.2. Skin cancer diagnosis

Diagnosis of skin cancer requires contemplation of alternative diagnoses, pertaining to benign including *Verruca vulgaris*, *Seborrheic keratosis*, *Actinic porokeratosis*, *eczema*, *Lentigo solaris*, *psoriasis*, *Lichen planus* etc. Malignant conditions involve extra-mammary Paget's disease *keratoacanthoma*, *SSCs*, *BSCs*, *Lentigo maligna* etc. Clinicians are expected to perform total body skin examination, at least for the individuals with high-risk [34]. Photodynamic visualization may be helpful in identification of actinic keratosis and histological confirmation is required in case of invasive suspected skin carcinoma [35]. The use of advanced and non-invasive optical technologies, like optical coherence tomography and dermatoscopy, may be useful in the improvement of diagnostic accuracy in skin cancers [36, 37].

1.7.3. Etiopathogenesis of skin cancer

Both SSCs as well as BSCs, get initiated through keratinocytes. BSCs are frequently reported carcinomas that occur due to higher level of radiotherapy [38]. Individuals whose immunity becomes deficient may be due to organ transplant and is also

inclined to tumour development. Such patients develop skin cancer more frequently than the normal individuals [39]. Furthermore, patients suffering from NMSCs are at higher risk of concurrent or later occurrence of second NMSCs [40]. Some vital etiological agents include the high level of radiation therapy, coal tar, arsenic, various hydrocarbons etc. [41]. Experimental evidence and epidemiological data indicate that ultraviolet-B (UV-B) radiations are the most important reason for the initiation of skin cancer [42]. Ozone layer depletion causes the continuous rise of UV-B levels in the atmosphere, thereby increasing the risk of skin cancer. Statistically, it is reported that each 1% reduction of ozone layer increases the incidence of tumours by 2-4% and risk of percentage increase of SSCs remain larger than BSCs [23, 43].

1.8. Colon cancer

The term "colon cancer" refers to gradually developing cancer that initiates as tissue or tumour growth on the inner walls of the colon [44]. Colon cancer is amplifying its threat globally due to increased mortality rate. Colon cancer is reported as the third most common cancer seen in both men and women, reported by ICMR, 2015. Currently, it imparts about 10% of the whole cancer burden. Moreover, it is expected to augment by 60% and more than 2.2 million new cases would occur by 2030 [45]. ICMR report 2015 has also stated that colon cancer constitutes 63,000 cases of deaths in men (10 % of all cancer cases) and 5,71,000 cases in women (9.4 % of all cancer cases). In India, the yearly prevalence of colon/ rectal cancer reported in men and women is 4.4 and 4.1 for every 1, 00,000 cases respectively [46, 47].

1.8.1. Reasons for increasing incidence of colon cancer

The rising occurrences of colon cancers are linked with various factors. Though family history may be a risk factor, the majority of the cases are shown to have a disease which was not reported in the family history. Some reasons enlisted for colon cancer are as below:

- Ageing is one of the common risk factor for colon cancer. About 81% of the cases occur in the population at the age of 45 plus. Out of this, > 65% of cancers are seen between the ages of 65 to 84.
- Alcohol consumption is other major risk factors in the development of colorectal cancer. This incidence risk is directly associated with the amount of alcohol consumption.

- Numerous studies have proved the link between diabetes and colon cancer. About 40% people with diabetes are likely to develop colon cancer.
- Diets rich in fat/ cholesterol are found to be linked with the development of colon cancer. Further, diets low in fiber, vegetables or fruits are associated with a elevated risk.
- Ethnicity is also a known factor, for instance. African Americans, show 40% more chances of colon cancer when compared with whites and have also reported 20% higher deaths.
- Family history is also a considerable reason. If a person has/ had a relative who has colon cancer, the chance of getting affected with the disease automatically rises.
- Reports from numerous studies have shown that 1 out of 4 cases of colon cancer displayed similar genetic link.
- Inflammatory bowel disease is characterized by the consequences of Crohn's disease and ulcerative colitis, both of which are linked with colon cancer development.
- Obesity is a strong factor for colon cancer. People with obesity are likely to show 30% more chances than those with normal weight.
- Smoking damages every organ-system of the body. Long-term smoking is linked with hastened polyp growth to develop tumour [44, 48-50].

1.8.2. Colon cancer diagnosis

Doctors use many tests/ diagnostic tools to diagnose cancer. They also examine whether it is benign or metastatic. For most of the cases, the biopsy is one of the genuine ways to ensure the presence of a cancerous area. In the biopsy, a small sample of tissue is excised for examination under a microscope, in a laboratory. All other tests just indicate the presence of cancer, but biopsy makes an unambiguous diagnosis of colorectal cancer. Sometimes, computed tomography (CT) scan or ultrasound is helpful to conduct a needle biopsy. Doctors consider signs/ symptoms, age, medical condition and family history as important factors with additional physical examination for diagnosing colorectal cancer. Colonoscopy is another way of diagnosis. It permits a view inside the whole rectum and colon while patients are sedated. Doctors also suggest laboratory testing of a tumour sample to screen specific genes, proteins or other factors involved. Blood tests may also be performed, as

colorectal cancer usually bleeds in the rectum or large intestine. Patients often become anaemic. Count of red blood cells may indicate the occurrence of bleeding. Blood test detecting the levels of carcinoembryonic antigen (CEA) protein may indicate the spread of tumour to other parts of the body. CEA is not an apt test as its levels rise in only about 60% of the people with colorectal cancer. A CT scan may be used to determine the tumour size. CT scan can also check for the spread of cancer to the organs like lungs, liver etc. Magnetic resonance imaging (MRI) is one of the best imaging tests to detect the exact location of colorectal cancer. An ultrasound forms a picture of internal organs to examine the spread of cancer. In positron emission tomography (PET) or PET-CT scan, a radioactive sugar substance is injected into the patient. This sugar substance gets taken up by the cells. Cancerous cells tend to use more energy and thus absorb more of the radioactive substance. A scanner then detects the substance and produces an image [51, 52].

1.8.3. Aetiology and pathogenesis of colon cancer

Just like any other form of cancer, colorectal cancer is likely to be multifactorial and may follow a two-step carcinogenesis model that is initiation and promotion. As per this model system, there is an involvement of a series of events in order to produce cancer, instead of a single cause. Initiation includes exposure to a carcinogenic agent which irreversibly causes genetic mutation and converts the normal cell to the cancerous one. Promotion includes agents which are not usually carcinogenic but promotes tumour once initiated [53-55].

Colorectal cancer originates from epithelial cell linings of the colon/ rectum, mostly due to some mutations in the Wingless/Integrated (Wnt) signalling pathway which raises signalling activity [56, 57]. Adenomatous polyposis coli (APC) gene is the most common mutated gene in almost all colorectal cancers, which produces the APC protein. This APC protein impedes the amassing of β-catenin protein. In absence of APC protein, β-catenin amasses to high levels and translocates inside the nucleus and binds to DNA to activate transcription of proto-oncogenes. Cancer may be due to the mutations in other genes like TCF7L2, AXIN1, AXIN2, etc. [58-60].

1.9. Cancer prevention

Cancer prevention includes the actions performed in order to decrease the chances of being affected by cancer. Cancer prevention decreases the cancer burden and reduces

the number of cancer deaths. Cancer prevention recommends a cost-effective strategy for the cancer control. National programs and policies may be implemented to increase awareness for reduction of exposure to cancer-causing risk factors and people should be provided with the information to adopt healthy lifestyles.

Genes, lifestyle and surrounding environment may enhance or reduce the cancer risks. Researchers have suggested various ways of cancer prevention. Moreover, the American Cancer Society reported that there is strong evidence which suggests that healthy behaviour may substantially reduce the risk of cancer development.

- Diet and lifestyle changes.
- To avoid things and environment prone to cancer.
- Not to use tobacco
- Regular medical checkup to find out pre-cancerous situations early, so that may be treated. May even have cancer screenings as per suggested guidelines.
- To take medicines to treat the precancerous condition, if detected.
- Perform adequate physical activities
- Have healthy foods
- Have vaccination against human papilloma virus [61-65].

1.10. Cancer treatment options

Standard cancer treatment includes the combination of radiation, surgery and chemotherapy. The treatment strategies depend on location, type, stage and extent of tumour. Common therapies include surgery, radiation therapy, hormone therapy, chemotherapy, immunotherapy and stem cell transplant.

- **Surgery** may be performed to remove tumour only when it is limited to its site of origin. Nearby tissues and lymph nodes may also be removed through surgery. Surgery may be performed through laser or by using conventional instruments.
- **Radiation therapy** treats cancer as well as certain diseases through ionizing radiation. The cancerous cells and its genetic contents are destroyed by the use of ionizing radiation in the treatment area.
- **Hormone therapy** changes the effects of the hormones which are involved in the growth of cancer. This particular therapy is commonly utilized in the treatment of breast and prostate cancer.
- **Chemotherapy** uses anti-cancer drugs for cancer treatment. These anti-cancer drugs destroy cancer cells by preventing its multiplication and growth at some or

other points of their life cycle. These drugs may be administered by different routes.

- **Biological therapy** makes use of the immune system to fight against cancer that may be indirect or direct. This uses natural/ herbal agents and also diminishes the side-effects that may have been developed due to other cancer treatments.
- **Stem cell transplant** (bone marrow transplant) may use one's own or donor's stem cells to grow healthy, mature and disease-free cells [66-68]**.**

1.11. Chemotherapy

Various known compounds have anticancer activity. These agents mostly have a narrow therapeutic window and do not have selectivity for cancer cells. The required goal of cancer chemotherapy should be the development or use of such agents/ drugs that may be able to kill tumour cells specifically or that may render them benign without upsetting normal cells of the body.

1.12. Limitations of conventional chemotherapy

Conventional chemotherapy targets DNA and results in improved survival of cancer patients. Though, it contains numerous limitations such as non-specific drug distribution, poor selectivity, fast clearance, systemic toxicity along with severe side effects. These limitations create the significant challenge in the effectual cancer treatment. Most of the anti-cancer drugs like doxorubicin, paclitaxel etc. have low selectivity and thus distributes systemically with lesser localization to tumour site. Therefore, higher doses are needed to reach pharmacological levels at the required site which in-turn lead to increased toxicity and severe side effects to the normal tissues [69, 70]. So as to circumvent toxic side effects, these drugs are often administered at lower doses than the required ones which subsequently result in failure of therapy along with the development of drug resistance as well as metastasis. Thus, cancer eradication still remains a major trouble due to its heterogeneous character and failure of chemotherapeutic agents to target tumour site without affecting healthy tissues.

Consequently, there is an overwhelming need to make use of such chemo-preventative and chemotherapeutic agents that are both effective as well as safe. One practical approach to this problem is the use of terrestrial plants and naturally existing/ agents of natural origin as a platform for drug development [4].

Another approach can be the development of a novel delivery system by making use of existing synthetic drugs that may show multiple functions including targeting, diagnosing and killing of tumour cells specifically. Naturally (derived from plants/ animals) existing agents are playing a dominant role in the development of traditional and sophisticated drug delivery system. The WHO has estimated that about 80% of the Asian and African countries using traditional medicines for prime healthcare. Plant products and compounds originated from plant products also play a significant role in the health care area of developed countries. The herbal cure is the most accepted version of traditional medicine and is very productive in the international market. The global market for herbal products is anticipated to raise $5 trillion by 2050 [4].

1.13. Efficient way out

Safe and site-specific drug delivery is a major obstacle for numerous diseases including cancer. Because of above-mentioned reasons there has been rising interest in the development of innovative approaches that may be safer and can affect only the required site. Paul Ehrlich introduced the theory of "Magic Bullet" for drug targeting [71]. It contained two things, one than the drug molecule should identify the target site and other that the drug molecule should effect therapeutically only at the targeted site. Cells or tissues can be targeted by encapsulating the drug moiety in a suitable pharmaceutical carrier which is a modified version of a magic bullet [72]. The nano-sized delivery system can be designed that could be utilized as both therapeutic and diagnostic agent. Numerous studies have shown that the limitations of conventional drug therapy can be conquered through nanotechnology [73, 74].

1.14. Nanotechnology in cancer

Nanotechnology is usually a multidisciplinary scientific field which undergoes a broad expansion. Nanotechnology has been derived from the Greek word 'nano' which means 'dwarf'. It is defined as a science/ engineering of assembling and constructing the objects at nano-scale, a thousand millionth a meter [75, 76]. The size of nanomaterials are ideal for increasing oral bioavailability, surface area, higher drug loading, rapid commencement of therapeutic action etc. Dissimilarly, conventional drugs rapidly get cleared from the body thereby reducing drug amount from tumour site [77]. Nanocarriers containing drugs increase its half-life, circulation time, allowing a greater amount of drug to reach the target site [78]. Anticancer drugs in

nanoformulations display a superior therapeutic index as a result of improved pharmacokinetics, distribution and accumulation of drug at the tumour site [79]. The nano-sized systems exhibit more permeability into tumour site, as tumour sites have a leaky vasculature. Smaller size facilitates topical, transdermal, nasal, oral, parenteral and ocular drug administration. Consequently, nano drug delivery systems can be successful tools for anticancer therapy. Numerous nanostructures including vesicular systems (niosomes, liposome) biodegradable polymers, lipidic nanoparticles, micelles, carbon nanotubes and metallic nanoparticles (gold, silver nanoparticles) have been studied for the treatment of cancer [80-82].

1.15. Mechanisms of drug targeting

The success key for cancer treatment is to increase the drug accumulation at the tumour site. Drug concentration reaching the cancerous tissue requires being precise, once the drug reaches the tumour site. It is required to selectively kill the cancer cells while avoiding harm to the healthy tissues in order to reduce toxicity and adverse effects. The two mechanisms involved in facilitating drug-loaded nanoparticles to reach the tumour site are passive and active approaches [72].

1.15.1. Passive drug targeting

In passive targeting, nanosized drug delivery systems utilize characteristics of the tumour vasculature to accumulate in the neoplastic site through enhanced permeability and retention (EPR) phenomenon, as demonstrated by Maeda and Matsumura [83-85]. The EPR concept relies on the pathophysiological characteristics of leaky vasculatures and lymphatic drainage [86]. EPR allows the diffusion of circulating nanoparticles to permeate tumour tissues, thereby avoiding healthy tissues [87, 88]. Mostly, for passive targeting, nanoparticulate delivery systems are surface-coated using biopolymers like polyethylene glycol (PEG) in various types of cancer [89, 90]. Nanoparticle accumulation in tumour tissue is difficult to determine as it depends on numerous factors like shape, size, zeta potential etc. of the nanoparticles. Thus, a small part of administered dose gets accumulated at the target site which becomes a momentous limitation for passive drug targeting [86]. Considering these limitations, active drug targeting is focused nowadays.

1.15.2. Active drug targeting

Active drug targeting is intended to deliver drug selectively to the tumour tissues. In this targeting strategy targeting moiety or ligand are attached over the surface of

nanocarriers. These moieties identify the tumour-specific epitopes and enable the nanocarriers to bind to these receptors, usually over-expressed at tumour site. These specific receptors are tumour markers and are either not expressed or expressed at lower levels on healthy/ normal cells [91]. For the efficient targeting of nanoparticles at tumour site it is necessary to have a sufficient amount of targeting moieties [92]. Presently many ways are existing for the production of active targeting drug carriers and numerous moieties are available including proteins, small molecules, aptamers, monoclonal antibodies and nucleic acids that specifically identify over-expressed receptors on tumour cells.

1.16. Different types of moieties/ ligands for active targeting

1.16.1. Protein/ peptides

Numerous proteins/ peptides have been scrutinized for tumour targeting potential [92]. Atypical glycosylation is seen in almost all types of experimental and human cancers. The glycosyl epitopes form antigens which can be utilized for targeting of tumour cells [93]. Lectins like proteins are of non-immune origin and have the potential ability to recognize aberrant glycosylation. Hence, lectins have been used in researches for targeting of glycosylation associated with metastasis [94, 95].

1.16.2. Monoclonal antibodies (mAb)

Cancer cell targeting with a mAb was explained by Milstein, 1981 [96]. These mAbs bind to the receptor present on the cell surface and responsible to induce various antibody depended anticancer mechanisms [97, 98]. The practicability of antibody depended on tissue targeting has been demonstrated clinically with seventeen mAbs approved by the United States Food and Drug Administration (US FDA) [99]. Bevacizumab (Avastin, approved in 2004), the first angiogenesis inhibitor used for the treatment of colorectal cancer is an anti-vascular endothelial growth factor (VEGF) mAb which restrain the growth of new blood vessels [100]. More than 200 drug delivery systems making use of antibodies or their fragments which are in preclinical/ clinical trials [101].

1.16.3. Aptamers

Aptamers are also an emerging class of targeting moieties that have single short stranded ribonucleic acid (RNA) or DNA sequence of oligonucleotides which is used as targeting moiety [102]. These aptamers form three-dimensional structures which

display high ligand binding specificity required for target affinity. They are lesser immunogenic in comparison to antibodies and can be synthesized chemically. Docetaxel entrapped nanoparticles containing aptamer (against prostate cancer cells) seen to deliver high selectivity as well as efficacy *in-vivo* [103].

1.16.4. Small molecules

Small molecules of molecular weight <500 Da are among a promising class of targeting ligands. They are small in size, having low synthesis cost with high stability. Docetaxel entrapped poly (lactic acid) (PLA) and polycaprolactone (PCL) based targeted nanocarrier was developed by Chandran et al. by making use of PMSA as the targeting moiety [104]. This target moiety found promising for the nanoparticles uptake by the cell over-expressing prostate-specific membrane antigen (PMSA). This small molecule has also been used as a targeting moiety for developing a polymeric nanoparticle (BIND-014) prepared from a hydrophilic PEG and hydrophobic PLA polymeric core. This was controlled-release, first targeted delivery system of polymeric nanoparticles that reached clinical phase I trials for cancer chemotherapy [105].

1.17. Niosomes

Niosomes are non-ionic surfactant based vesicular system. It is a biocompatible, biodegradable and nonimmunogenic nanocarrier system [106, 107]. Niosomes are mostly formed by cholesterol and non-ionic surfactants [108]. The unique bilayer structures of niosomes make it capable of encapsulating both categories of drugs (hydrophilic and lipophilic). Hydrophilic drugs get entrapped in the aqueous core or get adsorbed on bilayer surfaces, on the other hand, lipophilic drugs get encapsulated inside the lipophilic realm of the bilayers [109]. Niosomes were first used in cosmetic industries and their applications have been explored for drug delivery. When compared with liposomes, niosomes exhibit higher chemical and physical stability with larger availability of surfactants at lesser cost. Moreover, niosomes display enhanced residence time of drugs and diminish the systemic absorption.

1.17.1. Preparation methods of niosomes

1.17.1.1. Thin film hydration method

The thin film hydration method is popular and is a relatively simple preparation method. In this, cholesterol, surfactants and some other additives like charge inducing

agents taken are together in a round-bottomed flask and dissolved in an organic solvent. After that organic solvent is evaporated using a rotary vacuum evaporator and thus a thin film is obtained. Then hydration of this thin film is done by using aqueous or buffer solution with constant shaking [106, 110].

1.17.1.2. Ether injection method

In this method, the additives and surfactants are dissolved in diethyl ether and this solution injected slowly in an aqueous drug solution by a needle. Then organic solvent is allowed to evaporate at specific temperature, with stirring [111, 112].

1.17.1.3. Reverse phase evaporation method

In reverse phase evaporation, surfactant and other additives are dissolved in a mixture of chloroform and ether and further added to drug-containing aqueous phase. The resultant mixture is sonicated to form an emulsion and further the organic phase allowed to evaporate [113, 114].

1.17.1.4. Multiple membrane extrusion method

Surfactant, cholesterol and additives are dissolved in chloroform and processed to form a thin film. The prepared film is hydrated using aqueous drug polycarbonate membranes. The resultant aqueous suspension is extruded with passages. This method is ideal for controlling size of niosomes [115].

1.17.1.5. Supercritical carbon dioxide fluid method

In this method, surfactant and several other additives are dissolved in ethanol in a view cell. The CO_2 gas is then introduced into this view cell. After attaining equilibrium with magnetic stirring, the pressure is released to get niosomal dispersion. This method enables easy scale-up as it is a one-step production method [116].

1.17.1.6. Transmembrane pH gradient method

In this, a thin lipid film is formed through conventional method on the walls of a round bottomed flask. The formed film is hydrated using a solution of citric acid with vortex mixing. The resultant product is freeze-thawed to form niosomes. Further aqueous solution containing drug can be added to this suspension and then phosphate buffer is added. pH has to be maintained between 7-7.2 [117].

1.17.1.7. Heating method

In the heating method, surfactants and cholesterol are hydrated separately in buffer and the obtained solution is heated up to 120°C with continuous stirring in order to

dissolve cholesterol. After temperature reduction, the surfactants and other ingredients are added to the cholesterol-containing buffer, with stirring to obtain niosomes [108].

1.17.1.8. Bubble method

In bubble method, surfactants, other ingredients and buffer are added into a three-necked glass flask. Components are dispersed at 70°C and mixed with homogenizer. Then the flask is placed on a water bath followed by nitrogen gas bubbling to obtain unilamellar niosomal vesicles [118].

1.18. Gold nanoparticles

Gold nanoparticles (GNP) have been in much consideration now-a-days due to their unique characteristics and possibility of multiple surface functionalizations. The GNP can be effectively surface functionalized with proteins, oligonucleotides, antibodies etc. The multi-functionality of GNP gave numerous materials that can be used for a variety of biomedical applications. GNP also serves as a potential platform for therapeutics as they have high surface area which provides a dense presence of multifunctional moieties which can be exploited for targeting [119-121].

1.18.1. Preparation methods of GNP

1.18.1.1. Turkevich method

Turkevich described this method of GNP development in 1951 which involves reduction of chloroauric acid ($HAuCl_4$) by aqueous solution of citrate. In this method, the $HAuCl_4$ solution is heated and the citrate solution is added in it with vigorous stirring. The color changes from pale yellow to wine red which indicates the formation of GNP. Citrate ion plays a double role of stabilizing and reducing agents. Particle size can be controlled by varying the amount of reducing agent [122, 123].

1.18.1.2. Chemical method

This method of GNP synthesis generally has two parts, one is the reduction part using reducing agents and the other is the stabilization using stabilizers. Sometimes agents behave both as reducing and stabilizing agent [124].

1.18.1.3. The Brust-Schiffrin method

Brust-Schiffrin method was described by Brust et. al. in 1994. This method provides the approach of synthesis of GNP which are thermally as well as air stable. In this method, $HAuCl_4$ from an aqueous solution get transferred to a toluene phase by the use of tetraoctylammonium bromide (TOABr) (phase-transferring agent) and sodium

borohydride ($NaBH_4$) used as a reducing agent with presence of dodecanethiol. The organic phase changes the color from orange to deep brown which indicates the formation of GNP [125].

1.18.1.4. Seeding growth method

In this method, the seed gets produced by reduction of $HAuCl_4$ by using a reducing agent. The produced seeds are then transferred to $HAuCl_4$ solution and allowed for reduction in the presence of a weak reducing agent. In this method, geometry of GNP can be varied by altering the concentration of reducing agents, seeds and structure directing agents. This method is simple, economical and quick [126].

1.18.1.5. Biological/ green method

In this method, nanoparticles are synthesized from biological/ natural agents such as microorganisms, plant extracts, enzymes, plant products etc. Furthermore, this method utilizes non-toxic solvents and environment-friendly procedures [127].

1.19. Green nanotechnology

Green nanotechnology in terms of nanoparticle production provides advancement over chemical/ physical methods as it is cost effective and is easily scaled up. Moreover, it is environment-friendly as it avoids the use of high pressure, energy, temperature and toxic chemicals. The principle of green chemistry includes the designing of processes to maximize the amount of raw material converted into the product, use of environment-benign substances, energy efficient processes, the reaction in water etc. [128]. Chemical method of nanoparticle synthesis is a most common approach but it may use expensive and toxic reducing/ stabilizing agents as well as monomers, which limit its applications. Additionally, such prepared nanoparticles may display harmful effects in biomedical applications. Therefore, the need of the hour is to develop some green nanotechnology based as well as cost-effective methods which do not involve the use of toxic chemicals and hazardous procedures [129].

1.19. Literature review

Madni *et al.*, (2018) prepared and evaluated proniosomes and niosomal gel containing Pentazocine for management of cancer pain. They tested the permeation of niosomal gel in the rabbit model and concluded that it can be proved as a promising approach for the therapy [130].

Behroozeh *et al.*, (2018) prepared and evaluated pegylated nano-niosomes containing gingerol against breast cancer cell lines (T47D). Results reported that IC50 value of the pegylated nanoniosomal gingerol was less than the standard drug [131].

Amiri *et al.*, (2018) prepared and characterized vinblastine containing pegylated niosomes against tumour cells. Results concluded that formulation enhanced drug bioavailability and therapeutic efficacy [132].

Chiang *et al.*, (2018) prepared the combination of fucoidan-based magnetic nanoparticles and immunomodulators for enhancement of tumour-localized immunotherapy and demonstrated the potential of nanomedicine in boosting of therapeutic index of combination immunotherapy [133].

Farooq *et al.*, (2018) prepared and evaluated gold nanoparticles containing bleomycin and doxorubicin for dual delivery against HeLa cells. Results obtained suggested the rationale for further progress of GNP assisted combination chemotherapy [134].

Li *et al.*, (2018) prepared and compared the effect of wrapping solid gold nanoparticles and hollow gold nanoparticles with doxorubicin-loaded thermosensitive liposomes for cancer thermo-chemotherapy. Results obtained from the studies displayed marked improvement in the therapeutic efficacy of the nanoparticles [135].

Bhattacharya and Prajapati (2017) developed and evaluated niosome based topical gel loaded with cyclophosphamide, for skin cancer. The result of the studies were satisfactory and indicating that a good formulation approach was designed for melanoma treatment [136].

Ilkhanizadeh *et al.*, (2017) made the comparison between effects of free and niosomal formulations of *Artemisia Annua L.* over chronic myelogenous leukaemia (K562) cell line and concluded that the use of the niosomal formulation of artemisinin could effectively improve its therapeutic index, release rate and apoptosis influence [137].

Chinembiri *et al.*, (2017) prepared and evaluated niosomes and SLNs containing *Withenia somnifera* crude extracts intended for topical delivery against skin cancer. It was concluded that SLNs and niosomes encapsulated the crude extracts and released the marker compounds to certain layers in the skin [138].

Meyer and Are (2017) discussed the status of colorectal cancer. They reported that colorectal cancer is the fourth most common cancer worldwide and millions of new cases are reported each year. Further in India, it is the fifth most common cancer after breast, cervix, oral, and lung cancer [139].

Abadeer and Murphy (2017) reported that gold nanoparticles are suitable for thermal destruction of cancer cells owing to their ease of surface functionalization and photothermal heating ability. They included *in-vitro* and *in-vivo* studies and progression of gold nanoparticle photothermal therapy toward clinical cancer treatment [140].

Bizzarri *et al.*, (2016) reviewed the broad spectrum anticancer activity of myo-inositol and inositol hexakisphosphate and concluded that inositol can down-regulate various enzymes linked with cancer development [141].

Fu *et al.*, (2016) analyzed inositol hexaphosphate (IP6) and inositol can inhibit colorectal cancer metastasis of the liver in BALB/c mice. Results displayed that the effect of the combined application was significantly greater than the effect of either compound alone [142].

Liu *et al.*, (2015) analyzed the potential of IP6 in the suppression of growth and apoptosis induction in HT-29 colorectal cancer cells in culture and concluded that by targeting PI3K/Akt pathway, IP6 suppresses cell survival and proliferation and induces death in HT-29 cells [143].

Wawszczyk *et al.*, (2015) assessed the antiproliferative effect of IP6 on human skin melanoma cells and demonstrated the antiproliferative and cytotoxic effect of IP6 in a wide range of concentrations. Thus, it could be a promising therapeutic agent in treating cancer [144].

Mevold *et al.*, (2015) prepared and evaluated core-shell gold nanoparticles containing IP6 for label-free and rapid detection by SERS nanotechnology and found that it can

be promising in the application of rapid and label-free biological detection of bacteria or tumour cells [145].

Gajendran *et al.*, (2014) demonstrated the efficacy of *Datura innoxia* for biosynthesis of silver nanoparticles (AgNPs). The results showed that biosynthesized AgNPs inhibited the proliferation of human breast cancer cell line MCF7 with an IC50 of 20 mg/ml at 24 h incubation [146].

Suman *et al.*, (2014) described the synthesis of gold nanoparticles using an aqueous root extract of *Morinda citrifolia*. Result showed that the extract containing protein might be responsible for the formation of the nanoparticles and may play an important role in the stabilization of the formed nanoparticles. The synthesized gold nanoparticles could have a high potential for use as an anticancer, antidiabetic agent [147].

Khazir *et al.*, (2014) stated that plants have the potential to be excellent lead structures and serve as a basis of promising therapeutic agents for cancer treatment. Many successful anti-cancer drugs currently in use or their analogues are plant-derived and many more are under clinical trials. This review aimed at highlighting the invaluable role that plants play, in the discovery of anticancer agents [4].

Quester *et al.*, (2013) summarized some of the most significant results using organisms to produce metallic nanoparticles as well as the microscopic analyses used to characterize the nanostructured material obtained, providing a valuable database for future research [148].

Marangoni *et al.*, (2013) prepared and characterized jacalin-gold nanoparticles conjugates as specific markers for cancer cells and revealed that the AuNPs/jacalin-FITC nanoconjugates exhibited higher affinity for leukemic K562 cells than for healthy mononuclear blood cells [149].

Siler *et al.*, (2013) studied the behaviour of a single gold or silver particle placed in an interference field of two counter-propagating plane waves. The results of the parametric studies focused on the optical forces acting upon a single particle and the heat absorbed by a single particle placed at various positions across the interference fringe [150].

Kumar and Randhawa (2013) reviewed lipid nanoparticles for delivery of lipophilic and labile drugs with controlled and targeted release kinetics which do not have the disadvantages of emulsions, suspensions, liposomes and polymer nanoparticles [151].

Sharma *et al.*, (2009) studied the structure, dynamics, and interactions of jacalin from molecular dynamics simulations examined in conjunction with the results of X-ray studies. Crystallographic results and simulations together displayed the complete description of protein-carbohydrate interactions in a better manner than X-ray studies alone [152].

1.20. Research envisaged

Cancer remains a life-threatening ailment worldwide. It is the third most deadly disease in developing nations like India. Existing treatments/ drugs are very expensive and add on to the patient's distress. There is an acute need to utilize potent, economic and naturally available agents for cancer prevention and cancer therapy. The proposed research work was aimed at the development of a green (utilization of minimum amount of organic solvents, utilizing natural entities over synthetic drugs etc.,) and effective treatment system for various types of cancers that could recognize and target only cancerous cells and would not affect healthier cells of the body.

To assist cancer prevention, many efforts are being made along with which, the use of natural constituents as chemopreventive as well as chemotherapeutic agents have shown a rise, because of their safety, availability and general acceptance. IP6 is one such natural bioactive constituent of cereals, legumes etc. Various researchers have already proven that intake of IP6 containing legumes is connected with the lowering of cancer incidences. Instead, this potent, bioactive, carbohydrate is not very popular in cancer therapy due to its shortcoming of fast chelation and elimination from the body, within an hour of administration.

Thus, it was envisaged to develop and analyze a suitable drug delivery system(s) of IP6 which would overcome its limitations and enhance its potential for cancer prevention and therapy.

1.20.1. Objectives of the work

The purpose of the present studies was to develop and characterize targeted nanoparticulate drug delivery system(s) containing IP6 for chemoprevention and chemotherapeutics which could augment its residence time thereby avoiding its fast elimination and taking full advantage of its effect against cancer.

The specific objectives were:

(1) Optimization, preparation and characterization of IP6 loaded niosomal gel for the topical application intended for skin cancer prevention.

(2) Preparation and evaluation of pectin encrusted gold nanocomposites containing IP6 and jacalin, for oral delivery to target colon cancer.

1.20.2. Hypothesis

It was hypothesized that present studies would successfully develop stable and safe nanoparticulate drug delivery system(s) of IP6 which would enhance its residence time and inhibit its fast elimination. Thus the potential of IP6 would be utilized to a maximum for effective cancer therapy.

1.21. Plan of work

1.21.1. Literature survey & procurement of materials

1.21.2. Identification of drug

1.21.3. Preparation of standard curve of drug through UV-Spectrophotometery

1.21.4. Preparation and evaluation of inositol hexaphosphate containing niosomal suspension for skin cancer prevention

- Literature survey & procurement of materials
- Optimization of niosomal vesicles
- Preparation of niosomal vesicles
- *In-vitro* characterization of niosomal vesicles
    - Size and size distribution
    - Encapsulation efficiency
    - Zeta potential measurement
    - *In-vitro* drug release
    - Morphological evaluation (microscopy, SEM and TEM)
    - Stability studies
- Niosomal suspension preparation and characterization
    - Pharmaceutical characterization
    - Skin permeation
    - Irritation test (HET-CAM)
    - Cell cytotoxicity assay on SK-MEL-2 cell lines
- *In-vivo* studies
    - SDS-PAGE and western blotting
    - Reverse transcription polymerase chain reaction (RT-PCR)
    - Histopathology

1.21.5. Preparation and evaluation of pectin encrusted gold nanocomposite containing inositol hexaphosphate and jacalin, against colon cancer

1. Literature survey & procurement of materials
2. Preparation of gold nanoparticles
3. *In-vitro* characterization of nanoformulation
    - UV- visible spectroscopy
    - Size and size distribution

- Encapsulation efficiency
- *In-vitro* drug release
- FTIR spectroscopy
- Morphological evaluation
- Cell viability assay
- Colony forming assay
- Cell cycle analysis
- Apoptosis analysis
- ROS generation
- *In-silico* studies

4. *In-vivo* studies
    - Hemodynamic changes
    - Weight variation, pH and total acidity estimation
    - Aberrant crypt foci
    - Biochemical estimation
    - Morphology by SEM and histopathology
    - Western blotting
    - RT-PCR
    - ^{1}H NMR spectroscopic analysis of serum sample

1.21.6. Computation and compilation of thesis

1.22. References

1. Saranath D, Khanna A. Current status of cancer burden: global and Indian scenario. Biomed Res J. 2014;1(1):1-5.
2. Hanahan D, Weinberg RA. The hallmarks of cancer. cell. 2000;100(1):57-70.
3. Sikora K. The impact of future technology on cancer care. Clinical Medicine. 2002;2(6):560-8.
4. Khazir J, Mir BA, Pilcher L, Riley DL. Role of plants in anticancer drug discovery. Phytochemistry Letters. 2014;7:173-81.
5. Nair MK, Varghese C, Swaminathan R. Cancer: Current scenario, intervention strategies and projections for 2015. Burden of Disease in India. 2005;219.
6. Mallath MK, Taylor DG, Badwe RA, Rath GK, Shanta V, Pramesh C, et al. The growing burden of cancer in India: epidemiology and social context. The Lancet Oncology. 2014;15(6):e205-e12.
7. Cancer, World Health Organization 2018 [cited 2018 20 August]. World Health Organization]. Available from: http://www.who.int/en/news-room/fact-sheets/detail/cancer.
8. Current Status Of Cancer In India – A Bird's Eye View 2017 [cited 2018 20 August]. Available from: http://www.carehospitals.com/blog/think-tank/current-status-of-cancer-in-india-a-birds-eye-view/.
9. Stoddart R. The Generation of Cancer: Initiation, promotion, progression and the multiple influences of the environment. SAGE Publications Sage UK: London, England; 1983.
10. Troll W, Wiesner R. The role of oxygen radicals as a possible mechanism of tumor promotion. Annual Review of Pharmacology and toxicology. 1985;25(1):509-28.
11. Farber E. The multistep nature of cancer development. Cancer research. 1984;44(10):4217-23.
12. Cooper GM, Hausman RE. The cell: Molecular approach: Medicinska naklada; 2004.
13. Pitot HC, Goldsworthy T, Moran S. The natural history of carcinogenesis: implications of experimental carcinogenesis in the genesis of human cancer. Journal of supramolecular structure and cellular biochemistry. 1981;17(2):133-46.
14. Yamagiwa K, Ichikawa K. Experimental study of the pathogenesis of carcinoma. The Journal of Cancer Research. 1918;3(1):1-29.
15. Melnikova VO, Ananthaswamy HN. Cellular and molecular events leading to the development of skin cancer. Mutation research/fundamental and molecular mechanisms of mutagenesis. 2005;571(1):91-106.
16. Cancer Treatment in India 2018 [cited 2018 20 August]. Available from: https://www.medicalindiatourism.com/cancer-treatment.html.
17. Carmeliet P, Jain RK. Molecular mechanisms and clinical applications of angiogenesis. Nature. 2011;473(7347):298.
18. Makale M. Cellular mechanobiology and cancer metastasis. Birth Defects Research Part C: Embryo Today: Reviews. 2007;81(4):329-43.

19. Vincent TL, Gatenby RA. An evolutionary model for initiation, promotion, and progression in carcinogenesis. International journal of oncology. 2008;32(4):729-37.
20. Yokota J. Tumor progression and metastasis. Carcinogenesis. 2000;21(3):497-503.
21. Cancer Development 2018 [cited 2018 20 August]. Available from: https://www.cancerquest.org/cancer-biology/cancer-development#footnoteref4_wftj65w.
22. Foster PJ, Dunn EA, Karl KE, Snir JA, Nycz CM, Harvey AJ, et al. Cellular magnetic resonance imaging: in vivo imaging of melanoma cells in lymph nodes of mice. Neoplasia. 2008;10(3):207-16.
23. Panda S. Nonmelanoma skin cancer in India: Current scenario. Indian journal of dermatology. 2010;55(4):373.
24. Skin cancers 2018 [cited 2018 20 August]. Available from: http://www.who.int/uv/faq/skincancer/en/index1.html.
25. Narayanan DL, Saladi RN, Fox JL. Ultraviolet radiation and skin cancer. International journal of dermatology. 2010;49(9):978-86.
26. Thomas RF, Scotto J. Estimating increases in skin cancer morbidity due to increases in ultraviolet radiation exposure. Cancer investigation. 1983;1(2):119-26.
27. Talvalkar G. Squamous cell carcinoma of the skin. Its incidence and etio-pathogenesis in 625 cases. Indian journal of cancer. 1970;7(1):24-33.
28. Fleming ID, Barnawell JR, Burlison PE, Rankin JS. Skin cancer in black patients. Cancer. 1975;35(3):600-5.
29. Schreiber MM, Shapiro SI, Berry CZ, Dahlen RF, Friedman RP. The incidence of skin cancer in southern Arizona (Tucson). Arch Dermatol. 1971;104(2):124-7.
30. Qureshi A, Wei-Passanese E, Li T, Han J. Host risk factors for the development of multiple non-melanoma skin cancers. Journal of the European Academy of Dermatology and Venereology. 2013;27(5):565-70.
31. Flohil SC, Seubring I, Van Rossum MM, Coebergh J-WW, De Vries E, Nijsten T. Trends in Basal cell carcinoma incidence rates: a 37-year Dutch observational study. Journal of Investigative Dermatology. 2013;133(4):913-8.
32. Boffetta P, Jourenkova N, Gustavsson P. Cancer risk from occupational and environmental exposure to polycyclic aromatic hydrocarbons. Cancer Causes & Control. 1997;8(3):444-72.
33. Leiter U, Garbe C. Epidemiology of melanoma and nonmelanoma skin cancer—the role of sunlight. Sunlight, vitamin D and skin cancer: Springer; 2008. p. 89-103.
34. Argenziano G, Zalaudek I, Hofmann-Wellenhof R, Bakos RM, Bergman W, Blum A, et al. Total body skin examination for skin cancer screening in patients with focused symptoms. Journal of the American Academy of Dermatology. 2012;66(2):212-9.
35. Apalla Z, Nashan D, Weller RB, Castellsagué X. Skin cancer: Epidemiology, disease burden, pathophysiology, diagnosis, and therapeutic approaches. Dermatology and therapy. 2017;7(1):5-19.
36. Giavedoni P, Puig S, Carrera C, editors. Noninvasive imaging for nonmelanoma skin cancer. Seminars in cutaneous medicine and surgery; 2016.

37. Menge TD, Pellacani G, editors. Advances in noninvasive imaging of melanoma. Seminars in cutaneous medicine and surgery; 2016.

38. Meibodi NT, Maleki M, Javidi Z, Nahidi Y. Clinicopathological evaluation of radiation induced basal cell carcinoma. Indian journal of dermatology. 2008;53(3):137.

39. Mokhtari M, Mesbah A, Rajabi P, Rajabi MA, Chehrei A, Mougouei K. Determination of the relationship between basal cell carcinoma and human papilloma virus, based on immunohistochemistry staining method. Indian journal of dermatology. 2009;54(3):225.

40. Schinstine M, Goldman GD. Risk of synchronous and metachronous second nonmelanoma skin cancer when referred for Mohs micrographic surgery. Journal of the American Academy of Dermatology. 2001;44(3):497-9.

41. Tadini G, Restano L, Gonzáles-Pérez R, Gonzáles-Ensenat MA, Vincente-Villa MA, Cambiaghi S, et al. Phacomatosis pigmentokeratotica: report of new cases and further delineation of the syndrome. Archives of dermatology. 1998;134(3):333-7.

42. Leaf A. Potential health effects of global climatic and environmental changes. New England Journal of Medicine. 1989;321(23):1577-83.

43. Scotto J, Fears TR, Fraumeni JF. Incidence of nonmelanoma skin cancer in the United States. US Department of Health and Human Services, Public Health Service, National Institutes of Health, National Cancer Institute; 1983.

44. Myers D. Causes and Risk Factors of Colon Cancer 2018 [cited 2018 20 August]. Available from: https://www.verywellhealth.com/colon-cancer-causes-risk-factors-796786.

45. Arnold M, Sierra MS, Laversanne M, Soerjomataram I, Jemal A, Bray F. Global patterns and trends in colorectal cancer incidence and mortality. Gut. 2017;66(4):683-91.

46. Katoch VM. Consensus Document for Management of Colorectal Cancer. Indian Council of Medical Research, 2015.

47. Shanthi N, Gupta R, Mahato K. Traditional and emerging applications of microspheres: A review. Int J PharmTech Res. 2010;2(1):675-81.

48. Colon Cancer Info 2014 [cited 2018 21 August]. Available from: http://www.beseengetscreened.com/get-informed/causes-and-prevention.

49. Geggel L. Colon Cancer: Causes, Symptoms and Treatments 2014 [cited 2018 20 August]. Available from: https://www.livescience.com/34716-colon-cancer-symptoms-colonoscopy.html.

50. Haggar FA, Boushey RP. Colorectal cancer epidemiology: incidence, mortality, survival, and risk factors. Clinics in colon and rectal surgery. 2009;22(4):191.

51. Colorectal Cancer: Diagnosis 2017 [cited 2018 21 August]. Available from: https://www.cancer.net/cancer-types/colorectal-cancer/diagnosis.

52. Meyerhardt JA, Giovannucci EL, Holmes MD, Chan AT, Chan JA, Colditz GA, et al. Physical activity and survival after colorectal cancer diagnosis. Journal of clinical oncology. 2006;24(22):3527-34.

53. Doughty DB, editor Colorectal cancer: Etiology and pathophysiology. Seminars in oncology nursing; 1986: Elsevier.

54. Hill M. Bacteria and the etiology of colonic cancer. Cancer. 1974;34(S3):815-8.

55. Nigro ND, Bull AW. The two-step concept of intestinal carcinogenesis. Experimental colon carcinogenesis. 1983:215-24.
56. Minde DP, Radli M, Forneris F, Maurice MM, Rüdiger SG. Large extent of disorder in Adenomatous Polyposis Coli offers a strategy to guard Wnt signalling against point mutations. PloS one. 2013;8(10):e77257.
57. Gilbert SF. Developmental Biology, Ninth Edition (Developmental Biology Developmental Biology). 9th ed: Sinauer Associates, Inc.
58. Markowitz SD, Bertagnolli MM. Molecular basis of colorectal cancer. New England Journal of Medicine. 2009;361(25):2449-60.
59. Mehlen P, Fearon ER. Role of the dependence receptor DCC in colorectal cancer pathogenesis. Journal of Clinical Oncology. 2004;22(16):3420-8.
60. Arnold CN, Goel A, Blum HE, Richard Boland C. Molecular pathogenesis of colorectal cancer: implications for molecular diagnosis. Cancer: Interdisciplinary International Journal of the American Cancer Society. 2005;104(10):2035-47.
61. Cancer Prevention Overview (PDQ®)–Patient Version. National Cancer Institute, 2018.
62. Cancer prevention, World Health Organization 2018 [cited 2018 21 August]. Available from: http://www.who.int/cancer/prevention/en/.
63. Cancer Prevention. Rogel Cancer Center, Michigan Medicine, 2018.
64. Cancer Prevention, American Association for Cancer Research 2018 [cited 2018 21 August]. Available from: https://www.aacrfoundation.org/Pages/prevention.aspx.
65. Block G, Patterson B, Subar A. Fruit, vegetables, and cancer prevention: a review of the epidemiological evidence. Nutrition and cancer. 1992;18(1):1-29.
66. Types of Cancer Treatment, National Cancer Institute 2017 [cited 2018 21 August]. Available from: https://www.cancer.gov/about-cancer/treatment/types.
67. Silver JK, Baima J. Cancer prehabilitation: an opportunity to decrease treatment-related morbidity, increase cancer treatment options, and improve physical and psychological health outcomes. American journal of physical medicine & rehabilitation. 2013;92(8):715-27.
68. How Cancer is Treated, Cancer.Net 2018 [cited 2018 21 August]. Available from: https://www.cancer.net/navigating-cancer-care/how-cancer-treated.
69. Park J-H, von Maltzahn G, Xu MJ, Fogal V, Kotamraju VR, Ruoslahti E, et al. Cooperative nanomaterial system to sensitize, target, and treat tumors. Proceedings of the National Academy of Sciences. 2010;107(3):981-6.
70. Reinbolt RE, Patel R, Pan X, Timmers CD, Pilarski R, Shapiro CL, et al. Risk factors for anthracycline-associated cardiotoxicity. Supportive Care in Cancer. 2016;24(5):2173-80.
71. Strebhardt K, Ullrich A. Paul Ehrlich's magic bullet concept: 100 years of progress. Nature Reviews Cancer. 2008;8(6):473.
72. Torchilin VP. Passive and active drug targeting: drug delivery to tumors as an example. Drug delivery: Springer; 2010. p. 3-53.
73. Chidambaram M, Manavalan R, Kathiresan K. Nanotherapeutics to overcome conventional cancer chemotherapy limitations. Journal of pharmacy & pharmaceutical sciences. 2011;14(1):67-77.

74. Sakamoto JH, van de Ven AL, Godin B, Blanco E, Serda RE, Grattoni A, et al. Enabling individualized therapy through nanotechnology. Pharmacological Research. 2010;62(2):57-89.

75. Swarbrick J. Encyclopedia of pharmaceutical technology: CRC Press; 2013.

76. Vyas SP, Khar RK. Targeted & controlled drug delivery: Novel carrier systems: CBS publishers & distributors; 2004.

77. Allen TM, Cullis PR. Drug delivery systems: entering the mainstream. Science. 2004;303(5665):1818-22.

78. Shaffer C. Nanomedicine transforms drug delivery. 2005.

79. Bae KH, Chung HJ, Park TG. Nanomaterials for cancer therapy and imaging. Molecules and cells. 2011;31(4):295-302.

80. Muthu MS, Kutty RV, Luo Z, Xie J, Feng S-S. Theranostic vitamin E TPGS micelles of transferrin conjugation for targeted co-delivery of docetaxel and ultra bright gold nanoclusters. Biomaterials. 2015;39:234-48.

81. Kim S-S, Rait A, Kim E, DeMarco J, Pirollo KF, Chang EH. Encapsulation of temozolomide in a tumor-targeting nanocomplex enhances anti-cancer efficacy and reduces toxicity in a mouse model of glioblastoma. Cancer letters. 2015;369(1):250-8.

82. Kesavan A, Ilaiyaraja P, Beaula WS, Kumari VV, Lal JS, Arunkumar C, et al. Tumor targeting using polyamidoamine dendrimer–cisplatin nanoparticles functionalized with diglycolamic acid and herceptin. European Journal of Pharmaceutics and Biopharmaceutics. 2015;96:255-63.

83. Bazak R, Houri M, El Achy S, Hussein W, Refaat T. Passive targeting of nanoparticles to cancer: A comprehensive review of the literature. Molecular and clinical oncology. 2014;2(6):904-8.

84. Maeda H, Matsumura Y. Tumoritropic and lymphotropic principles of macromolecular drugs. Critical reviews in therapeutic drug carrier systems. 1989;6(3):193-210.

85. Matsumura Y, Maeda H. A new concept for macromolecular therapeutics in cancer chemotherapy: mechanism of tumoritropic accumulation of proteins and the antitumor agent smancs. Cancer research. 1986;46(12 Part 1):6387-92.

86. Maeda H. The enhanced permeability and retention (EPR) effect in tumor vasculature: the key role of tumor-selective macromolecular drug targeting. Advances in enzyme regulation. 2001.

87. Jain RK. Delivery of molecular and cellular medicine to solid tumors. Microcirculation. 1997;4(1):1-23.

88. Jain RK, Stylianopoulos T. Delivering nanomedicine to solid tumors. Nature reviews Clinical oncology. 2010;7(11):653.

89. Hatakeyama H, Akita H, Harashima H. A multifunctional envelope type nano device (MEND) for gene delivery to tumours based on the EPR effect: a strategy for overcoming the PEG dilemma. Advanced drug delivery reviews. 2011;63(3):152-60.

90. Knop K, Hoogenboom R, Fischer D, Schubert US. Poly (ethylene glycol) in drug delivery: pros and cons as well as potential alternatives. Angewandte chemie international edition. 2010;49(36):6288-308.

91. Ruoslahti E, Bhatia SN, Sailor MJ. Targeting of drugs and nanoparticles to tumors. The Journal of cell biology. 2010;188(6):759-68.

92. Sahoo SK, Misra R, Parveen S. Nanoparticles: a boon to drug delivery, therapeutics, diagnostics and imaging. Nanomedicine in Cancer: Pan Stanford; 2017. p. 73-124.

93. Hakomori S. Glycosylation defining cancer malignancy: new wine in an old bottle. Proceedings of the National Academy of Sciences. 2002;99(16):10231-3.

94. Danella Polli C, Pereira Ruas L, Chain Veronez L, Herrero Geraldino T, Rossetto de Morais F, Roque-Barreira MC, et al. Jacalin-activated macrophages exhibit an antitumor phenotype. BioMed Research International. 2016;2016.

95. Lis H, Sharon N. Lectins: carbohydrate-specific proteins that mediate cellular recognition. Chemical reviews. 1998;98(2):637-74.

96. Warenius H, Galfre G, Bleehen N, Milstein C. Attempted targeting of a monoclonal antibody in a human tumour xenograft system. European Journal of Cancer and Clinical Oncology. 1981;17(9):1009-15.

97. Chames P, Van Regenmortel M, Weiss E, Baty D. Therapeutic antibodies: successes, limitations and hopes for the future. British journal of pharmacology. 2009;157(2):220-33.

98. Clynes RA, Towers TL, Presta LG, Ravetch JV. Inhibitory Fc receptors modulate in vivo cytoxicity against tumor targets. Nature medicine. 2000;6(4):443.

99. Gabizon AA. Pegylated liposomal doxorubicin: metamorphosis of an old drug into a new form of chemotherapy. Cancer investigation. 2001;19(4):424-36.

100. Ferrara N. VEGF as a therapeutic target in cancer. Oncology. 2005;69(Suppl. 3):11-6.

101. Carter P. Improving the efficacy of antibody-based cancer therapies. Nature Reviews Cancer. 2001;1(2):118.

102. Orava EW, Cicmil N, Gariépy J. Delivering cargoes into cancer cells using DNA aptamers targeting internalized surface portals. Biochimica et Biophysica Acta (BBA)-Biomembranes. 2010;1798(12):2190-200.

103. Farokhzad OC, Cheng J, Teply BA, Sherifi I, Jon S, Kantoff PW, et al. Targeted nanoparticle-aptamer bioconjugates for cancer chemotherapy in vivo. Proceedings of the National Academy of Sciences. 2006;103(16):6315-20.

104. Chandran SS, R. Banerjee S, C. Mease R, Pomper MG, R. Denmeade S. Characterization of a targeted nanoparticle functionalized with a urea-based inhibitor of prostate-specific membrane antigen (PSMA). Cancer biology & therapy. 2008;7(6):974-82.

105. Von Hoff D, Mita MM, Ramanathan RK, Weiss GJ, Mita AC, LoRusso PM, et al. Phase 1 study of PSMA-targeted docetaxel-containing nanoparticle BIND-014 in patients with advanced solid tumors. Clinical Cancer Research. 2016:clincanres. 2548.015.

106. Ag Seleci D, Seleci M, Walter J-G, Stahl F, Scheper T. Niosomes as nanoparticular drug carriers: fundamentals and recent applications. Journal of Nanomaterials. 2016;2016.

107. Rajera R, Nagpal K, Singh SK, Mishra DN. Niosomes: a controlled and novel drug delivery system. Biological and Pharmaceutical Bulletin. 2011;34(7):945-53.

108. Moghassemi S, Hadjizadeh A. Nano-niosomes as nanoscale drug delivery systems: an illustrated review. Journal of Controlled Release. 2014;185:22-36.

109. Your Source of Information 2008 [cited 2018 21 August]. Available from: http://jeepakistan.blogspot.com/2008/05/d.html.

110. Baillie A, Florence A, Hume L, Muirhead G, Rogerson A. The preparation and properties of niosomes—non-ionic surfactant vesicles. Journal of pharmacy and pharmacology. 1985;37(12):863-8.

111. Marwa A, Omaima S, Hanaa E-G, Mohammed A-S. Preparation and in-vitro evaluation of diclofenac sodium niosomal formulations. International Journal of Pharmaceutical Sciences and Research. 2013;4(5):1757-65.

112. Srinivas S, Kumar YA, Hemanth A, Anitha M. Preparation and evaluation of niosomes containing aceclofenac. Dig J Nanomater Bios. 2010;5(1):249-54.

113. Kiwada H, NIIMURA H, FUJISAKI Y, YAMADA S, KATO Y. Application of synthetic alkyl glycoside vesicles as drug carriers. I. Preparation and physical properties. Chemical and pharmaceutical bulletin. 1985;33(2):753-9.

114. Moghassemi S, Parnian E, Hakamivala A, Darzianiazizi M, Vardanjani MM, Kashanian S, et al. Uptake and transport of insulin across intestinal membrane model using trimethyl chitosan coated insulin niosomes. Materials Science and Engineering: C. 2015;46:333-40.

115. Chandu VP, Arunachalam A, Jeganath S, Yamini K, Tharangini K, Chaitanya G. Niosomes: a novel drug delivery system. International journal of novel trends in pharmaceutical sciences. 2012;2(1):25-31.

116. Manosroi A, Chutoprapat R, Abe M, Manosroi J. Characteristics of niosomes prepared by supercritical carbon dioxide (scCO2) fluid. International journal of pharmaceutics. 2008;352(1-2):248-55.

117. Mayer L, Bally M, Cullis P. Uptake of adriamycin into large unilamellar vesicles in response to a pH gradient. Biochimica Et Biophysica Acta (BBA)-Biomembranes. 1986;857(1):123-6.

118. Talsma H, Van Steenbergen MJ, Borchert JC, Crommelin DJ. A novel technique for the one-step preparation of liposomes and nonionic surfactant vesicles without the use of organic solvents. Liposome formation in a continuous gas stream: The 'Bubble'method. Journal of pharmaceutical sciences. 1994;83(3):276-80.

119. Brown SD, Nativo P, Smith J-A, Stirling D, Edwards PR, Venugopal B, et al. Gold nanoparticles for the improved anticancer drug delivery of the active component of oxaliplatin. Journal of the American Chemical Society. 2010;132(13):4678-84.

120. Mukherjee P, Bhattacharya R, Bone N, Lee YK, Patra CR, Wang S, et al. Potential therapeutic application of gold nanoparticles in B-chronic lymphocytic leukemia (BCLL): enhancing apoptosis. Journal of nanobiotechnology. 2007;5(1):4.

121. Yeh Y-C, Creran B, Rotello VM. Gold nanoparticles: preparation, properties, and applications in bionanotechnology. Nanoscale. 2012;4(6):1871-80.

122. Hu M, Chen J, Li Z-Y, Au L, Hartland GV, Li X, et al. Gold nanostructures: engineering their plasmonic properties for biomedical applications. Chemical Society Reviews. 2006;35(11):1084-94.

123. Turkevich J, Stevenson PC, Hillier J. A study of the nucleation and growth processes in the synthesis of colloidal gold. Discussions of the Faraday Society. 1951;11:55-75.

124. Herizchi R, Abbasi E, Milani M, Akbarzadeh A. Current methods for synthesis of gold nanoparticles. Artificial cells, nanomedicine, and biotechnology. 2016;44(2):596-602.

125. Brust M, Walker M, Bethell D, Schiffrin DJ, Whyman R. Synthesis of thiol-derivatised gold nanoparticles in a two-phase liquid–liquid system. Journal of the Chemical Society, Chemical Communications. 1994(7):801-2.

126. Siti RM, Khairunisak AR, Azlan AA, Noordin R, editors. Green synthesis of 10 nm gold nanoparticles via seeded-growth method and its conjugation properties on lateral flow immunoassay. Advanced Materials Research; 2013: Trans Tech Publ.

127. Shankar SS, Rai A, Ankamwar B, Singh A, Ahmad A, Sastry M. Biological synthesis of triangular gold nanoprisms. Nature materials. 2004;3(7):482.

128. Saxena A, Tripathi R, Zafar F, Singh P. Green synthesis of silver nanoparticles using aqueous solution of Ficus benghalensis leaf extract and characterization of their antibacterial activity. Mater Lett. 2012;67(1):91-4.

129. Singh M, Kalaivani R, Manikandan S, Sangeetha N, Kumaraguru A. Facile green synthesis of variable metallic gold nanoparticle using Padina gymnospora, a brown marine macroalga. Applied Nanoscience. 2013;3(2):145-51.

130. Madni A, Rahim MA, Mahmood MA, Jabar A, Rehman M, Shah H, et al. Enhancement of Dissolution and Skin Permeability of Pentazocine by Proniosomes and Niosomal Gel. AAPS PharmSciTech. 2018:1-10.

131. Behroozeh A, Tabrizi MM, Kazemi SM, Choupani E, Kabiri N, Ilbeigi D, et al. Evaluation the Anti-Cancer Effect of PEGylated Nano-Niosomal Gingerol, on Breast Cancer Cell lines (T47D), In-Vitro. Asian Pacific journal of cancer prevention: APJCP. 2018;19(3):645.

132. Amiri B, Ahmadvand H, Farhadi A, Najmafshar A, Chiani M, Norouzian D. Delivery of vinblastine-containing niosomes results in potent in vitro/in vivo cytotoxicity on tumor cells. Drug development and industrial pharmacy. 2018;44(8):1371-6.

133. Chiang C-S, Lin Y-J, Lee R, Lai Y-H, Cheng H-W, Hsieh C-H, et al. Combination of fucoidan-based magnetic nanoparticles and immunomodulators enhances tumour-localized immunotherapy. Nature nanotechnology. 2018:1.

134. Farooq MU, Novosad V, Rozhkova EA, Wali H, Ali A, Fateh AA, et al. Gold nanoparticles-enabled efficient dual delivery of anticancer therapeutics to HeLa cells. Scientific reports. 2018;8(1):2907.

135. Li Y, He D, Tu J, Wang R, Zu C, Chen Y, et al. The comparative effect of wrapping solid gold nanoparticles and hollow gold nanoparticles with doxorubicin-loaded thermosensitive liposomes for cancer thermo-chemotherapy. Nanoscale. 2018;10(18):8628-41.

136. Bhattacharya S, Prajapati BG. Formulation, Design and Development of Niosome Based Topical Gel for Skin Cancer.

137. Ilkhanizadeh B, Mehrshad A, Seddighnia A, Zarei L. Comparison between effects of free and niosomal formulations of Artemisia annua L.(asteraceae) on chronic myelogenous leukemia (K562) cell line. International Journal of Pharmacology. 2017;13(2):191-7.

138. Chinembiri TN, Gerber M, du Plessis LH, du Preez JL, Hamman JH, du Plessis J. Topical delivery of Withania somnifera crude extracts in niosomes and solid lipid nanoparticles. Pharmacognosy magazine. 2017;13(Suppl 3):S663.

139. Meyer B, Are C. Current Status and Future Directions in Colorectal Cancer. Springer; 2017.

140. Abadeer NS, Murphy CJ. Recent progress in cancer thermal therapy using gold nanoparticles. The Journal of Physical Chemistry C. 2016;120(9):4691-716.

141. Bizzarri M, Dinicola S, Bevilacqua A, Cucina A. Broad spectrum anticancer activity of myo-inositol and inositol hexakisphosphate. International journal of endocrinology. 2016;2016.

142. Fu M, Song Y, Wen Z, Lu X, Cui L. Inositol hexaphosphate and inositol inhibit colorectal cancer metastasis to the liver in BALB/c mice. Nutrients. 2016;8(5):286.

143. Liu G, Song Y, Cui L, Wen Z, Lu X. Inositol hexaphosphate suppresses growth and induces apoptosis in HT-29 colorectal cancer cells in culture: PI3K/Akt pathway as a potential target. International journal of clinical and experimental pathology. 2015;8(2):1402.

144. Wawszczyk J, KAPRAL M, Lodowska J, Jesse K, Hollek A, GLARZ LW, editors. Antiproliferative effect of inositol hexaphosphate on human skin melanoma cells in vitro. Paper presented at IX MKNOL Conference; 2014.

145. Mevold AH, Liu J-Y, Huang L-Y, Liao H-L, Yang M-C, Chan T-Y, et al. Core-shell structure of gold nanoparticles with inositol hexaphosphate nanohybrids for label-free and rapid detection by SERS nanotechnology. Journal of Nanomaterials. 2015;2015:5.

146. Gajendran B, Chinnasamy A, Durai P, Raman J, Ramar M. Biosynthesis and characterization of silver nanoparticles from Datura inoxia and its apoptotic effect on human breast cancer cell line MCF7. Materials Letters. 2014;122:98-102.

147. Suman T, Rajasree SR, Ramkumar R, Rajthilak C, Perumal P. The Green synthesis of gold nanoparticles using an aqueous root extract of Morinda citrifolia L. Spectrochimica Acta Part A: Molecular and Biomolecular Spectroscopy. 2014;118:11-6.

148. Quester K, Avalos-Borja M, Castro-Longoria E. Biosynthesis and microscopic study of metallic nanoparticles. Micron. 2013;54:1-27.

149. Marangoni VS, Paino IM, Zucolotto V. Synthesis and characterization of jacalin-gold nanoparticles conjugates as specific markers for cancer cells. Colloids and Surfaces B: Biointerfaces. 2013;112:380-6.

150. Šiler M, Chvátal L, Zemánek P. Metallic nanoparticles in a standing wave: optical force and heating. Journal of Quantitative Spectroscopy and Radiative Transfer. 2013;126:84-90.

151. Kumar S, Randhawa JK. High melting lipid based approach for drug delivery: solid lipid nanoparticles. Materials Science and Engineering: C. 2013;33(4):1842-52.

152. Sharma A, Sekar K, Vijayan M. Structure, dynamics, and interactions of jacalin. Insights from molecular dynamics simulations examined in conjunction with results of X-ray studies. Proteins: Structure, Function, and Bioinformatics. 2009;77(4):760-77.

Chapter 2

Drug profile and analytical methods

2. Drug profile and analytical methods

2.1. The drug Inositol hexaphosphate (IP6)

IP6 is a natural bioactive constituent of grains, legumes and cereal products [1, 2]. Chemically, IP6 is a simple carbohydrate with six phosphates attached to each carbon (inositol-1,2,3,4,5,6-hexaphosphate). It is a principal means of storage of phosphorus in several plant tissues [3, 4]. It possesses various health benefits including strong antioxidant properties, lowering of serum cholesterol and many more. It has also been revealed to have momentous potential as an antiangiogenic agent that only affects malignant cells and does not invade the normal cells/ tissues of the body. Moreover, various researches proved that intake of IP6 containing legumes is linked with the lessening of incidences of cancers [5, 6]. In studies, IP6 was found effectual in both pre as well as post-initiation phases of cancer and has also been known to induce differentiation and apoptosis. A number of *in-vitro* and *in-vivo* studies have shown anti-cancer properties of IP6 including skin, colon, prostate, lung, metastatic and mammary cancers [3, 7, 8]. IP6 forms tight chelates with many polyvalent and nutritionally important minerals of the body (calcium, copper, magnesium, iron etc.). It is therefore considered that IP6 diminishes the bioavailability of many of these dietary minerals and is infamous as an anti-nutrient [9]. IP6 gets very rapidly absorbed when administered intra-gastrically and gets distributed to various organs as fast as an hour following its administration [10].It thereby gets eliminated from the body without showing its potential as an antiangiogenic agent.

2.1.1. Synonyms: Phytate, IP6, Fitic acid, Inositol hexaphosphate

2.1.2. Chemical name: Phytic acid

2.1.3. Molecular formula: $C_6H_{18}O_{24}P_6$

2.1.4. Molecular weight: 660.04g/mole

2.1.5. Colour: White

2.1.6. Taste: Sour

2.1.7. Solubility: Freely soluble in water, soluble in 50% acetone, almost insoluble in anhydrous ether, chloroform and n-hexane and insoluble in oil.

2.1.8. Storage conditions: Required to be stored in a dry place and an air-tight container.

2.1.9. Chemical structure

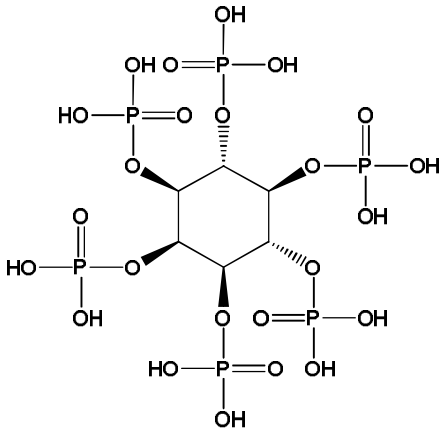

2.1.10. Stability: Highly hygroscopic in nature, thus has to be kept away from moisture. It is stable at room temperature, incompatible with strong oxidizing agents.

2.1.11. Mechanisms of action: The mechanism of action for IP6 is not completely known. A recent study stated that IP6 functions as an antioxidant by chelating divalent cations such as copper and iron, preventing the formation of reactive oxygen species, responsible for cell injury and carcinogenesis. The chelation hypothesis, however, does not completely explain IP6's antineoplastic activity. It is reasonable to conclude that, in addition to its antioxidant role, IP6 probably exerts its action via control of cell division. In a recent study, it has been shown that IP6 decreased S phase and arrested cells in the G0/G1 phase of the cell cycle. A significant decrease in the expression of proliferation markers indicated that IP6 disengaged cells from actively cycling. In addition, IP6 has been shown to enhance natural killer cell (NK-cell) activity, thereby boosting NK-cell cytotoxicity [11, 12].

2.1.12. Analytical profile of the drug

A UV-visible spectroscopy method as reported by Haug and Lantzsch, was utilized to determine the concentration of drug in pharmaceutical dosage forms and in biological samples [1].

2.1.13. Identification of drug

2.1.13.1. Melting point

The melting point of IP6 was determined using a melting point apparatus. For the

determination of melting point, the drug sample was filled in three different capillaries and the melting point determined through conventional method [13]. The melting range was recorded which begins when the sample first starts to melt and ends when the sample completely melts. It was found to be in the range of 22-25°C.

2.1.13.2. Fourier transforms infrared spectrum (FTIR) analysis

To obtain the FTIR spectrum of pure IP6, the drug was scanned in the range of 4000-600 cm^{-1} using a Nicolet 6700, Thermoscientific, spectrophotometer (shown in Figure 2.1). The FTIR spectrum of IP6 gave the characteristic peak at 3430.3 cm^{-1} which relates to OH stretching. Peaks near 1662.1 cm^{-1} were probably due to the carboxyl group and at 1061.5 cm^{-1} was allocated to the phosphate radical or hydrogen phosphate radical [14].

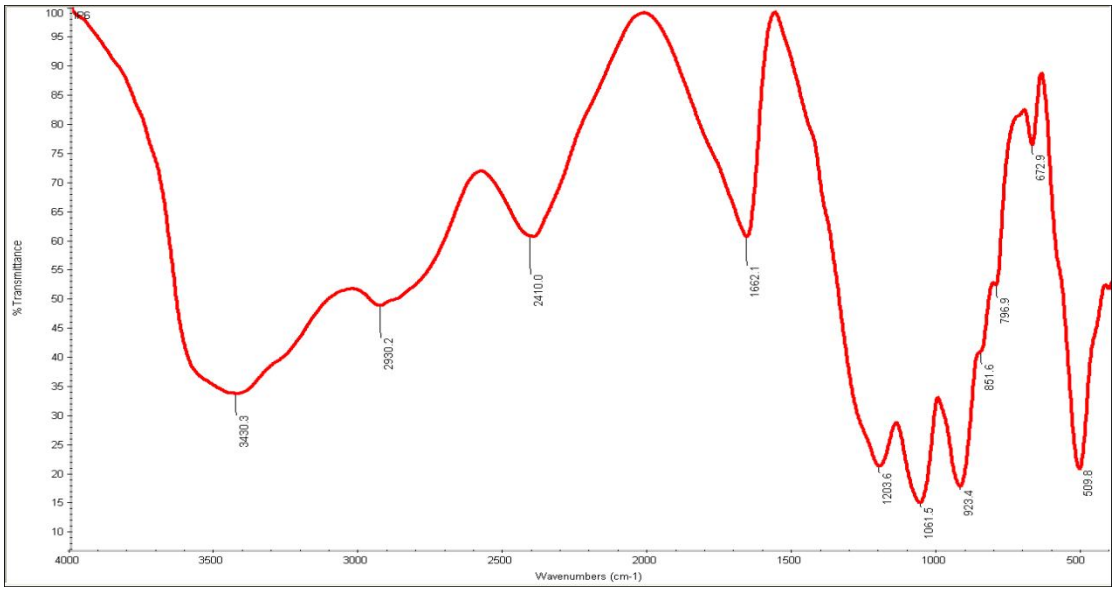

Figure 2.1 FTIR spectrum of IP6

2.1.13.3. Establishment of calibration plot of IP6 using UV- visible spectrophotometer

To accomplish the *in-vitro* drug dissolution studies, *ex-vivo* drug permeability and solubility analysis of the drug, standard plots of the pure drug were constructed by a previously established method [1, 15]. An indirect method was used for the detection of IP6. For this, the aqueous IP6 solution was heated with the ferric solution of known iron content. The decrease in iron content (determined through colorimetry with 2, 2'-bipyridine) was measured as the content of IP6. The absorbance was measured after a

while to facilitate bipyridine and iron phytate reaction, due to which colour changed with time [1].

2.1.13.3.1. Scanning and determination of maximum wavelength (λmax)

Standard solution of IP6 (100 µg/mL) was prepared and scanned in the range of 400-600 nm by using a UV-visible spectrophotometer (LT-2910, Labtronics, India) and taking distilled water as the blank solution [1]. The λmax of the drug was found to be 520 nm.

2.1.13.3.2. Preparation of calibration plot

i. **IP6 solution-** A drug stock solution (100µg/ml) was prepared with distilled water and named as the solution (i). Further, serial dilutions of concentration of 3µg/mL, 9µg/mL, 15µg/mL, 12µg/mL, 21µg/mL, 27µg/mL and 30µg/mL were prepared from above stock solution.

ii. **Ferric solution-** Ferric solution was prepared by dissolving 0.2g ammonium iron (III) sulphate.12 H_2O in 2N HCl (100 ml) and the volume was made up to 1000 ml using distilled water. This solution was named as the solution (ii).

iii. **2, 2′-Bipyridine solution-** Solution (iii) was prepared by dissolving 10g of 2,2'-bipyridine and 10 ml thioglycolic acid in distilled water and volume was made up to 1000 ml [1].

2.1.13.3.3. Procedure-

- Drug solution (0.5mL) was pipetted into different test tubes ranging from the concentration of 3 to 30µg/mL.
- Solution (ii) (1mL) was added to it and covered properly with parafilm. Tubes were heated in a boiling water bath for 30 min, by taking care for the first 5 min that the tubes remain well covered.
- Then, the tubes were cooled in ice water for 15 min and allowed to adjust to room temperature.
- Once the tubes had reached the room temperature, the content of the tubes was mixed and centrifuged for 30 min at 3000g each.
- 1 ml of the supernatant was taken out and transferred to another test tube in which 1.5 ml of solution (iii) was added.

- After that, solutions were scanned from a range of 400 to 600 nm. Scanning revealed absorbance maxima at 520 nm (Figure 2.2). This wavelength was found to be similar to the reported value [1].
- Thus absorbance was measured at 520 nm against distilled water. The experiment was repeated in triplicate.

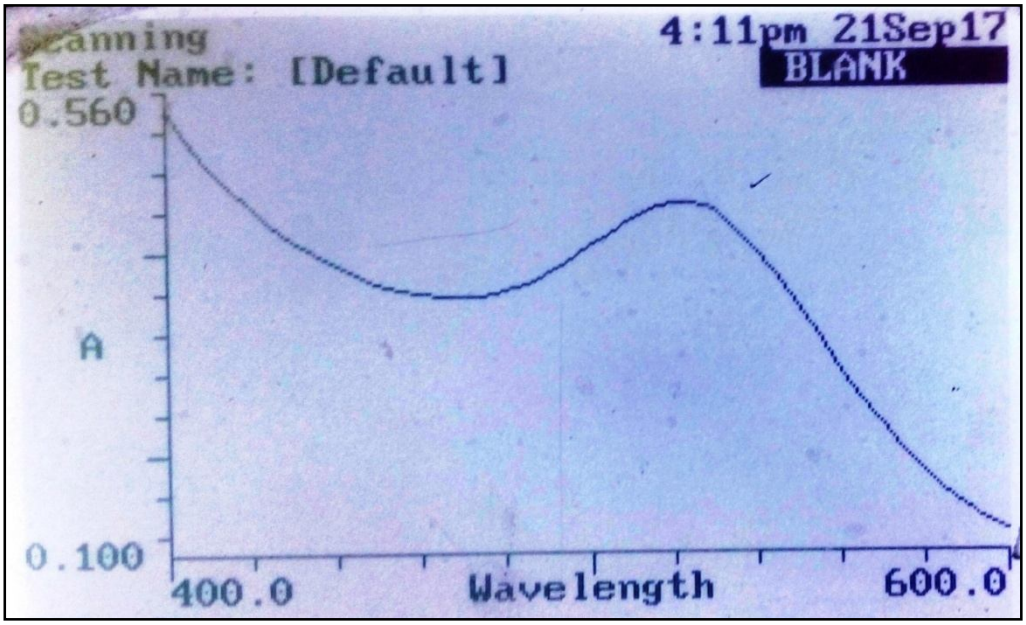

Figure 2.2 UV-visible spectra of IP6

Table 2.1 Concentration, average absorbance and regression equation for IP6

S. No.	Concentration (µg/ml)	Average absorbance (mean±SD), n=3	Regression equation
1.	3	0.970±0.02	y = -0.030x + 1.041 R^2 = 0.997
2.	9	0.740±0.09	
3.	15	0.579±0.02	
4.	21	0.392±0.02	
5.	27	0.189±0.01	
6.	33	0.040±0.00	

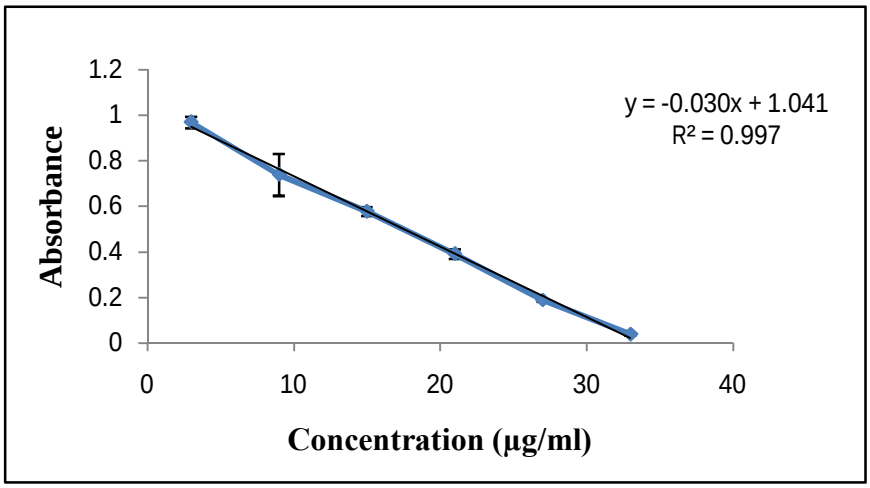

Figure 2.3 Standard curve of IP6 in methanol

2.1.14. Discussion

The results of melting point estimation as well as FTIR analysis were similar to earlier reports [14], thereby indicating the purity of the drug sample. The prepared standard curve was utilised for all subsequent estimations.

2.1.14. References

1. Haug W, Lantzsch HJ. Sensitive method for the rapid determination of phytate in cereals and cereal products. Journal of the Science of Food and Agriculture. 1983;34(12):1423-6.
2. March J, Villacampa A, Grases F. Enzymatic—spectrophotometric determination of phytic acid with phytase from Aspergillus ficuum. Analytica chimica acta. 1995;300(1-3):269-72.
3. Saad N, Esa NM, Ithnin H, Shafie NH. Optimization of optimum condition for phytic acid extraction from rice bran. African Journal of Plant Science. 2011;5(3):168-75.
4. Wang K, Liu P, Ye Y, Li J, Zhao W, Huang X. Fabrication of a novel laccase biosensor based on silica nanoparticles modified with phytic acid for sensitive detection of dopamine. Sensors and Actuators B: Chemical. 2014;197:292-9.
5. Izadi Z, Divsalar A, Saboury AA, Sawyer L. β-lactoglobulin–pectin Nanoparticle-based Oral Drug Delivery System for Potential Treatment of Colon Cancer. Chemical biology & drug design. 2016;88(2):209-16.
6. Shukla K, Raj P, Kumar A, Kumar M, Kaithwas G. Effect of monotherapy and combination therapy of pantoprazole and aprepitant in gastric esophageal reflux disease in albino rats. The Scientific World Journal. 2014;2014.
7. Pandey M, Gupta KP. Epigenetics, an early event in the modulation of gene expression by inositol hexaphosphate in ethylnitrosourea exposed mouse lungs. Nutrition and cancer. 2011;63(1):89-99.
8. Gupta KP, Singh J, Bharathi R. Suppression of DMBA-induced mouse skin tumor development by inositol hexaphosphate and its mode of action. Nutrition and cancer. 2003;46(1):66-72.

9. Shamsuddin AM. Inositol phosphates have novel anticancer function. The Journal of nutrition. 1995;125(suppl_3):725S-32S.

10. Shamsuddin AM. Metabolism and Cellular Functions of IP6. A Review. Anticancer Research. 1999;19(5):3733-6.

11. Singh RP, Agarwal C, Agarwal R. Inositol hexaphosphate inhibits growth, and induces G1 arrest and apoptotic death of prostate carcinoma DU145 cells: modulation of CDKI-CDK-cyclin and pRb-related protein-E2F complexes. Carcinogenesis. 2003;24(3):555-63.

12. Baten A, Ullah A, Tomazic VJ, Shamsuddin AM. Inositol-phosphate-induced enhancement of natural killer cell activity correlates with tumor suppression. Carcinogenesis. 1989;10(9):1595-8.

13. Deman J, Deman L, Blackman B. Melting-point determination of fat products. Journal of the American Oil Chemists' Society. 1983;60(1):91-4.

14. Daneluti ALM, Matos JdR. Studies of thermal behavior of phytic acid. Brazilian Journal of Pharmaceutical Sciences. 2013;49(2):275-83.

15. Abdelbary AA, AbouGhaly MH. Design and optimization of topical methotrexate loaded niosomes for enhanced management of psoriasis: application of Box–Behnken design, in-vitro evaluation and in-vivo skin deposition studies. International journal of pharmaceutics. 2015;485(1-2):235-43.

Chapter 3

Optimization, preparation and characterization of inositol hexaphosphate loaded niosomal gel for the topical application intended for skin cancer prevention

Experimental

The entire work has been divided into two parts. Two formulations were developed and characterized maintaining a common thread of inositol hexaphosphate (IP6) loaded novel drug delivery system against cancer. The first part includes the optimization, preparation and characterization of IP6 loaded niosomal gel for the topical application intended for skin cancer prevention. The second part discusses the preparation and evaluation of pectin encrusted gold nanocomposites containing IP6 and jacalin, for oral delivery to target colon cancer.

3. Optimization, preparation and characterization of IP6 loaded niosomal gel for the topical application intended for skin cancer prevention

3.1. Background

Cancer is a life-threatening disease globally [1]. About 3-8% rise in skin cancer has been recorded every year [2]. People rely on natural medicines as first-line treatment, because of their perception of availability, safety and general acceptance for cancer prevention/ treatment [3, 4].

IP6 is a natural constituent of grains, legumes and cereal products [5, 6]. It has been found to have considerable potential as an agent that only affects malignant cells and does not affect normal cells/ tissues of the body. Numerous studies have proved the chemopreventive and anti-cancer properties of IP6 in the skin, colon, lung, prostate and mammary cancers [7-9]. IP6 is also available in the form of capsules and dietary powder. Metallic nanoparticle-based IP6 micelles have been reported to improve its stability [10]. IP6 considered as an anti-nutrient as it forms tight chelates with polyvalent and nutritionally important minerals (like calcium, magnesium, iron and copper) thereby leading its fast elimination.

IP6, when administered orally, gets distributed to various organs within an hour of administration. Administration through the topical route also leads to its chelation and fast elimination [11, 12].

Recently niosomes have received much attention as a prospective drug delivery system. When compared with liposomes, niosomes provide higher chemical and physical stability with low cost and greater availability of surfactants. Furthermore, niosomes show

improved residence time of drugs in the epidermis thereby reducing the systemic absorption [13, 14].

Besides having a great potential as an antiangiogenic agent, IP6 is underutilized because of its rapid absorption and excretion. This demanded development of a delivery system that can control its biotransformation. Thus, the central endeavour of the present work was to develop and evaluate a niosomal delivery system containing IP6 for deterrence of preneoplastic skin damage.

3.2. Materials

Table 3.1 List of various chemicals utilized during formulation studies

Materials	**Source**
Acetone	ThermoFischer Scientific (Qualigens)
Ammonium iron (III) sulphate.12 H_2O	Sigma Co. (St. Louis, MO, USA)
Antibodies	Santa Cruz , USA
Calcium chloride	HiMedia Laboratories Pvt.Ltd. Mumbai, India
Cholesterol	HiMedia Laboratories Pvt.Ltd. Mumbai, India
Dicetyl phosphate (DCP)	S.D. Fine chemicals Ltd., Mumbai, India
DMBA	Sigma Co. (St. Louis, MO, USA)
dNTPs	Bangalore Genei (India)
Ethanol	S.D. Fine chemicals Ltd., Mumbai, India
Fetal bovine serum	Sigma Co. (St. Louis, MO, USA)
Hydroxy quinone	Sigma Co. (St. Louis, MO, USA)
IP6	Sigma Co. (St. Louis, MO, USA)
Isopropyl alcohol	ThermoFischer Scientific (Qualigens)
Magnesium chloride	HiMedia Laboratories Pvt.Ltd.Mumbai, India
[Methyl-^{3}H] S-adenosyl methionine	AmershamBiosciences-GE Healthcare (USA)
MTT (3-(4,5-Dimethylthiazol-2-Yl)-2,5-Diphenyltetrazolium Bromide)	Sigma Co. (St. Louis, MO, USA)
PCR primers	Bangalore Genei (India)

Materials	**Source**
Potassium chloride	HiMedia Laboratories Pvt.Ltd. Mumbai, India
RNase	Sigma Co. (St. Louis, MO, USA)
RT-PCR kit	Bangalore Genei (India)
Sodium chloride	HiMedia Laboratories Pvt.Ltd. Mumbai, India
Sodium hydroxide	SDFCL Pvt. Ltd., Mumbai, India
Sodium metabisulfite	Sigma Co. (St. Louis, MO, USA)
Span 80	HiMedia Laboratories Pvt.Ltd. Mumbai, India
Taq DNA polymerase	Bangalore Genei (India)
Thioglycollic acid	Merckmillipore
2,2'-bipyridine	Abcam

3.3. Experimental design

A 2^3 (two-level, three-factor) full factorial experimental design (using Design Expert® software) was utilized for statistical optimization of the formulation variables, which was implemented in the preparation of IP6 niosomes. This statistical optimization was performed in order to get higher encapsulation efficiency and optimum vesicle size. A total of nine experiments were run. For the purpose, three independent variables and two dependent variables were taken. The compositions, used for the preparation of IP6 loaded niosomes prepared according to 2^3 full factorial design is shown in Table 3.2.

Table 3.2 Factorial design for optimization of IP6 loaded niosomes

Factors (independent variables)	**Levels**	
	Low	**High**
X1- Cholesterol: surfactant ratio (molar ratio)	1:1	1:2.5
X2- Sonication time (minute)	1	2
X3- DCP (µM)	0	5
Responses (dependent variables)	**Constraints**	
Y1- Particle size (nm)	Optimum	
Y2- Encapsulation efficiency (%)	Maximize	

3.4. Preparation and characterizations of IP6 loaded niosomes

Unilamellar niosomal vesicles were prepared from surfactant, cholesterol and dicetylphosphate (DCP), according to the following technique. Accurately weighed amounts of cholesterol and Span 80 in different molar ratios, as shown in Table 3.2, was taken in a round-bottomed flask and were dissolved in 10 ml of chloroform. DCP was added as a negative charge inducing agent, in requisite batches. A rotary evaporator (IKA® Rotavapor, Bangalore, India) was used to evaporate chloroform at 45°C and 120 rpm under reduced pressure to form a thin film. The formed thin film was then hydrated with 5 ml of aqueous drug solution, at 45°C and 120 rpm. The dispersion was sonicated for a minute at 80% energy using probe-type sonicator (Labsonic®-M, Sartorius Stedium) and set aside at 4ºC for 24 h, for maturation [15, 16].

3.5. Particle size and size distribution

Particle size and polydispersity index (PDI) of IP6 loaded niosomes was determined with the help of dynamic light scattering (DLS) using Malvern Zetasizer Nano ZS (Malvern Instruments, UK) at 25ºC by assessment of autocorrelation function at 90°C. The experiment was performed in triplicate [15].

3.6. Encapsulation efficiency

The percentage encapsulation efficiency of IP6 in niosomes was determined indirectly, by ultra-centrifuging 2 ml of niosomal suspension at 16,700 rpm for 60 min by using a cooling centrifuge (REMI CPR-24, Mumbai, India) at 4°C in order to separate free drug from niosomes. The supernatant (0.5 ml) was then taken to estimate non-encapsulated drug via UV-visible spectroscopy at 520 nm. The percent drug encapsulated was calculated through the subsequent equation [5, 17].

$$\%\ \text{Drug encapsulation efficiency} = \frac{\text{Initial amount} - \text{Observed amount}}{\text{Initial amount of drug}} \text{X } 100 \qquad \text{Equation-1}$$

3.7. Zeta potential measurement

Zeta potential of the niosomal formulation containing IP6 was measured by using Malvern Zetasizer Nano ZS. It was determined by assessing the electrophoretic mobility of niosomes in a U type tube, at a temperature of 25°C [18].

3.8. *In-vitro* drug release studies

In-vitro drug release of IP6 from niosomes was determined via pre-treated dialysis bag (Himedia dialysis membrane, 12,000-14,000 molecular weight cut-off). One end of the bag was sealed with closure clip, 2 ml volume of niosomal suspension was filled into it and sealed with another clip. Thus prepared dialysis bag was placed in 50 ml of PBS (pH 6.8), which acted as a receptor medium, at the temperature of 37±2°C and continuously stirred at 100 rpm. At the definite time intervals, 0.5 ml of dialysate was withdrawn and measured spectrophotometrically, sink conditions were maintained throughout [15, 16].

3.9. Morphological evaluation of niosomes

Shape and morphology of prepared niosomes were examined by optical microscopy, scanning electron microscopy (SEM) and transmission electron microscopy (TEM). For microscopy, the sample was stratified over the glass slide, mounted with the coverslip and observed under an optical microscope at 100X using immersion oil. The sample for SEM was layered over micro coverslip, air dried and sputter coated with Au/Pd. Thus, prepared samples were observed under a Jeol (JSM- 6490LV), Japan, electron microscope at 10kV accelerating voltage and 100X magnifications. The hydrated niosomes was examined using TEM. A drop of previously diluted suspension was laminated over a 400-mesh copper grid, which was left to adhere on carbon substrate for about 1 min. Excess of the suspension was removed by filter paper. The sample was then air-dried and evaluated under instrument (H- 7500, Hitachi Made, Japan) at 100 kV accelerating voltage and 20000 magnifications [16, 19].

3.10. Stability studies of IP6 containing niosomes

The optimized batch was tested for stability as per International Conference on Harmonisation (ICH) guidelines. The rationale of stability testing is to corroborate the properties of formulation changes with respect to time and varying conditions of temperature and humidity [20]. Stability studies were carried out by assessing the capability of niosomes to retain the desired properties. The formulation was kept for analysis at room temperature condition *viz.* 30°C±2°C/ 60%±5% RH. Samples were analyzed at 15^{th}, 30^{th}, 60^{th}, 90^{th}, 120^{th} and 180^{th} day and were tested for particle size, PDI, zeta potential and percent encapsulation efficiency [21].

3.11. Preparation and characterization of IP6 loaded niosomal suspension

3.11.1. Preparation of different phases

Oil phase (Phase A) was prepared by using light liquid paraffin (5% w/w), which was used as blending base and isopropyl myristate (2.5% w/w), as an emollient/ lubricant. These two were taken together in a beaker and heated up to 80°C over a hot plate with gentle mixing, until a clear solution was obtained. To this clear solution, ethylene glycol monostearate (1% w/w) was used as a pearlising agent and myristyl myristate (1% w/w) as an emollient/ skin conditioner was added one by one with stirring, to obtain a clear solution. Phase B (aqueous phase) was prepared by taking water (q.s.) and disodium EDTA (0.05% w/w) as a co-preservative and heated up to 80°C with continuous stirring. Carbopol 934 (1% w/w) was added to above solution with high-speed stirring (1000-1500 rpm) till a uniform dispersion was obtained. Phase C was prepared by taking propylene glycol (2% w/w) used as humectants/ plasticizer, methylparaben (0.2% w/w) (water-soluble preservative) and propylparaben (0.3% w/w) (oil soluble preservative) and mixing all together gently with slow heating. Glycerin (3% w/w) was also added to act as humectant, plasticiser and was mixed well.

3.11.2. Emulsification

When both oily and aqueous phases (phase A and B) were heated separately till 80^{o}C, the oil phase was added slowly to the aqueous phase with high stirring (1500 to 2000 rpm) and stirring was continued for 5 min of complete addition. After a while stirring speed was stepped down to 500-1000 rpm and continued for 10 min. Thus formed emulsion was allowed to cool to room temperature and phase C was added with slow stirring. The emulsion was neutralized with triethanolamine to adjust the pH to the range of 6.5 to 7. To the above suspension, IP6 and niosomal formulation loaded with IP6 was dispersed, as required and kept for further evaluation [15].

3.11.3. Determination of pH

The pH of the niosomal suspension was determined via the previously described method, by using digital pH meter, NIG-333 (Naina Solar Limited, New Delhi, India). Measurements were carried out in triplicate [22].

3.11.4. Determination of viscosity

A Brookfield digital viscometer (Labtronics, model LT-730, India) with spindle no.3 at 60 rpm was used to determine the viscosity in cps of the suspension formulation, in triplicate. The experiment was performed at room temperature [15, 22].

3.11.5. Texture analysis

Texture analysis of niosomal suspension was done using CT3 Texture Analyzer, Brookfield Engineering Laboratories, USA. Firmness, spreadability and extrudability altogether deals with texture profile of formulations. For estimation of firmness, TA-10 probes, fixture TA-BT-KI, with a hold time of 2 sec and trigger load 5 gm were used. Male and female cone probe with trigger load 2 gm and TA DEC (dual extrusion cell) were utilized for estimation of spreadability and extrudability. All other instrumental settings of equipment were done according to suggested stipulations [22, 23].

3.11.6. *Ex-vivo* skin permeation studies

Ex-vivo skin permeation of IP6 from niosomal suspension was estimated using full thickness abdominal skin which was extracted from Swiss albino mice of 12-15 g of body weight. The surface area of release membrane was taken as 2 cm^2. Assembly was prepared such that, receptor compartment had a volume of 25 ml phosphate buffer saline (PBS) of pH 6.8 with continuous stirring and was thermostated at a temperature of 37±1°C throughout the experiment. Specified amount (equivalent to 5mg of IP6) of the niosomal suspension was applied evenly on the epidermal side of the skin and covered with aluminium foil in order to prevent its drying out. At predetermined time intervals, aliquots of 0.5 ml were withdrawn and replaced by the equal volume of PBS maintaining sink condition throughout the experiment. After 24 h of the experiment, the skin front was rinsed twice with 0.5 ml of double distilled water. The withdrawn aliquots and washing solutions were examined for content of IP6 by UV- visible spectrophotometery. The steady-state flux (Jss) of IP6 was obtained from the slope by plotting the cumulative amount of drug permeated (µg) versus time (h) using linear regression analysis [24, 25]. The permeability coefficient (Kp) of the IP6 through the mice membrane was calculated using the subsequent formula, i.e. Kp = Jss.H/C.

Where, H is membrane thickness and C is the initial concentration of IP6 applied.

3.11.7. Irritation test: Hen's Egg Test on the Chorioallantoic Membrane (HET-CAM)

A modified HET-CAM test was done to estimate the irritation tolerability of prepared niosomal formulation loaded with IP6. Briefly, fertilized eggs of white leghorn hens were procured from a poultry farm, kept for incubation at a temperature of 37±0.5°C and rotated slowly with care at every 12 h, ensuring that the air sac is upright. Eggs albumin (3ml) was taken out from the pointed end of the eggs, on the third day of the experiment using sterile technique. Three eggs were utilized for each formulation within the weight range of 50 to 60 g and candling was done to remove the flawed eggs. The openings of eggs were instantaneously sealed by using parafilm (American Can Company, Neenah, Wisconsin) with the help of a heated spatula. Then the eggs were kept in an equatorial arrangement, allowing the development of chorioallantoic membrane (CAM) at some distance from the eggshell. When the CAM developed completely, at the tenth day of the experiment, a casement (2 × 2 cm^2) was made on eggs' equator and 0.5 ml of test formulations instilled over CAM surface through the casement. This was left for about 20 sec and then rinsed with 5 ml of warm saline. After that, the membrane was examined for the vascular wrecks and the time consumed for haemorrhagic damage and coagulation was documented for up to 300 sec. NaCl solution (0.9% w/v) was used as the control, which has already been reported to be practically non-irritant. The scores were calculated by subsequent formula and were analyzed in accordance with the scoring schemes as revealed in Table 3.3, [26].

$$\text{Scores} = \left[\frac{(301-\text{H})}{300}\right] \times 5 + \left[\frac{(301-\text{L})}{300}\right] \times 7 + \left[\frac{(301-\text{C})}{300}\right] \times 9 \qquad \text{Equation-2}$$

where, H= Haemorrhage time (sec), L= Lysis time (sec), C= Coagulation time (sec)

Table 3.3 Scoring chart for HET-CAM test

Scores range	Inference
0-0.9	Non-irritant or practically none
1-4.9	Weak or slight irritation
5-8.9 or 5-9.9	Moderate irritation
9-21 or 10-21	Strong or severe irritation

3.11.8. *In-vitro* cytotoxicity against human cancer cell lines

Anti-cell-apoptotic activity of IP6 loaded niosomal suspension and pure IP6 were determined by sulforhodamine-B (SRB) assay using SK-MEL-2, a human melanoma cell line. The test samples were diluted using Dulbecco's modified eagle medium (DMEM) and supplemented with 2% inactivated fetal bovine serum to obtain the required concentration of the stock solution and then filtered and centrifuged. Serial dilutions from the range 0.5 to 2 mM were prepared from the above stock solution. The cell suspension which was used had a density of approximately 10,000 cells/ 0.1 ml, instilled in a 96-well plate and kept for 24 h for incubation. After incubation, different concentrations of test samples (100 µl) were added to the wells and allowed for incubation for 72 h at 37°C. Cells were then fixed at the bottom of the wells with cold trichloroacetic acid (TCA) at 4°C for 1 h, and then rinsed with distilled water and air dried. Thereafter, 50 µl of each SRB solution was added to wells and allowed for staining, for 30 min. The plate was washed with 1 % v/v acetic acid to remove unused dye and air dried. Further, the plate was shaken gently for 5 min after addition of 100 µl of Tris buffer (pH 10.5;10 mM). The optical density (OD) was measured by using a microplate reader. Percent growth inhibition caused by pure IP6 and IP6 loaded formulation was calculated by using the following equation. Inhibitory concentration 50 (IC50) values were calculated by linear regression [27].

$$\%\ \text{Growth inhibition} = 100 - \left[\frac{\text{OD (test)} - \text{OD (blank)}}{\text{OD (control)} - \text{OD (blank)}}\right] * 100 \qquad \text{Equation-3}$$

3.12. *In-vivo* studies

Female Swiss albino mice were procured from the in-house animal breeding colony of CSIR-IITR, Lucknow. Animals were fed with synthetic pellet diet and water *ad libitum*. The experimental studies were approved by the Institutional Animal Ethics committee of Indian Institute of Toxicology Research, Lucknow (IAEC approval IITR/IAEC/04/2015). All the animals were kept in polypropylene cages, in a well-ventilated animal house maintaining photoperiodic conditions at the temperature of 22°C±2°C. Animals were handled as per norms of IAEC and care was taken to follow all the guidelines with a humane approach.

3.12.1. Treatment schedule for animals

All animals were divided into 6 groups, containing 12 animals each, Table 3.4. Two days prior to the experiment, the dorsal side of mice skin was shaved at an area of 2 cm^2 with the help of an electric clipper in interscapular region. DMBA (0.005µg/kg) dissolved in 100µL of acetone was applied topically on the shaved back of animals. All other treatments were also given similarly subsequent to DMBA application. After that, animals were sacrificed at 4^{th}, 8^{th}, 16^{th} and 24^{th} h of treatments. Animals were euthanized by cervical dislocation and skins were extracted, snap frozen in liquid nitrogen and stored at -80°C, till further use [27].

Table 3.4 Treatment details for animals

Groups	**Treatment**
Group I (Negative control)	Placebo (plain suspension) formulation
Group II (Toxic control)	DMBA+ placebo formulation
Group III (Standard)	DMBA+IP6(5mg) in acetone
Group IV (Test 1)	DMBA+F1:Dose1 (5mg IP6, niosomal formulation)
Group V (Test 2)	DMBA+F1:Dose2 (3mg IP6, niosomal formulation)
Group VI (Test 3)	DMBA+F2 (5mg IP6 dispersed in suspension)

3.12.2. SDS- PAGE and western blotting

Epidermal tissues were extracted using a freeze-thaw method and were quantified with the help of Bradford protein assay technique. A 10% of epidermal tissue lysate was prepared for protein analysis by using 20 mM Tris buffer (pH 7.5) which contained sucrose (250 mM), $MgCl_2$ (2 mM), Tris-HCl (20mM), EGTA (0.5 mM), EDTA (2 mM), DTT (100 mM), PMSF (100 mM), Na_3VO_4 (30 mM) and protease inhibitor cocktail. The tissue lysate equivalent to 50 µg protein was resolved using SDS-PAGE of 10% gel. Segregated proteins were assigned to the methanol soaked PVDF membrane and probed with ODC, PCNA, cyclin D1 and COX-2 primary antibodies followed by the horseradish peroxidase-conjugated apt secondary antibodies. Antibody binding signals were examined by Chemiluminescence HRP detection system using a Versa Doc and band

strength was estimated by Syngene gene tool. PVDF membranes were stripped by making use of stripping buffer of pH 6.8 and then reprobed with β-actin antibody [28].

3.12.3. Reverse transcription polymerase chain reaction (RT-PCR)

Skin tissue samples from each group were assessed for their mRNA content by using RT-PCR. Total RNA was extorted through Trizol reagent in accordance with the manufacturer's stipulations and DNA contaminations were segregated using DNaseI treatment. c-DNA was produced from total RNA by taking 2ng RNA equivalent volume by utilizing the c-DNA preparation kit. Synthesized c-DNA was used for quantification of particular mRNA by mouse-specific primers, mentioned in Table 3.5. A 20 µl of reaction mixture restrained 100 ng of c-DNA, 1.5 mM of $MgCl_2$, 10 pM each primer, 1.5 mM of dNTPs and 1 unit Ampli Taq DNA polymerase enzyme. Thus produced product was then augmented by thermal cycles (denaturation at 95 °C for 5 min, 95 °C for 60 sec, annealing temperature for 60 sec and at 72 °C for 60 sec) × 35 subsequently final extensions of 72°C for 4 min. Thus obtained PCR products were resolved and visualized by using 1.5% of the agarose gel containing ethidium bromide. Quantifications were performed with the use of gene tool Syngene software [28].

Table 3.5 Nucleotide sequences and product size used for RNA analysis by RT-PCR

Gene	**Sequence**	**Product size (bp)**	***T*m (◦C)**
ODC	F 5'-TGGAGTGAGAATCATAGCTG-3' R 5'-TTGGCCTCTGGAACCCATTG-3'	410	58
PCNA	F 5'- GAAGCACCAAATCAAGAGAA -3' R 5'- TCACCCCATTCTTTGCACAG -3'	193	55
COX-2	F 5'-GTGGAAAAACCTCGTCCAGA-3' R 5'-TGATGGTGGCTGTTTTGGTA-3'	256	60
Cyclin D1	F 5′-TGTTCGTGGCCTCTAAGATGAAG-3′ R 5′-AGGTTCCACTTGAGCTTGTTCAC-3′	136	60
β-Actin	F 5′-TGTGATTGGTGGGAATGGGTCAG-3′ R 5′-TTTGATGTCACGCACGATTTCC-3′	514	60

3.12.4. Histopathology

Skin tissues, extracted from mice were stored in 10% buffered formalin for histopathological analysis. The skin tissues were usually processed, fixed with paraffin

wax and were sectioned (3-5 µm) with the use of rotary Microtome. Obtained sections were unflustered over a glass slide where it was deparaffinized and stained with hematoxylin and eosin dye. These sections were then observed under the microscope at 40X.

3.12.5. Statistical analysis

All the data of studies were subjected to statistical analysis using one-way ANOVA following Student-Newman-Keuls tests for the post hoc analysis. Values are mentioned as mean±SE, n=3. Significance was determined in the terms of 'p' values, where 'p' value of <0.05 was taken as statistically significant.

3.13. Results

3.13.1. Particle size and size distribution

As mentioned in Table 3.6 and shown by Design Expert® software, the range of particle size observed was from 268.9±3.8 nm to 965.5±5.2 nm and the PDI value ranged from 0.212±0.18 to 0.431±0.15. The contour plot, Figure 3.1(a) revealed that independent variables showed different effects on particle size.

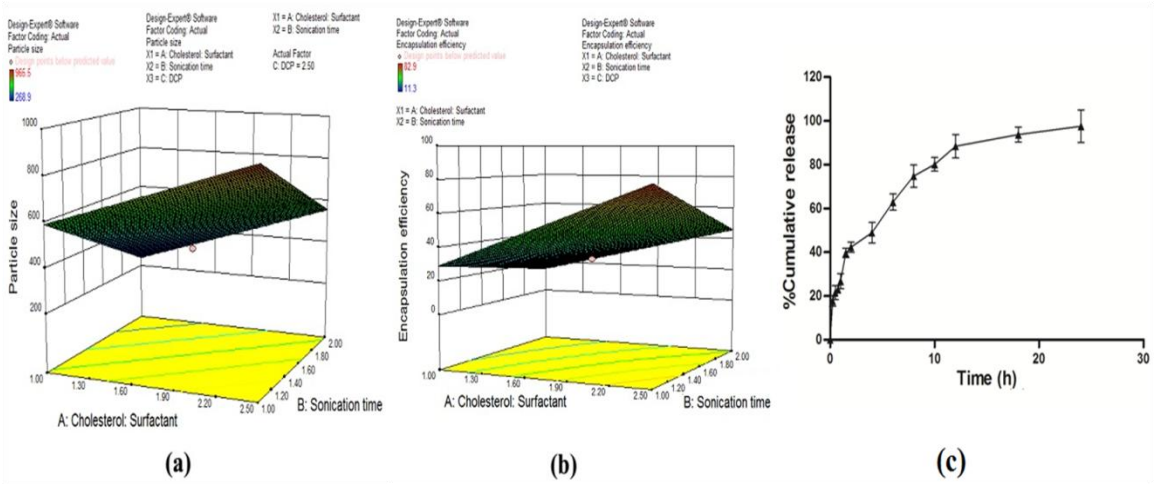

Figure 3.1 (a) Response 3D plot, effect of cholesterol: surfactant molar ratio, sonication time and DCP conc. on particle size, (b) response 3D plot, effect of cholesterol: surfactant molar ratio, sonication time and DCP conc. on encapsulation efficiency and (c) percent of IP6 released as a function of time (h) from IP6 loaded niosomes of optimized batch NIO6.

Table 3.6 Encapsulation efficiency, particle size, polydispersity index and zeta potential values of IP6 loaded niosomes (n=3)

Run	Encapsulation efficiency (%±SD)	Particle size (nm±SD)	PDI (values±SD)	Zeta potential (values±SD)
NIO1	28.5±5.3	589.2±48.3	0.219±0.04	-6±0.21
NIO2	79.2±6.2	942.8±71.2	0.412±0.17	-7±0.13
NIO3	11.3±2.9	268.9±35.8	0.268±0.07	-6±0.11
NIO4	46.9±3.9	532.6±43.3	0.321±0.09	-8±0.14
NIO5	32.7±3.4	576.2±57.6	0.318±0.12	-31±0.23
NIO6	82.9±2.6	965.5±65.2	0.386±0.08	-36±0.36
NIO7	21.4±8.9	302.0±47.3	0.431±0.05	-30±0.23
NIO8	48.3±5.1	563.3±54.2	0.298±0.03	-29±0.31
NIO9	29.8±2.9	428.2±53.5	0.212±0.08	-18±0.39

3.13.2. Encapsulation efficiency

As displayed in Table 3.6 and estimated by Design Expert® software, IP6 was efficiently incorporated into niosomal vesicles with encapsulation efficiency ranging from 11.3±2.9 to 82.9±2.6%. ANOVA test suggested that the DCP concentration found insignificant in affecting encapsulation efficiency. On the contrary, cholesterol: surfactant ratio and sonication time showed a vital effect, Figure 3.1(b).

3.13.3. Zeta potential measurement

Zeta potential of niosomes are shown in Table 3.6. Batches which did not contain DCP revealed lower values and those which contained it, displayed higher values of charge.

3.13.4. *In-vitro* drug release studies and release kinetics

The *in-vitro* drug release of NIO6, optimized formulation, at end of 24 h was found to be 97.61±1.39, Figure 3.1(c). The release kinetics of NIO6 was best explained by Higuchi's equation, as the plot showed the maximum linearity (R^2= 0.9627) and followed zero order (R^2 = 0.8107) kinetics, Table 3.7.

Table 3.7 *In-vitro* drug release studies

Batch	Zero order		First order		Higuchi		Korsmeyer Peppas	
NIO6	K	R_2	K	R_2	K	R_2	N	R_2
	3.8564	0.8107	0.0425	0.3764	20.901	0.9627	0.546	0.438

3.13.5. Morphology of niosomes

To observe the morphology of niosomes, various microscopic studies of the optimized formulation were performed. They were found to be homogeneous and spherical in shape as shown, Figure 3.2.

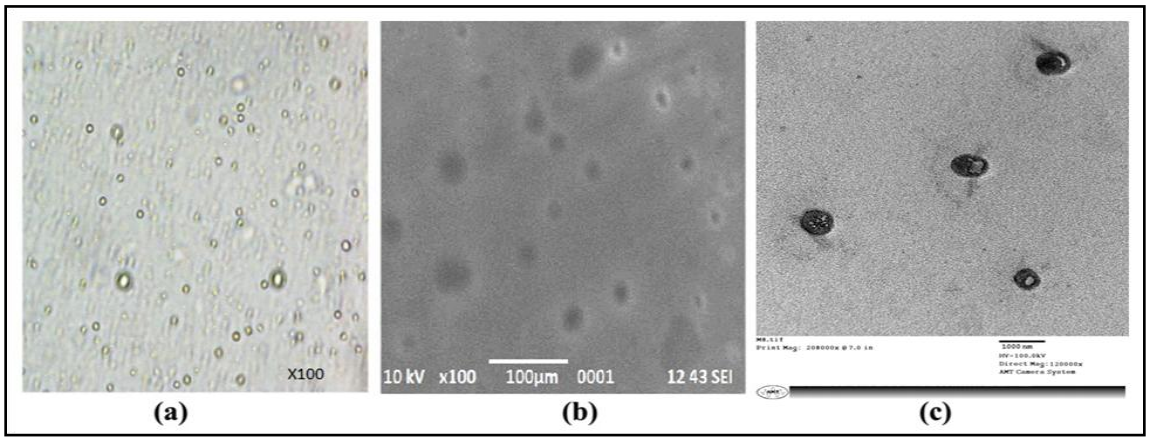

Figure 3.2 Morphological evaluation of optimized niosome batch (NIO6): (a) optical microscopy image (b) SEM image and (c) TEM image

3.13.6. Stability studies of IP6 loaded niosomes

Optimized formulation of IP6 loaded niosomes was kept for stability testing at aforesaid conditions. Results of stability studies showed that prepared niosomal formulation was stable up to 180 days at room temperature (Table 3.8). All the parameters were found to be stable during the analysis. None of the samples showed significant degradation on storage at the condition of 30°C±2°C/ 60%±5%. Thus, shelf-life of prepared formulation is estimated to be high.

Table 3.8 Effect of storage on particle size, PDI, zeta potential and encapsulation efficiency (n=3)

Days interval	Particle size (nm±SD)	PDI (values±SD)	Zeta potential (values±SD)	Encapsulation efficiency (%±SD)
Initial	965.5±65.2	0.386±0.08	-36±0.28	82.9±2.6
15th day	966.3±71.2	0.312±0.02	-36±0.31	81.2±3.8
30th day	972.3±63.2	0.319±0.03	-35±0.42	81.3±3.6
60th day	979.0±76.3	0.421±0.08	-35±0.52	80.0±4.8
90th day	983.5±87.4	0.376±0.07	-34±0.35	78.3±2.8
120th day	988.0±75.7	0.436±0.07	-32±0.38	78.1±4.3
180th day	990.3±82.3	0.348±0.08	-32±0.56	76.0±3.6

3.13.7. Suspension characterization

On visual inspection, the developed niosomal suspension revealed good homogeneity. pH of the suspension was found to be 6.9±0.002 and its viscosity was seen to be 9650±50.0 cp with spindle number 3. An innovative instrumental technique was utilized to imitate human sensorial perception by using various texture constraints including spreadability, firmness and extrudability. Firmness was found to be 19 g. The spreadability value was found to be 1.5 mJ. The work done to extrude the sample from a packaging tube uniformly is its extrudability and it was found to be 55.6 mJ. *Ex-vivo* skin permeation studies were done with Swiss albino mice skin in which niosomal and plain IP6 suspensions were compared, Table 3.9. Observation detailed that none/ negligible quantity of IP6 was left unabsorbed on the skin surface after 24 h, in the case of both, plain IP6 suspension as well as niosomal suspension of IP6.

Table 3.9 Cumulative amount permeated, flux and permeability coefficient of IP6 across excised mice skin, n=3.

Formulation	Cumulative amount permeated (µg/cm^2)	Flux (µg/cm^2/h)	Permeability coefficient (cm^2/h)*10^3
IP6 Plain Suspension	3791.5±176.3	148.6±9.2	297.2±18.3
IP6 Niosomal Suspension	448.5±25.1	11.6±1.1	23.2±2.3

3.13.8. Irritation test: HET-CAM

A HET-CAM (Figure 3.3) study is a quick, insightful and economical test to examine the skin irritancy of the formulations. CAM of chick embryo involves complete tissue with veins, arteries and capillaries which responds to injury with the intact inflammatory process. The irritation score was observed to be in the range of 0 to 0.42±0.03.

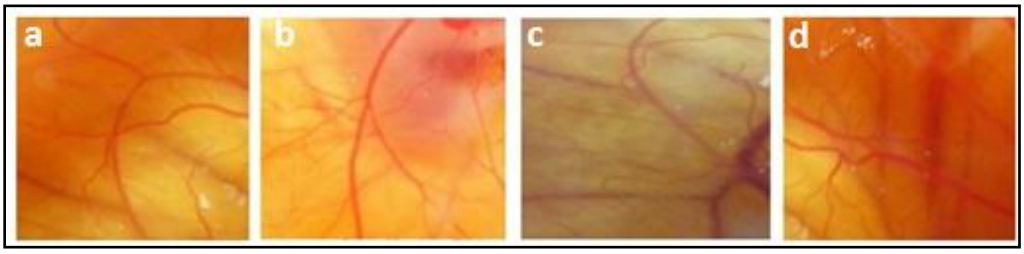

Figure 3.3 HET-CAM images (a) normal saline, (b) niosomal suspension of IP6 (Dose 1), (c) niosomal suspension of IP6 (Dose 2), (d) IP6 in suspension

3.13.9. *In-vitro* cytotoxicity studies

The cell proliferation or apoptosis studies displayed significant changes in the tested cell lines and lead to inhibition of cell proliferation and apoptosis after the application of the niosomal formulation. Cells of SK-MEL-2 cell lines were examined with photomicrographs and revealed that after the treatment with the formulation, cells were scattered with minimal attachment and pigmentation, as displayed in Figure 3.4. IP6 pure displayed IC50 value at the concentration of 1.39 mM , whereas niosomal suspension displayed a value of 0.96 mM, i.e., niosomal suspension loaded with IP6 was significantly ($p<0.05$) more effective than pure IP6.

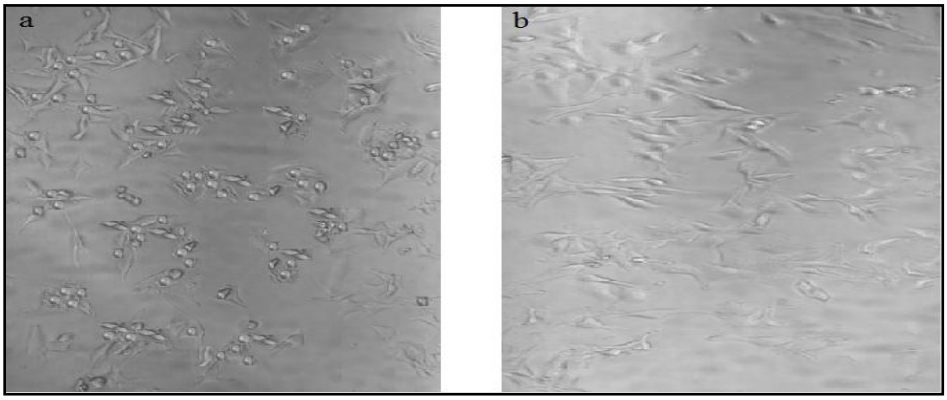

Figure 3.4 Cell line SK-MEL-2 (a) before niosomal suspension application (b) after niosomal suspension application

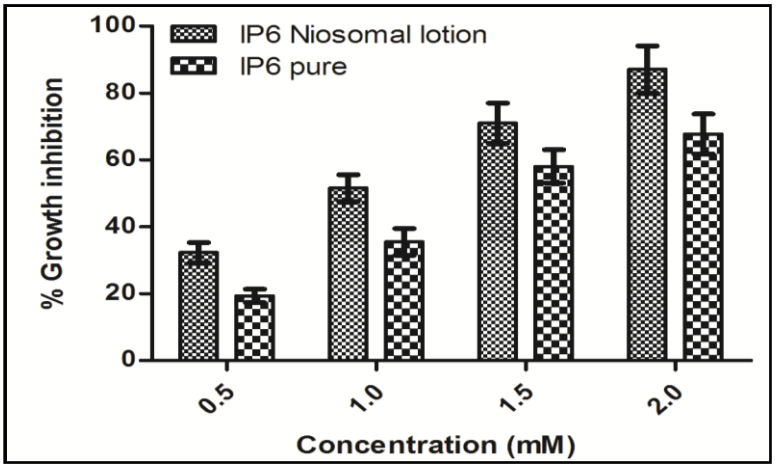

Figure 3.5 *In-vitro* percent cell growth inhibition of SK-MEL-2 human cancer cell-lines by IP6 in niosomal suspension and pure IP6 against control (normal saline) through SRB assay (n=3)

3.13.10. *In-vivo* studies

3.13.10.1. *To evaluate the effects of IP6 formulations on DMBA altered ODC, PCNA, COX-2 and cyclin D1 expression*

To explicate the effect of formulations on DMBA induced changes in the expression of ODC, PCNA, COX-2 and cyclin D1, mice skin was treated different IP6 formulations. Expressions of aforesaid genes were quantified by western blot and RT-PCR for protein and m-RNA levels respectively. All the comparisons were made with respect to negative control and it was taken as the baseline, with no up or down-regulation.

Table 3.10 Effects of IP6 and formulations on DMBA altered ODC expression

ODC	4th hour		8th hour		16th hour		24th hour	
	Western blot (%)	RT-PCR (%)	Western blot (%)	RT-PCR (%)	Western blot (%)	RT-PCR (%)	Western blot (%)	RT-PCR (%)
Group I	0	0	0	0	0	0	0	0
Group II	45	45	61	57	196	194	110	108
Group III	1	0	4	3	31	29	55	52
Group IV	34	31	7	4	3	0	0	0
Group V	32	29	18	15	7	5	13	13
Group VI	10	9	14	12	21	19	35	35

Table 3.11 Effects of IP6 and formulations on DMBA altered PCNA expression

PCNA	4th hour		8th hour		16th hour		24th hour	
	Western blot (%)	RT-PCR (%)	Western blot (%)	RT-PCR (%)	Western blot (%)	RT-PCR (%)	Western blot (%)	RT-PCR (%)
Group I	0	0	0	0	0	0	0	0
Group II	50	49	71	71	202	201	122	119
Group III	4	4	4	4	34	32	64	59
Group IV	39	38	11	11	4	4	2	1
Group V	38	37	22	22	10	9	19	14
Group VI	13	11	18	16	23	22	35	29

Table 3.12 Effects of IP6 and formulations on DMBA altered COX-2 expression

COX-2	4th hour		8th hour		16th hour		24th hour	
	Western blot (%)	RT-PCR (%)	Western blot (%)	RT-PCR (%)	Western blot (%)	RT-PCR (%)	Western blot (%)	RT-PCR (%)
Group I	0	0	0	0	0	0	0	0
Group II	62	58	82	81	224	218	235	231
Group III	2	1	9	9	39	36	101	96
Group IV	22	17	3	2	0	0	0	0
Group V	37	31	20	20	15	14	11	10
Group VI	3	0	14	13	32	28	34	32

Table 3.13 Effects of IP6 and formulations on DMBA altered cyclin-D1 expression

Cyclin-D1	4th hour		8th hour		16th hour		24th hour	
	Western blot (%)	RT-PCR (%)	Western blot (%)	RT-PCR (%)	Western blot (%)	RT-PCR (%)	Western blot (%)	RT-PCR (%)
Group I	0	0	0	0	0	0	0	0
Group II	54	54	81	80	226	225	229	224
Group III	19	19	43	42	87	86	101	96
Group IV	29	26	50	50	1	0	0	0
Group V	42	40	55	54	8	7	12	10
Group VI	21	19	34	33	36	36	92	88

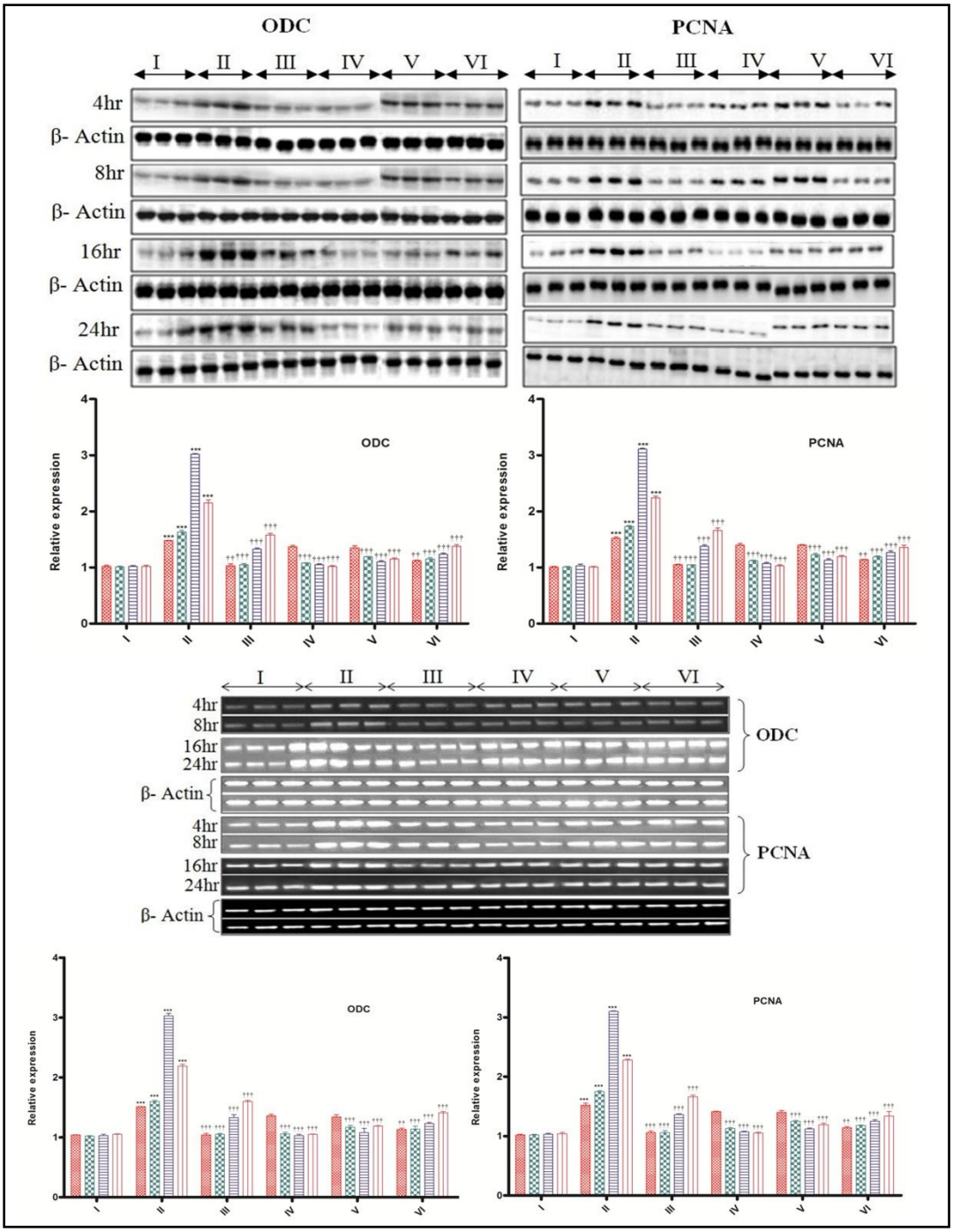

Figure 3.6 Effect of IP6 and formulations on DMBA induced deregulation of ODC and PCNA. Three individual samples from each group were analyzed and subjected to statistical analysis (n = 3). Image A and B show qualitative and quantitative analysis at the protein level and at mRNA level shown by C and D. I-Placebo formulation, II-DMBA+ Placebo formulation, III-DMBA+IP6 in acetone, IV- DMBA+F1(Dose1), V-DMBA+F1(Dose2), VI- DMBA+F2. *p< 0.05, ** p < 0.01, *** p < 0.001 (With respect to control), †p< 0.05, †† p < 0.01, ††† p < 0.001 (With respect to DMBA) 4^{th} h, 8^{th} h, 16^{th} h, 24^{th} h

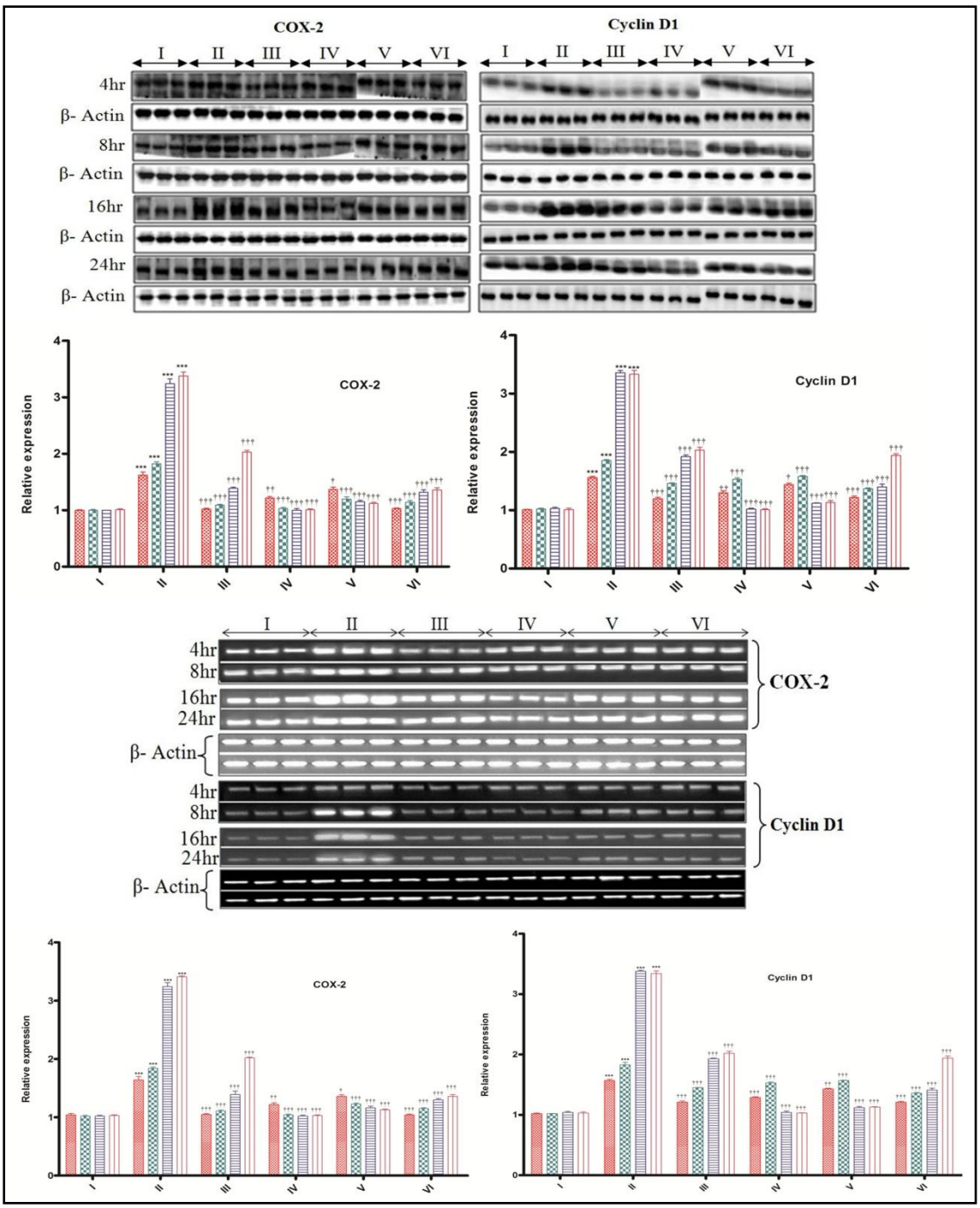

Figure 3.7 Effect of IP6 and formulations on DMBA induced deregulation of COX2 and cyclin D1. Three individual samples from each group were analyzed and subjected to statistical analysis (n = 3). Image A and B show qualitative and quantitative analysis at the protein level and at mRNA level shown by C and D. I-Placebo formulation, II-DMBA+ Placebo formulation, III-DMBA+IP6 in acetone, IV- DMBA+F1(Dose1), V-DMBA+F1(Dose2), VI- DMBA+F2. *p< 0.05, ** p < 0.01, *** p < 0.001 (With respect to control), †p< 0.05, †† p < 0.01, ††† p < 0.001 (With respect to DMBA) 4^{th} h, 8^{th} h, 16^{th} h, 24^{th} h

3.13.10.2. Histopathology

Skin tissue samples of the control group animals showed no alterations in the epidermal thickness when analyzed for histopathology, Figure 3.8(I). Conversely, significant hyperplasia was seen in DMBA treated skin with the increase in time points. DMBA effect was seen to commence from 4^{th} h and reached the maximum at 16^{th} and 24^{th} h, as depicted through the double-headed arrow, Figure 3.8(II). Concomitant application of IP6 formulations displayed varying consequences with varying doses and formulations, Figure 3.8. IP6 in acetone, as shown in Figure 3.8(III), was seen to circumvent the effect of DMBA initially but with increasing time, its effect diminished. Conversely, IP6 suspension displayed a better reduction in skin thickness when compared with the standard. Niosomal suspension containing IP6 revealed a maximum reduction in skin thickness, Figure 3.8(IV) and 3.8(V).

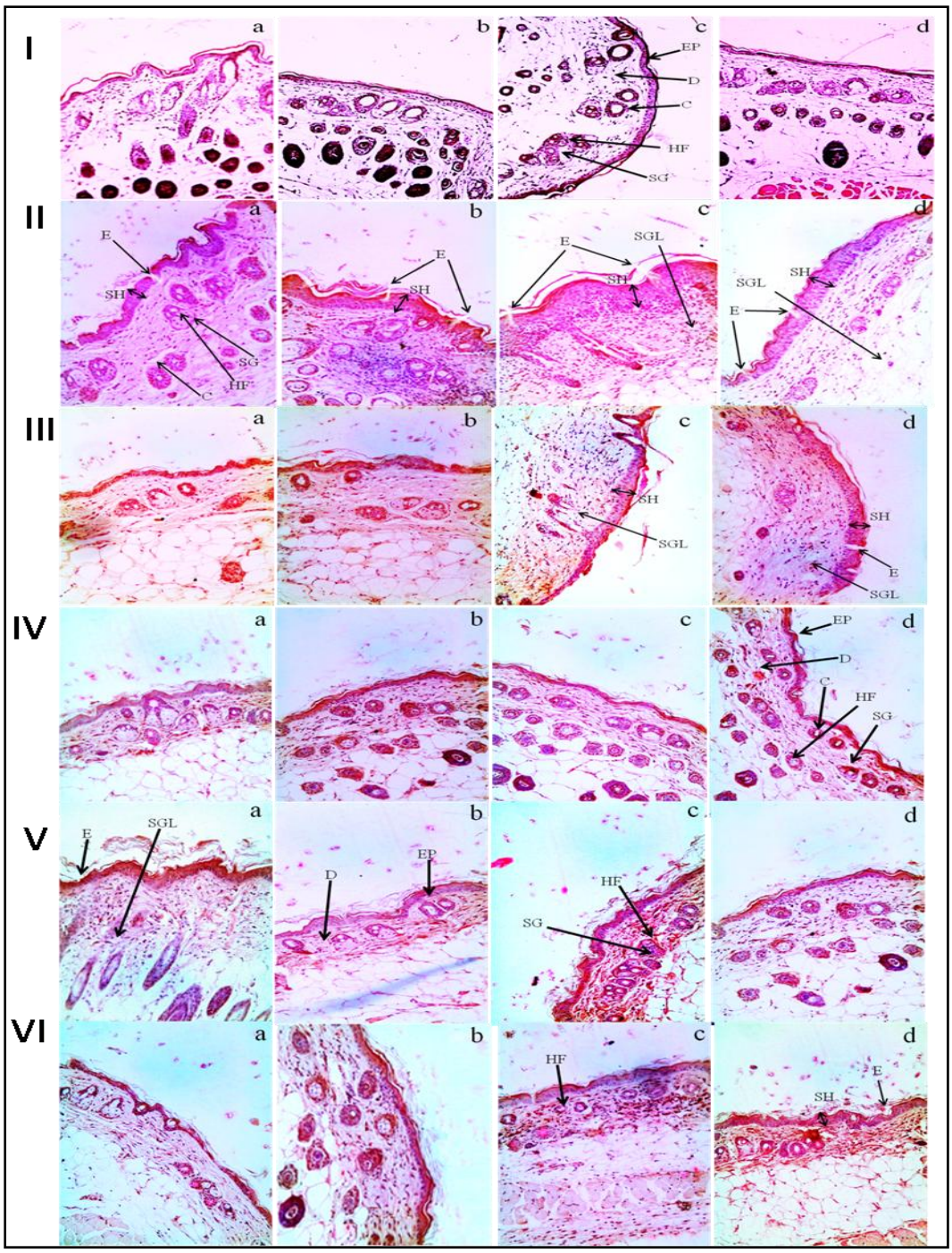

Figure 3.8 Histopathological examination (100×) of mice skin at a- 4th h, b- 8th h, c-16th h, d-24th h after exposure of DMBA and IP6, in various forms. Most affected epidermis thickness is shown by the double head arrow, SH- squamous hyperplasia. D- dermis, EP- epidermis, C- capillary, HF- hair follicle, SG- sebaceous gland, SGL- sebaceous gland loss, E- erosion. I-Placebo formulation, II-DMBA+ Placebo formulation, III-DMBA+IP6 in acetone, IV- DMBA+F1:(Dose1), V-DMBA+F1:(Dose2) and VI- DMBA+F2. Double headed arrow showing skin thickness.

3.14. Discussion

The central venture of current work was to facilitate topical delivery of IP6 with avoidance of systemic absorption. As earlier reports suggested that the vesicles with diameter ≤ 600 nm deliver their contents into deeper layers of skin and consequently raise the possibility of systemic absorption [29, 30]. Therefore, the IP6 loaded niosomal formulations which showed the particle size of less than 600 nm were not considered further for the studies. It was observed that when cholesterol concentration increased with respect to surfactant, the particle size decreased and it may be due to the fact that higher quantity of cholesterol results in dense and well-organized vesicles with a reduction of diameter and consequent rise in matrix cohesion [19]. Conversely, it has also been reported that particle size may increase with increasing amount of surfactant concentration, above a threshold value, as observed in the current studies [16, 31]. Furthermore, the DCP addition showed a trivial rise in particle size which might be due to its negative charge induction which increases the hydrophilicity of the vesicle bilayer thereby increasing water intake of the bilayers which could result in increased particle size [22]. Conclusively, as described by 3D plots, Figure 3.1(a), cholesterol: surfactant ratio and sonication time are seen to effect particle size directly.

It was seen that encapsulation efficiency moved parallel with particle size. Greater encapsulation was observed in larger vesicles and vice-versa. This result illustrated that reduction in cholesterol concentration, with respect to surfactant and inclusion of the DCP lead to significant rise of EE%, as shown by 3D plot, Figure 3.1(b). This might be attributed to the fact that in certain cases, the increasing cholesterol may interrupt the normal linear structure of the vesicular membrane and thus lead to the reduction of drug encapsulation [30]. Zeta potential relates the magnitude of the electrical charge present at the surface of particles and indicates the extent/ degree of repulsion present between the adjacent particles. Either negative or positive, high zeta potential bestows the stability by resisting their aggregation [18]. The negative value displayed by IP6 loaded niosomes may be due to the presence of negative charge inducing agent i.e. DCP. Observations were in-line with the characteristic property of DCP.

Physicochemical analysis revealed that niosomal suspension loaded with IP6 had a pH similar to skin pH range and spreadability value indicated that the suspension could be

applied by application of a small amount of shear. The cumulative percent of the amount of IP6 permeated from plain IP6 suspension was higher than that of niosomal suspension. The lower flux of IP6 containing niosomal suspension displayed prolonged drug release behaviour [26, 32].

HET-CAM studies revealed that the irritation score of all the formulations was found to be in the range of non-irritant category, Figure 3.3 and Table 3.3. Studies revealed that the formulation was well tolerated and gentle. IP6 in niosomal suspension displayed superior inhibition of cell proliferation/ apoptosis than the pure form of IP6, Figure 3.4 & 3.5 which may be attributed to the fact that niosomes in suspension displayed better interaction with lipid layer of the cell and hence micronized drug particles could have penetrated easily to lead to maximum cell death. Inhibitory effect of the niosomal suspension was seen to be in concordance with previous reports which projected that IP6 is a potential antineoplastic agent. Thus it was considered worth evaluating the *in-vivo* efficacy of prepared formulations against DMBA induced dysregulation of markers pertaining to cellular proliferation/ differentiation and inflammation. It was seen that the topical application of DMBA up-regulated the expression of ODC and PCNA at 4^{th} h and it reached its maximum till 16^{th} h.

ODC imparts a vital role in differentiation, cell growth, transformation as well as apoptosis [32]. It has been well studied and reported as an important marker for cellular proliferation in non-melanoma skin cancer, both preclinically and clinically [33].[38] Topical application of DMBA caused significant upregulation of the ODC levels and was consequently reflected by the increased mRNA expression. In the same line, the upregulation of PCNA protein was observed at 16^{th} h of the DMBA application, Table 3.11. PCNA is produced in the early G1 phase of cell cycle and contributes to the DNA replication, repair and cell cycle progression. It is a well-recognized marker of raised cellular proliferation in the clinical cases of squamous cell carcinoma and it was evident in the current experiment as well [34-36]. Overall, ODC and PCNA comprise a team of biological markers that are responsible for raised proliferation, differentiation and subsequent progression of carcinogenesis. Treatment with IP6 loaded niosomal suspension as well as plain IP6 suspension conveyed favourable outcome towards the normal regulation of the ODC and PCNA at all the time points studied, Figure 3.6 and

Table 3.10 and 3.11. The IP6 mediated decrease in cellular proliferation is linked with the reduction of DNA synthesis and a decrease in PCNA with the consequent increase in p^{21}WAF-1/CIP1, which is coupled with cell senescence and loss of function [37-39]. p^{21}WAF-1/CIP1 is a cyclin/CDK complex inhibitor that binds to the PCNA and causes G1 arrest. Based on the above findings, we scrutinized the expression of cyclin D1. Substantiating the results obtained for PCNA and ODC levels, IP6 loaded niosomal formulation was also seen to down-regulate the cyclin D1 expression and was followed by curtailment in the mRNA levels (Table 3.13). The biological effects of IP6 loaded niosomal formulation towards cancer progression were found to be in-line with the previous reports of pure IP6 [12].

To further boost our deliberations, we scrutinized the COX-2 expression which is a well recognized inflammatory marker for tumor progression [40]. DMBA application provoked a significant upregulation of COX-2 protein and mRNA expression as well. Topical application of the IP6 loaded niosomal formulation showed a significant lowering of the COX-2 protein, (Table 3.12). Overall, IP6 loaded niosomal formulation marginalized the deleterious effect of DMBA and revealed favourable normal regulation when compared with IP6 alone and IP6 plain suspension as well.

Conclusively, the studies substantiate that results of the *in-vivo* studies demonstrated that the IP6 loaded niosomal formulation F1-Dose1 (5mg) was seen as most effective for prevention of above-mentioned gene upregulation. This result may be attributed to the synchronised release, Figure 3.1(c) of IP6 from the niosomal suspension with the upregulation of carcinogenic genes following DMBA application. It was observed that gene upregulation of aforesaid genes almost increased with time, except COX-2 which was seen to rise till 16^{th} h and decreased at 24^{th} h. This behaviour matched with the *in-vitro* release pattern of the drug from niosomal formulation and thus was able to control upregulation proficiently. F1-Dose2 (3mg) also displayed the similar pattern of results but showed the lesser effect which may be due to the result of the reduced quantity of IP6. F2 (plain IP6 suspension) was found inferior to F1 formulations, though improved performance was demonstrated when compared to IP6 in acetone, with increasing time points. This result transpired possibly due to the fact that drug dissolved in acetone penetrated deeply and drug exposure took place at once and formed chelates might

rapidly get absorbed and distributed to various organs as early as an hour after administration, without showing its maximum effect at the required site. It was hypothesized that drug particles entangled in suspension base would also contribute to the slower drug penetration.

3.15. Conclusion

The controlled release and stable niosomal suspension containing IP6 was developed and optimized successfully against dysregulation of cellular differentiation and epidermal hyperplasia in mice skin. The developed formulation was found to be non-irritant, aesthetic and had desirable properties for the topical application. *In-vitro* as well as *in-vivo* findings of the present studies proved that IP6 loaded niosomal suspension could constitute a promising approach for preclusion of DMBA induced dysregulation of cellular markers pertaining to proliferation/ differentiation, inflammation and hyperplasia. Further studies may be performed to recognize the effect of IP6 loaded formulations on various carcinomas and successive scale-up from bench to bedside.

3.16. References

1. Siegel RL, Miller KD, Jemal A. Cancer statistics, 2016. CA: a cancer journal for clinicians. 2016;66(1):7-30.
2. Xu C, Huang M-T, Shen G, Yuan X, Lin W, Khor TO, et al. Inhibition of 7, 12-dimethylbenz (a) anthracene-induced skin tumorigenesis in C57BL/6 mice by sulforaphane is mediated by nuclear factor E2–related factor 2. Cancer research. 2006;66(16):8293-6.
3. Steward W, Brown K. Cancer chemoprevention: a rapidly evolving field. British journal of cancer. 2013;109(1):1.
4. Singh R, Sharma J, Goyal P. Prophylactic role of Averrhoa carambola (star fruit) extract against chemically induced hepatocellular carcinoma in Swiss albino mice. Advances in pharmacological sciences. 2014;2014.
5. Haug W, Lantzsch HJ. Sensitive method for the rapid determination of phytate in cereals and cereal products. Journal of the Science of Food and Agriculture. 1983;34(12):1423-6.
6. March J, Villacampa A, Grases F. Enzymatic—spectrophotometric determination of phytic acid with phytase from Aspergillus ficuum. Analytica chimica acta. 1995;300(1-3):269-72.
7. Saad N, Esa NM, Ithnin H, Shafie NH. Optimization of optimum condition for phytic acid extraction from rice bran. African Journal of Plant Science. 2011;5(3):168-75.

8. Wang K, Liu P, Ye Y, Li J, Zhao W, Huang X. Fabrication of a novel laccase biosensor based on silica nanoparticles modified with phytic acid for sensitive detection of dopamine. Sensors and Actuators B: Chemical. 2014;197:292-9.

9. Pandey M, Gupta KP. Epigenetics, an early event in the modulation of gene expression by inositol hexaphosphate in ethylnitrosourea exposed mouse lungs. Nutrition and cancer. 2011;63(1):89-99.

10. Wang N, Yang H-F, Zhu X, Zhang R, Wang Y, Huang G-F, et al. Synthesis of anti-aggregation silver nanoparticles based on inositol hexakisphosphoric micelles for a stable surface enhanced Raman scattering substrate. Nanotechnology. 2009;20(31):315603.

11. Shamsuddin AM. Inositol phosphates have novel anticancer function. The Journal of nutrition. 1995;125(suppl_3):725S-32S.

12. Shamsuddin AM. Metabolism and Cellular Functions of IP6. A Review. Anticancer Research. 1999;19(5):3733-6.

13. Balakrishnan P, Shanmugam S, Lee WS, Lee WM, Kim JO, Oh DH, et al. Formulation and in vitro assessment of minoxidil niosomes for enhanced skin delivery. International journal of pharmaceutics. 2009;377(1-2):1-8.

14. Paolino D, Cosco D, Muzzalupo R, Trapasso E, Picci N, Fresta M. Innovative bola-surfactant niosomes as topical delivery systems of 5-fluorouracil for the treatment of skin cancer. International journal of pharmaceutics. 2008;353(1-2):233-42.

15. Muzzalupo R, Tavano L, La Mesa C. Alkyl glucopyranoside-based niosomes containing methotrexate for pharmaceutical applications: evaluation of physico-chemical and biological properties. International journal of pharmaceutics. 2013;458(1):224-9.

16. Ruckmani K, Sankar V. Formulation and optimization of zidovudine niosomes. Aaps Pharmscitech. 2010;11(3):1119-27.

17. Abdelbary AA, AbouGhaly MH. Design and optimization of topical methotrexate loaded niosomes for enhanced management of psoriasis: application of Box–Behnken design, in-vitro evaluation and in-vivo skin deposition studies. International journal of pharmaceutics. 2015;485(1-2):235-43.

18. Kanoujia J, Singh M, Singh P, Parashar P, Tripathi CB, Arya M, et al. Genipin crosslinked soy-whey based bioactive material for atorvastatin loaded nanoparticles: preparation, characterization and in vivo antihyperlipidemic studies. RSC Advances. 2016;6(96):93275-87.

19. Tavano L, Aiello R, Ioele G, Picci N, Muzzalupo R. Niosomes from glucuronic acid-based surfactant as new carriers for cancer therapy: preparation, characterization and biological properties. Colloids and Surfaces B: Biointerfaces. 2014;118:7-13.

20. Branch SK. Guidelines from the international conference on harmonisation (ICH). Journal of pharmaceutical and biomedical analysis. 2005;38(5):798-805.

21. Arya M, Tiwari P, Tripathi CB, Parashar P, Singh M, Sinha P, et al. Colloidal vesicular system of Inositol hexaphosphate to counteract DMBA induced dysregulation of markers pertaining to cellular proliferation/differentiation and inflammation of epidermal layer in mouse model. Molecular pharmaceutics. 2017;14(3):928-39.

22. Bendas ER, Abdullah H, El-Komy MH, Kassem MA. Hydroxychloroquine niosomes: a new trend in topical management of oral lichen planus. International journal of pharmaceutics. 2013;458(2):287-95.

23. Singh M, Kanoujia J, Singh P, Tripathi CB, Arya M, Parashar P, et al. Development of an α-linolenic acid containing soft nanocarrier for oral delivery: in vitro and in vivo evaluation. RSC Advances. 2016;6(81):77590-602.

24. Shinde UA, Kanojiya SS. Serratiopeptidase niosomal gel with potential in topical delivery. Journal of pharmaceutics. 2014;2014.

25. Jigar V, Puja V, Krutika S. Formulation and evaluation of topical niosomal gel of erythromycin. Int J Pharm Pharm Sci. 2011;3(1):123-6.

26. Gupta H, Aqil M, Khar RK, Ali A, Bhatnagar A, Mittal G. Sparfloxacin-loaded PLGA nanoparticles for sustained ocular drug delivery. Nanomedicine: nanotechnology, biology and medicine. 2010;6(2):324-33.

27. Singh P, Arya M, Kanoujia J, Singh M, Gupta KP, Saraf SA. Design of topical nanostructured lipid carrier of silymarin and its effect on 7, 12-dimethylbenz [a] anthracene (DMBA) induced cellular differentiation in mouse skin. RSC Advances. 2016;6(88):84965-77.

28. Tiwari P, Gupta KP. Modulation of miR-203 and its regulators as a function of time during the development of 7, 12 dimethylbenz [a] anthracene induced mouse skin tumors in presence or absence of the antitumor agents. Toxicology and applied pharmacology. 2014;278(2):148-58.

29. Khazir J, Mir BA, Pilcher L, Riley DL. Role of plants in anticancer drug discovery. Phytochemistry Letters. 2014;7:173-81.

30. Abdelbary G, El-gendy N. Niosome-encapsulated gentamicin for ophthalmic controlled delivery. Aaps Pharmscitech. 2008;9(3):740-7.

31. Singh AP, Saraf SK, Saraf SA. SLN approach for nose-to-brain delivery of alprazolam. Drug delivery and translational research. 2012;2(6):498-507.

32. Ferreira LS, Ramaldes GA, Nunan EA, Ferreira LA. In vitro skin permeation and retention of paromomycin from liposomes for topical treatment of the cutaneous leishmaniasis. Drug development and industrial pharmacy. 2004;30(3):289-96.

33. Elmets CA, Athar M. Targeting ornithine decarboxylase for the prevention of nonmelanoma skin cancer in humans. Cancer Prevention Research. 2010;3(1):8-11.

34. Liang S-B, Furihata M, Takeuchi T, Iwata J, Chen B-K, Sinobe H, et al. Overexpression of cyclin D1 in nonmelanocytic skin cancer. Virchows Archiv. 2000;436(4):370-6.

35. Dornelas MT, Rodrigues MF, Machado DC, Gollner ÂM, Ferreira AP. Expression of cell proliferation and apoptosis biomarkers in skin spinocellular carcinoma and actinic keratose. Anais brasileiros de dermatologia. 2009;84(5):469-75.

36. Hoshino Y, Teranishi Y, Terashima S, Ito F, Konno A, Inoue H, et al. A ornithine decarboxylase activity and proliferating cell nuclear antigen in gastric cancer. Nihon Geka Gakkai zasshi. 1994;95(10):743-52.

37. Saied I, Shamsuddin A. Up-Regulation of the Tumor Suppressor Gene p53 and WAF1 Gene Expression by IP~ 6 in HT-29 Human Colon Carcinoma Cell Line. Anticancer Research. 1998;18(3):1479-84.

38. Yang G, Shamsuddin A. IP6-induced growth inhibition and differentiation of HT-29 human colon cancer cells: involvement of intracellular inositol phosphates. Anticancer research. 1995;15(6B):2479-87.

39. Sakamoto K, Venkatraman G, Shamsuddin AM. Growth inhibition and differentiation of HT-29 cells in vitro by inositol hexaphosphate (phytic acid). Carcinogenesis. 1993;14(9):1815-9.

40. Edelman MJ, Hodgson L, Wang X, Kratzke RA, Vokes EE. Cyclooxygenase-2 (COX-2) as a predictive marker for the use of COX-2 inhibitors in advanced non–small-cell lung cancer. Journal of Clinical Oncology. 2012;30(16):2019.

Chapter 4

Preparation and evaluation of pectin encrusted gold nanocomposites containing inositol hexaphosphate and jacalin, for oral delivery to target colon cancer

Preparation and evaluation of pectin encrusted gold nanocomposites containing inositol hexaphosphate (IP6) and jacalin, for oral delivery to target colon cancer

4.1. Background

Colon cancer is expanding its threat due to a high mortality rate. Globally, it is found to be the third most common cancer, in both genders. At present, it constitutes about 10% of the whole cancer burden. Furthermore, colorectal cancer is about to amplify by 60% and >2.2 million new cases have been forecasted by 2030 [1].

To facilitate cancer prevention, numerous efforts are being made, amongst which the use of naturally occurring constituents as antiangiogenic agents have shown a rise. This is due to their safety, availability and general acceptance [2].

IP6, as mentioned earlier is one such naturally occurring agent, linked with the lessening of incidences of colon cancers [3, 4], but is underutilized due to its fast chelation and elimination from the body, within an hour of oral administration [5]. To abolish its flaw and maximize the chemotherapeutic activity, a surface-modified nanoformulation of IP6 may be developed. Gold nanoparticles have drawn consideration owing to their distinctive properties as controlled drug delivery agents, contrast agents and biosensors for cancer detection and treatment [6-8].

Active targeting of a nanoparticulate system may be done to make delivery efficient at the required site and it may be accomplished through surface functionalization with proteins, antibodies and aptamers. Accordingly, conjugation of biomolecules to the gold core may impart to its additional interaction and advanced potential [9-11].

Uncharacteristic glycosylation has usually seen in all types of human as well as experimental cancers and associated glycosyl epitopes form antigens which can be exploited for binding/ targeting [12]. Lectins proteins are of non-immune origin and possess the ability to spot aberrant glycosylation. Therefore, lectins are being used by researchers to target glycosylation-related to metastasis [13, 14]. Jacalin is one such lectin, obtained from seeds of jackfruit [15] and it has a high capability of identifying tumour-linked antigenic disaccharides [16, 17] which get over-expressed in nearly 85% of human and experimental carcinomas including colon, breast etc. [18].

Efforts were made for improving the residence time of IP6 and targeting of the formulation at the required site to accomplish superior anticancer efficiency.

4.2. Materials

Table 4.1 List of various chemicals utilized during formulation studies

Materials	**Source**
2,2'-bipyridine	Abcam
Acetone	ThermoFischer Scientific (Qualigens)
Antibodies	Cell Signaling Technology, USA and Alexis Biochemicals, USA
Chloroauric acid	Loba Chemie, Mumbai
Crystal violet	Sigma Co. (St. Louis, MO, USA)
DCFH-DA dye	Sigma Co. (St. Louis, MO, USA)
DMH	Acros Organics (Thermo Fisher Scientific, New Jersey, US)
DMSO	Himedia Laboratories, Mumbai, India
dNTPs	Bangalore Genei (India)
Ethanol	S.D. Fine chemicals Ltd., Mumbai, India
Fetal bovine serum	Sigma Co. (St. Louis, MO, USA)
Formalin	Sigma Co. (St. Louis, MO, USA)
Horseradish peroxidase-conjugated secondary antibody	Bangalore Genei (India)
Hydroxy quinone	Sigma Co. (St. Louis, MO, USA)
IP6	Sigma Co. (St. Louis, MO, USA)
Jacalin	Sigma Co. (St. Louis, MO, USA)
Magnesium chloride	Himedia Laboratories, Mumbai, India
Methanol	ThermoFischer Scientific (Qualigens)
[Methyl-3H] S-adenosyl methionine	AmershamBiosciences-GE Healthcare (USA)
Methylene blue	ThermoFischer Scientific (Qualigens)
MTT (3-(4,5-Dimethylthiazol-2-yl)-diphenyl tetrazolium bromide)2,5-	Sigma Co. (St. Louis, MO, USA)
NMR tube	Wilmad Glass, USA
PCR primers	MWG Bio Tech, Germany
Pectin	Acros Organics (Thermo Fisher Scientific, New Jersey, US)
Phenolphthalein	Sigma Co. (St. Louis, MO, USA)
Potassium chloride	Himedia Laboratories, Mumbai, India

Propidium Iodide	Sigma Co. (St. Louis, MO, USA)
PVDF membrane	Millipore Co. USA
RNase	Sigma Co. (St. Louis, MO, USA)
RT-PCR kit	Bangalore Genei (India)
Sodium chloride	Himedia Laboratories, Mumbai, India
Sodium hydroxide	SDFCL Pvt. Ltd., Mumbai, India
Sodium metabisulfite	Sigma Co. (St. Louis, MO, USA)
Taq DNA polymerase	Bangalore Genei (India)
Thioglycollic acid	Merckmillipore

4.3. Preparation of IP6 loaded jacalin-pectin-gold nanoparticles (IJP-GNP)

A green method was utilized for the reduction of chloroauric acid by making use of pectin for the synthesis of pectin-gold nanoparticles (P-GNP). A 0.5% w/v of pectin solution was prepared with distilled water. Aliquots (9 ml each) of pectin solution were taken in three different test tubes and 1 ml of 1 mM (F1), 2 mM (F2) and 3 mM (F3) chloroauric acid solution was added respectively. The three test tubes were allowed to react in a water-bath at 55°C till dark reddish purple colour was obtained. Colour change indicated the formation of P-GNP. To the P-GNP suspensions, IP6 (1 mg/ml) and jacalin (1 mg/ml) (for surface modified batch) solutions were added in a ratio of 1:1 and gently stirred at 4°C for 24 h, protected from light. Free IP6 and jacalin were separated out by centrifugation at a temperature of 4°C at 20,000 rpm for 30 min. The supernatant was separated used to estimate free IP6 and the pellets were collected, washed and redispersed with deionized water and stored for further characterization. The prepared formulations (F1, F2 and F3) were analyzed for UV spectroscopy, particle size, polydispersity index (PDI) and drug loading. The formulations found best according to these parameters were considered optimized and taken for further analysis [19, 20].

4.4. *In-vitro* characterization of IJP-GNP

4.4.1. UV–visible spectroscopy

The UV–visible spectroscopy is an indirect and proficient technique for examining the synthesis of GNP. The change in surface plasmon resonance of IJP-GNP was

estimated by a UV-visible spectrophotometeric method. The wavelength range for analysis was set from 400 to 600 nm [21, 22].

4.4.2. Particle size and PDI

The particle size and PDI of IJP-GNP were evaluated through the standard method by using a particle size analyzer, laser light scattering-based equipment [21].

4.4.3. Drug loading

The drug loading was determined indirectly by estimating non-bound drug which was separated by centrifugation of IJP-GNP suspension at 20,000 rpm for 30 min. The supernatant was taken to estimate free IP6 by UV-visible spectroscopy at 520 nm. The percentage drug loading was calculated by using the following equation [19, 23, 24].

$$\%\ \text{Drug loading} = \frac{\text{Total amount of drug} - \text{Non bound drug in supernatant}}{\text{Total amount of drug}} \text{X } 100 \quad \text{Equation 1}$$

4.4.4. *In-vitro* drug release studies

The *in-vitro* drug release studies were carried out with pre-treated dialysis membrane of 12,000-14,000 kDa molecular weight cut-off. One end of the bag was closed with a clip and respective formulation (F1, F2 and F3) (equivalent to 2 mg of IP6) was filled into it and the other end was sealed with the clip. The prepared dialysis bag was placed in a beaker containing dissolution medium (HCl buffer- 50 ml) of pH 1.2 with continuous stirring (100 rpm) for two hours. Subsequently, pH of dissolution media was adjusted to 6.8 with PBS and the experiment was continued for 3 more hours. At the end of the third hour, dissolution media was degassed with CO_2 for 15 minutes, to maintain anaerobic conditions. Rat cecal content (4 % w/v) was added at pH 7.4 and experiment was continued for 12 hours with continuous CO_2 purging. The entire experiment was conducted at a temperature of 37±2°C, maintaining sink conditions. Dialysate (0.5 ml each) was withdrawn at the predetermined intervals from 0 hours to 12 hours and examined spectrophotometrically [19, 20, 25].

4.4.5. Fourier transform infrared (FTIR) spectroscopy

FTIR spectroscopy was used to examine the chemical nature/ identification of chemical groups involved in reaction of pectin, chloroauric acid, jacalin, IP6 and IJP-GNP. The FTIR spectra of samples were recorded spectrometrically at room temperature (Nicolet 6700, Thermo Scientific, USA) by earlier reported methods [26].

4.4.6. Morphological evaluation

Morphology and shape of prepared IJP-GNP was observed by utilizing transmission electron microscopy (TEM). For TEM, a drop of IJP-GNP suspension was layered on a 400-mesh copper grid and left to be air-dried over carbon substrate. The prepared slide was observed under an electron microscope (H- 7500, Hitachi Made, Japan) at an accelerating voltage of 100 kV and at a magnification of 30,000X [21].

4.5. *In-vitro* cell line studies

4.5.1. Cell viability assay

Effect of formulations, P-GNP, IP-GNP and IJP-GNP on the viability of different cells were determined by MTT assay, IP6 was taken as standard. Briefly, cells were seeded in 96-well plate at a density of 1×10^4 cells. Cells were treated with different concentrations of treatment at 24 h, 48 h and 72 h. At the end of treatment, 20 µl MTT (5 mg/ml) was added in each well. After incubation of 3 h, media along with MTT was removed. 200 µl DMSO was added to dissolve the formazan crystal and absorbance was recorded at 540 nm using ELISA plate reader [27].

4.5.2. Colony forming assay

HCT 15 cells were seeded (500 cells/well) in six-well plates. Seeded cells were allowed to grow for 24 h and 48 h and then treated with IJP-GNP. At the end of incubation, cells were washed, fresh media was added and cells were allowed to grow for 6 to 7 days. Then, cells were again washed with PBS, fixed with ice-cold methanol and stained by 1% w/v crystal violet solution. Excess staining was removed by washing with PBS and images were observed and recorded using an inverted fluorescent microscope (Nikon Eclipse Ti-S, Tokyo, Japan) at a magnification of 20X [28].

4.5.3. 4,6-diamidino-2- phenylindole (DAPI) staining

The HCT-15 cells with the concentration of 10^4 cells/ml were allowed to grown on coverslips after treatment with IJP-GNP for 24 h and 48 h. Nuclei showed changes, which were examined by DAPI staining using an earlier reported method. After washing with PBS, the cells were fixed for 5 min by using cold methanol, at room temperature and again washed with PBS and incubated with DAPI solution (2 mg/ml in PBS) at room temperature, for 10 min. Specimens were analyzed and images were

captured using an inverted fluorescent microscope (Nikon Eclipse Ti-S, Tokyo, Japan) at 20X magnification [29].

4.5.4. Cell cycle analysis

The HCT-15 cells (1×10^6) were seeded in T-25 culture flask and allowed to grow for 24 h. After 24 h, cells were treated with IJP-GNP for 24 h and 48 h. At end of incubation, cells were harvested, fixed with ice-cold ethanol (70%) and incubated for 1 h at 4°C. Thereafter, cells were centrifuged and resuspended in 300 ml PBS and incubated with 30 mg of RNase and 15 mg of propadium iodide (PI) for 30 min at room temperature, in dark. Thus prepared samples were analyzed by flow cytometry using a FACS Calibur instrument (BD Biosciences) [30].

4.5.5. Apoptosis analysis

To determine the effect of IJP-GNP on apoptosis in HCT-15 cells, AnnexinV-FITC/PI dual staining was performed by making use of flow cytometry. Cells of 1×10^6 cells concentration were seeded in six-well plates, allowed to grow for 24 h and treated with different concentration at 24 h and 48 h. At the end of incubation, cells were harvested, washed with PBS and stained with AnnexinV-FITC and PI using apoptosis detection kit (Sigma Co. St. Louis, MO, USA). Samples were examined by a flow cytometer using FACS Caliber instrument (BD Biosciences) [29].

4.5.6. ROS generation assay

ROS generation was assayed using 2,7-dichlorodihydrofluorescein diacetate (DCFH-DA) dye through a flow cytometer. HCT-15 cells (1×10^6) were seeded in 6 well plates for 24 h. Seeded cells were treated with different concentration of IJP-GNP for 24 h and 48 h. At the end of incubation, cells were harvested by trypsinization, fixed with cold methanol and incubated with 30 µg/ml of DCFH-DA dye for 30 minutes at room temperature, in dark. At the end of incubation, cells were centrifuged and resuspended in 300 ml of PBS. Specimens were analyzed by fluorescence microscopy (Evos Flc microscope, Invitrogen), at a wavelength of 485nm and 520nm for excitation and emission respectively. Production of ROS was quantified by using Image J software (Image J, National Institutes of Health, and Bethesda, MD). A total number of 50 cells from each group were quantified for fluorescence intensity and analyzed statistically with respect to untreated (control) group [29].

4.6. *In-silico* approach to studies inter-molecular interactions between IP6, P-GNP and jacalin protein

4.6.1. Preparation of structure

The 3-dimensional structure of jacalin protein (Figure 4.1) was retrieved from the Protein Data Bank (PDB ID: iku8) (www.rcsb.org) which was used for the present docking studies. Energy minimization and force field CHARM m were applied to remove the bad steric clashes. In this execution, all computations were performed in the vacuum without any reaction field [31].

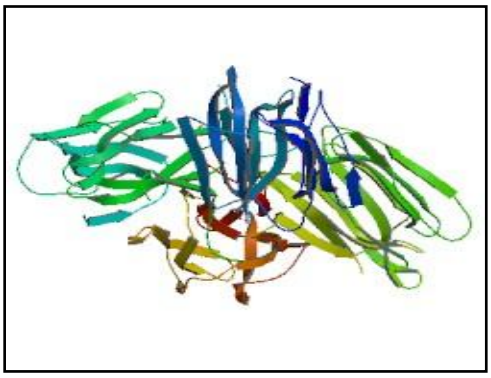

Figure 4.1: 3-Dimensional structure of jacalin protein (iku8)

4.6.2. Preparation of ligand complex structure of jacalin, P-GNP and IP6

The SMILES (Simplified Molecular Input Line Entry Specification) notations of the inhibitors were obtained from the Pub Chem database.

4.6.3. ADME and druglikeness analysis

Molecular properties like membrane permeability, bioavailability etc. of compounds are always coupled with several basic molecular descriptors like log P, molecular weight or number of hydrogen bond acceptors/ donors in a molecules [32]. These molecular characteristics are utilized in formulating the "rule of five" [33]. Lipinski's rule states that molecules with good membrane permeability have molecular weight ≤500, hydrogen bond donor ≤5 and acceptor ≤10. In the present studies, these molecular properties and druglikeness score of chloroauric salt and inositol hexaphosphate were estimated by utilizing Molinspiration tool [34].

4.6.4. Molecular interaction analysis

The *in-silico* docking analyses were carried out using PatchDock. The jacalin protein was docked with IP-GNP and resultant pdb file obtained after jacalin, P-GNP and IP6

docking was used as IJP-GNP complex and was further docked by uploading the receptor and molecules in PatchDock Server, an automatic server for molecular docking. The final figures were produced with the help of Discovery Studio 4.5 Visualizer [35].

4.7. *In-vivo* studies

The study was approved and conducted as per guidelines IAEC (approval no.: SDCOP&VS/AH/CPCSEA/01/0028). Animals were handled as per norms of IAEC and care was taken to follow guidelines with a humane approach. Albino Wistar rats (weighing 100-120 g) were used for the studies. All the animals were housed in polypropylene cages with well-ventilated, standard conditions of temperature (22±2°C) and photoperiodic cycle (12 h dark/ light) with free access to the commercial pellet diet and water *ad libitum*. Before commencing the studies, animals were acclimatized for at least a week. All animals were divided into 5 groups containing 8 animals each. DMH was administered at a dose of 20 mg/kg/week, subcutaneously and all other treatment details as per Table 4.2, were given for six weeks. At the end of the 6^{th} week, animals were euthanized with cervical dislocation. Before sacrifice, animals were scrutinized for their electrocardiogram (ECG) and heart rate variability (HRV) paradigms and blood was collected by retro-orbital plexus. The blood serum, colon tissue and colon content were collected and stored for further analysis.

Table 4.2 Treatment detail for animals

Groups	Treatment
Normal control	1mM EDTA+saline (2 ml/kg/day, oral)
Toxic control	DMH
Standard	DMH+ IP6 (2 mg/kg/day, oral)
IP-GNP	DMH+ IP-GNP (IP6 equivalent to 2 mg/kg/day, oral)
IJP-GNP	DMBA+ IJP-GNP (IP6 equivalent to 2 mg/kg/day, oral)

4.7.1. Hemodynamic changes

Animals were anaesthetized by using a combination injection of ketamine hydrochloride (100 mg/kg) and diazepam (5mg/kg) which was given intramuscularly, and animals were mounted on a wax tray. ECG signals were then recorded by placing platinum hook electrodes on the skin of the dorsal and ventral thorax of the animals. Electrodes were attached with channel power lab (ML-826) and bio-amplifier (ML-136) in order to change the analogue signals to digital ones. The recorded ECG

signals were saved and analyzed offline. HRV analysis was done on different segments of ECG signals. Raw signals were analyzed manually to make sure that all the R waves are alleged correctly and HR was figured out by plotting the R wave number vs. time. Time and frequency domains of HRV were also determined offline.

4.7.2. Estimation of weight variation and pH

Weight variations among the animals of each group were determined by utilizing the following equation. The collected colon content was examined for colonic pH by making use of a pen-type digital pH meter (Hanna Instrument HI 98107) [36, 37].

$$\%\,\text{Weight variation} = \left[\frac{\text{Final weight} - \text{Initial weight}}{\text{Final weight}}\right] * 100 \qquad \text{Equation 2}$$

4.7.3. Estimation of total acidity

For estimation of total acidity, 01 ml of gastric juice was diluted with distilled water. From it, 50 ml was taken in a conical flask. Two drops of phenolphthalein indicator were added to it and titrated with 0.01N NaOH until a pink colour sustained. The volume of 0.01N NaOH was recorded which was used up to obtain the pink colour. The total acidity was expressed as mEq/L in the following equation [36, 37].

$$\text{Total Acidity} = \frac{\text{Vol .of NaOH} \times \text{N} \times 100}{0.1\text{mEq /L}} \qquad \text{Equation 3}$$

4.7.4. Biochemical estimation

For biochemical estimation, the distal part of colon tissue (10% w/v) was homogenized by using 0.15 M KCl and centrifuged at 4°C and at an rpm of 10,000. Thus obtained supernatant was analyzed for numerous antioxidant markers including protein carbonyl, thiobarbituric acid reactive substances (TBARS), glutathione (GSH), superoxide dismutase (SOD) and catalase by following the established procedure of our laboratory [38].

4.7.5. Morphological evaluation

4.7.5.1 Aberrant crypt foci (ACF)

ACF analysis was performed following the method described by Bird, 1987. Briefly, colon tissue was opened longitudinally, rinsed with normal saline and fixed flat in 10% of buffered formalin for 24 hours. Thereafter the tissue was stained by using 0.1% methylene blue in PBS for 10 min and then placed on a glass slide. The tissue

was observed through a light microscope at a magnification of 40X. ACF was exemplified by nearby normal crypts through an increase in size, augmented distance from the lamina and perceptible pericryptal zone. ACF in total and number in crypts in each focus were counted for at least two foci per slide [39].

4.7.5.2. Morphological evaluation by scanning electron microscopy (SEM)

The colon tissue was scrutinized for its morphology by SEM. Tissue samples were fixed for 6 h by using 2.5% glutaraldehyde at 4°C and rinsed with 0.1 M PBS with 3 changes, each for 15 min at 4°C. Osmium tetroxide (1% w/v) was utilized for fixation, at 4°C for 2 h and samples washed with 0.1 M PBS for 3 changes, each for 15 min at 4°C. Tissue specimens were dehydrated by making use of increasing acetone concentrations viz. 30%, 50%, 70%, 90%, 95% and 100% v/v, for 30 min each at 4°C and then air dried. Air dried samples were mounted on an aluminium stub and observed under SEM Jeol (JSM- 6490LV, Japan) at 500X magnification [40, 41].

4.7.5.3. Morphological evaluation by histopathology

The colon tissue samples were fixed overnight with paraformaldehyde and further treated overnight with 70% v/v isopropanol. Then specimens were exposed to isopropanol with variable concentrations (70%, 90%, and 100% v/v) and dehydrated using 100% v/v xylene. The prepared tissue specimens were embedded with paraffin wax to prepare blocks, sectioned with a microtome and stained with haematoxylin and eosin. Stained sections were examined under a digital biological microscope, (N120, BR Biochem Life Sciences, New Delhi, India) at a magnification of 40X [40, 41].

4.7.6. Western blotting

The total protein was extracted from the colon tissue by using a freeze-thaw method and was quantified through Bradford protein assay. Tissue lysate was prepared by utilizing 20 mM Tris buffer of pH 7.5. Prepared tissue lysate, equivalent to 50 μg of proteins was resolved using 10 % SDS-PAGE and transferred on to methanol soaked PVDF membrane (Millipore Co. USA) utilizing transfer buffer. Subsequently, PVDF membrane was blocked by using blocking solution for 3 h and probed overnight with primary antibodies of dilution 1:1000, against PI3K (#4257), Akt (#4691) (Cell Signaling Technology, USA) and COX-2 (ALX-210-711-1) (Alexis Biochemicals, USA). Primary antibody incubation was followed by horseradish peroxidase-conjugated secondary antibody (Bangalore Genei, India) incubation. Then, antibody

binding signals were visualized with the help of Chemiluminescence HRP detection system (Millipore) over Versa Doc (Bio-Rad) and simultaneously band strength was estimated by Syngene gene tool. Utilized PVDF membranes were stripped and reprobed by using β-actin antibody(4970) (Cell Signaling Technology Inc, USA) [42].

4.7.7. Reverse transcription polymerase chain reaction (RT-PCR)

RT-PCR (Applied Biosystems, Verity, USA) was used for estimating colon tissue samples for their mRNA content. Total RNA content of colon tissue sample was extracted by using Trizol reagent (Invitrogen) according to manufacturer's directives. DNA contaminations were removed by utilizing DNaseI. c-DNA synthesis was done by using c-DNA preparation kit and taking RNA equivalent to 2ng. c-DNA was used for quantification of particular mRNA through primers (MWG Bio Tech, Germany) mentioned in Table 4.3. A 20 µl of the reaction mixture was prepared by making use of 100 ng of c-DNA, dNTPs (1.5 mM), $MgCl_2$ (1.5 mM), 10 pM each primer and 1 unit Ampli Taq DNA polymerase enzyme. The product was amplified using thermal cycles (denaturation at 94°C for 5 min, 95°C for 60 sec, annealed at 72°C for 60 sec)×35 and final extensions of 4 min at 72°C. A 1.5% of the agarose gel containing ethidium bromide was used to resolve/ visualize prepared PCR products. Quantification was made by utilizing gene tool Syngene software. β-actin was used as an internal control [24].

Table 4.3 Nucleotide sequences and product size used for RNA analysis by RT-PCR

Gene	Sequence	Product size (bp)
PI3K	F 5'-GGACCCGATGCGGTTAGA-3' R 5'-GATGATGGTCGTGGAGGC-3'	141
Akt	F 5'-ATGGCACCTTCATTGGCTAC-3' R 5'-GGGCCGGACTCGTCATAC-3'	222
COX-2	F 5'-GTGGAAAAACCTCGTCCAGA-3' R 5'-TGATGGTGGCTGTTTTGGTA-3'	256
β-Actin	F 5′-TGTGATTGGTGGGAATGGGTCAG-3′ R 5′-TTTGATGTCACGCACGATTTCC-3′	514

4.8. ^{1}H NMR spectroscopic analysis of serum samples

4.8.1. Serum sample preparation

The stored serum samples were thawed at room temperature and centrifuged at a relative centrifugal force of 16,278 for 5 min, just before acquiring the NMR data. A

total of 440 µl of sample was filled in 5 mm NMR tube for data acquisition: 220 µl of serum was taken and final volume adjusted by adding 220 µl of saline sodium PBS of strength 20 mM and pH 7.4 with 0.9 % saline prepared in D_2O as described earlier [43]. A sealed co-axial containing the known concentration of 0.1 mM TSP (Sodium salt of 3-trimethylsilyl-(2, 2, 3, 3-d4)-propionic acid) was also inserted in NMR tubes to provide lock for NMR experiments, and as an external standard reference to aid chemical shift referencing for metabolite quantification and assignment [44].

4.8.2. NMR measurements

All the NMR spectra were acquired at 300K on Bruker Avance-III NMR spectrometer operating at a proton frequency of 800.21 MHz and equipped with Cryoprobe. The raw NMR data was processed in the Bruker software Topspin-v2.1 (Bruker BioSpin GmbH, Germany). For each serum sample, the 1D ^{1}H transverse relaxation-edited CPMG (Carr–Purcell–Meiboom–Gill) NMR spectra were recorded using the standard Bruker's pulse program library sequence (cpmgpr1d) with pre-saturation of the water peak with continuous irradiation during the recycle delay (RD) of 5 sec. Each spectrum consisted of the accumulation of 128 scans and lasted for about 15 min. To remove broad signals from triglycerides, proteins, cholesterol and phospholipids, a total spin-spin relaxation time of 60 min (n=300 and 2τ=200µs) was applied. Each FID (free induction decay) was zero filled and Fourier-transformed (FT) to 64 K data points following manual phase and baseline-correction. A line broadening factor of 0.3 Hz and a sine-bell apodisation function was applied to FIDs before FT.

4.8.3. Spectral assignment

The 1D ^{1}H CPMG NMR spectra of metabolite resonances were assigned using the Chenomx NMR Suite (Chenomx Inc., Edmonton, AB, Canada) [45]. The remaining peaks in the spectra were assigned by comparing them with the chemical shifts of distinct metabolites reported previously in the literature [46, 47], BMRB (Biological Magnetic Resonance Data Bank) [48] and HMDB (The Human Metabolome Database) databases [49].

4.8.4. Multivariate statistical analysis

Before multivariate analysis, all the NMR spectra were manually phased, baseline corrected and referenced internally to Lactate peak (at δ =1.33 ppm). The CPMG δ (0.5−9.5 ppm) spectra were binned and automatically integrated using AMIX package

(Version 3.9.15, Bruker). The region δ (4.66-5.2 ppm) distorted due to water suppression was excluded from the CPMG data set. The selected regions were reduced to spectral bins of δ (0.01 ppm) and each spectral bin further normalized by total spectral intensity. The binned data from CPMG experiments were submitted to a multivariate data analysis performed using the open access web-based metabolomics data processing tool, named MetaboAnalyst [50, 51]. Principal Component Analysis (PCA) was used for the initial overview of the grouping trend within the data set and outlier detection. The data were modelled with the supervision method of Partial Least Squares Discriminant Analysis (PLS-DA) to reveal class separations between the groups and to further identify the metabolites responsible for class separation [52]. For both PCA and PLS-DA, the data were scaled using Pareto scaling. To avoid the over-fitting of the PLS-DA model, 10-fold cross-validation algorithm helps to evaluate 100% classification accuracy using the top 5 latent variables, which were used. The quality of the models was described by the cross-validation parameters R^2 and Q^2, representing the explained variance and predictive capability of the model, respectively. The PLS-DA model was further used to identify the metabolites responsible for the discrimination based on their higher values of variable importance on projection (VIP) scores. The VIP score represents a weighted sum of squares of the PLS loadings and takes into account the amount of explained Y-variation in each dimension to measure the impact of each metabolite. A $p \leq 0.05$ was considered significant, calculated by Mann-Whitney test for pairwise comparisons.

4.9. Results

4.9.1. Preparation and *in-vitro* characterization of IJP-GNP

IJP-GNP was prepared through a green method of reduction of chloroauric acid using pectin, loaded with IP6 and surface modified with jacalin.

4.9.2. UV spectroscopy

The UV-visible spectroscopy is an efficient method for investigating the biosynthesis of GNP. The absorption maxima were evident between 520–530 nm.

4.9.3. Particle size and PDI

Particle size analysis showed that the size of IJP-GNP increased with the increasing concentration of chloroauric acid. The size of formulations, F1, F2 and F3 were found

to be 67.4±2.38nm, 128.29±3.12nm and 283 ± 4.94nm respectively. The prepared IJP-GNP showed PDI values of 0.24, 0.29 and 0.32 respectively.

4.9.4. Drug loading

Drug loading of IP6 in IJP-GNP decreased with increasing amount of chloroauric acid. F1, F2 and F3 revealed percentage drug loading of 81.63±1.21%, 78.86±1.98% and 76.1±2.69 % respectively.

4.9.5. FTIR spectroscopy

FTIR spectroscopy of pectin, chloroauric acid, IP6, jacalin and IJP-GNP was analyzed, Figure 4.2. All the excipients displayed their characteristic peaks. In case of pectin, the peaks were observed at 2935.8 cm^{-1} and 1746.8 cm^{-1} which correspond to C-H and C=O bond (indicating -$COCH_3$ groups) vibrations [53]. For chloroauric acid, the peaks at 1631.4 cm^{-1} and 3389.8 cm^{-1} corresponds to C-O and -OH stretching respectively [54]. The peaks near 1654.4 cm^{-1} showed the main vibrational bands of amide groups of jacalin [55] and the bands near 1378.8 cm^{-1} displayed vibrational mode of the COOH and C-O groups of aspartic acid, glutamic acid like amino acids, present in jacalin. Peak near 3430.3 cm^{-1} in case of IP6 relates to OH stretching [56]. IJP-GNP revealed the shift in peaks of hydroxyl and carbonyl groups and also displayed all the characteristic peaks of IP6 and jacalin.

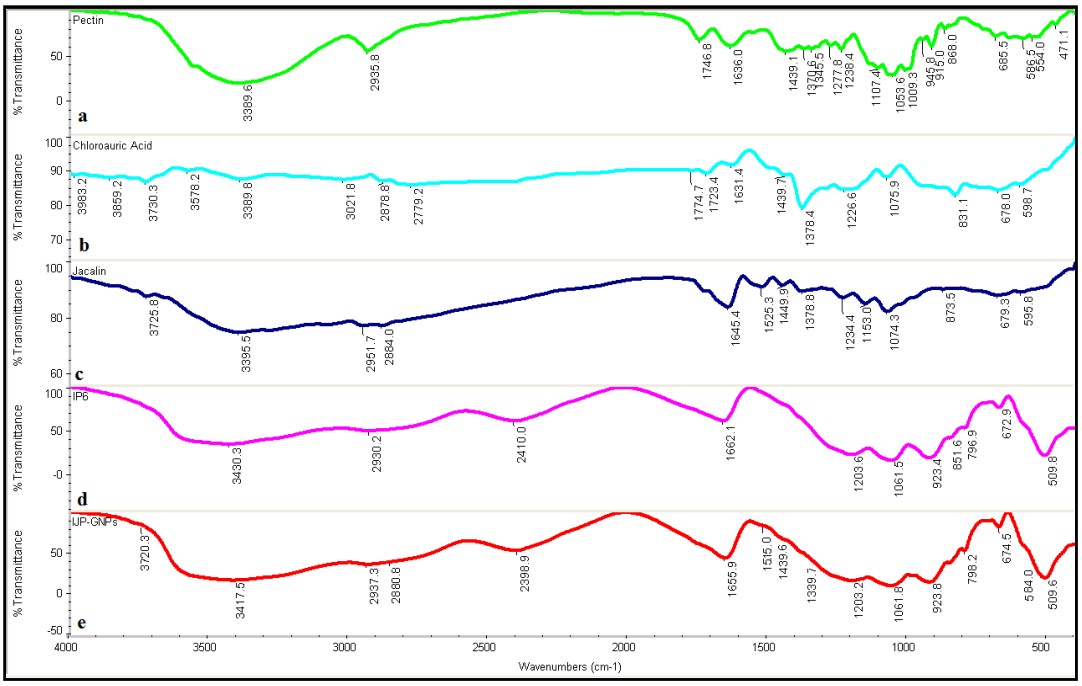

Figure 4.2 FTIR spectrums: a- pectin, b- chloroauric acid, c- jacalin, d- IP6 and e- IJP-GNP

4.9.6. *In-vitro* drug release studies

In-vitro drug release from IJP-GNP was observed to be significantly low in acidic pH. The release increased after changing the pH of media to 6.8 and was found to be higher with media having pH 7.4 containing cecal content. (Figure 4.3(A)).

4.9.7. Morphological evaluation

Morphological evaluation of P-GNP through TEM displayed spherical shape, while IJP-GNP revealed a corona surrounding the surface (Figure 4.3(B)).

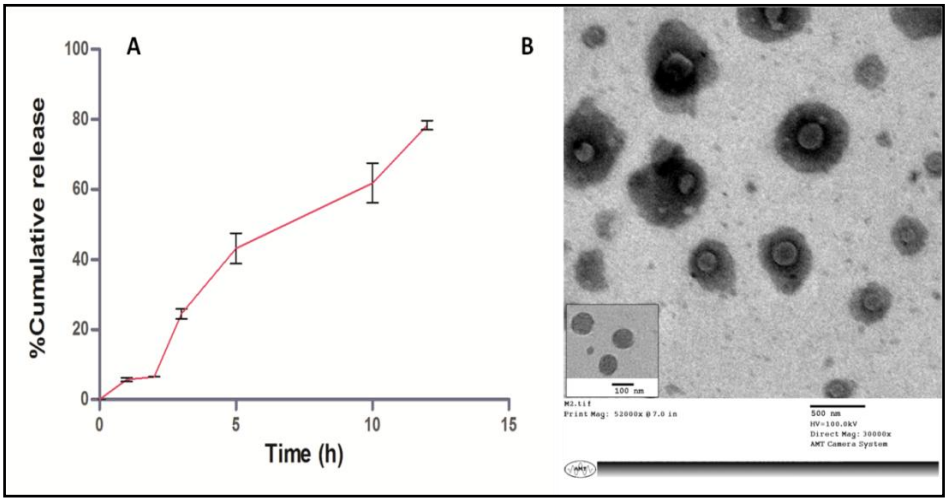

Figure 4.3 A- Percent of IP6 released as a function of time (h) from IJP-GNP. B- Morphological evaluation of P-GNP (inset) and IJP-GNP through TEM analysis

4.9.8. Cytotoxicity evaluation

All the synthesized formulations were appraised for their anti-cancer activity along with IP6 (as standard) against the development of HCT-15 colon cancer cell lines, in a dose as well as time-dependent way by utilizing MTT assay. The assay was performed for assessing cell growth inhibition, as shown in Table 4.4. Out of four treatments, IJP-GNP demonstrated critical cytotoxicity at lower concentrations (conc. 5, 10, 15, 20, 25 µM/ml) and rest were seen active at higher concentration. Formulations IJP-GNP and IP-GNP viably stalled the development of HCT-15 cells. IJP-GNP was found to be the most effective formulation in this arrangement with least IC50 (15 µM/ml) at 24 h treatment and sub IC50 (10 µM/ml) at 48 h against standard medication IC50 (30 µM/ml) at 24 h and sub IC50 (15 µM/ml) at 48 h against colon cancer cells. Furthermore, IP6 containing formulations did not display cytotoxicity against human normal colon epithelial cell (NCM460).

Table 4.4 The *in-vitro* cytotoxicity estimated as IC50 after 24 h, 48 h and 72 h

Treatment	IC50 values (µM /ml)					
	24 h	**24 h**	**48 h**	**48 h**	**72 h**	**72h**
	HCT 15	**NCM460**	**HCT 15**	**NCM460**	**HCT 15**	**NCM460**
P-GNP	62±0.03	>100	70± 0.02	>100	85±0.04	>100
IP-GNP	17±0.04	>100	15± 0.02	>100	10± 0.02	>100
IJP-GNP	15±0.02	>100	10± 0.02	>100	08± 0.02	>100
IP6	30±0.08	>100	32±0.01	>100	35.6±0.03	>100

4.9.9. Colony forming assay

The HCT-15 cells apparently formed 192 colonies after 12 h treatment of IJP-GNP. The number of colonies was reduced with augmentation in time of treatment with IJP-GNP formulation. The untreated HCT-15 cells were seen to generate the most extreme of 210 colonies after 24 h, Figure 4.4. The figure displayed the time and dose-dependent inhibition of colony development by IJP-GNP treatment.

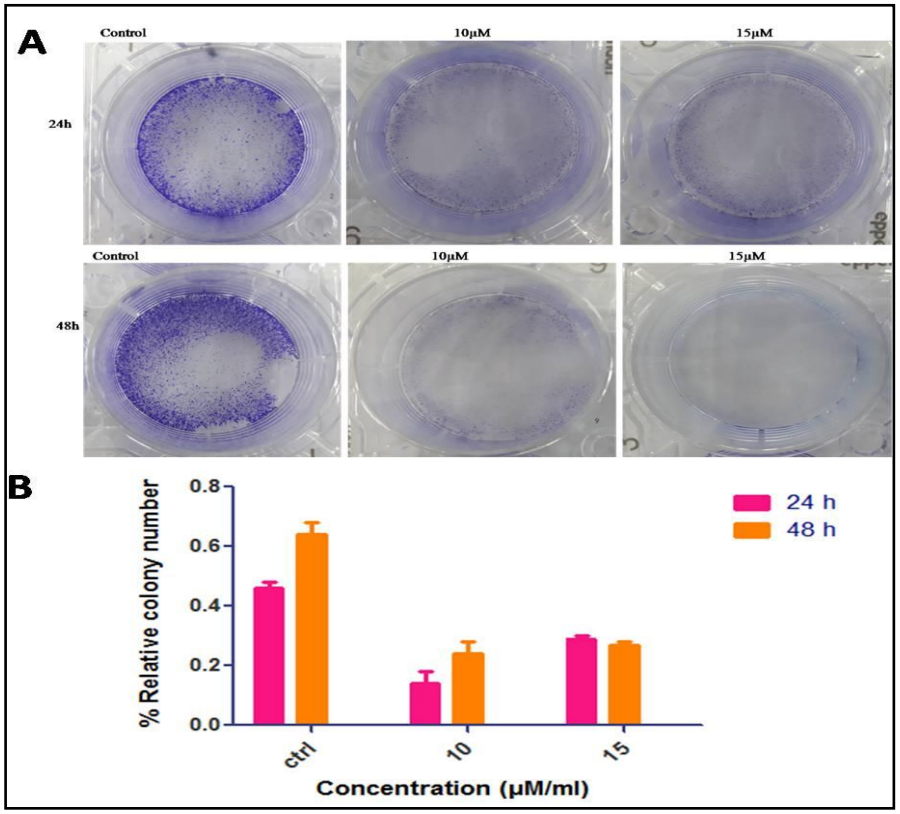

Figure 4.4 Effects of IJP-GNP on colony formation in HCT 15 cells. Cells were treated with 10 µM/ml and 15 µM/ml for 24 h and 48 h, stained with 0.5% crystal violet and was analyzed by flow camera , (A) Pictorial representation (B) Graphical representation

4.9.10. Cell cycle analysis

The flow cytogram displayed the percentage of HCT cell lines in the G0/G1 stage for IJP-GNP when contrasted with the sub IC50 and control. It was seen that IJP-GNP trigger G0/G1 cell cycle arrest when compared to untreated control cells, Figure 4.5, while, a consequent decrease of the synthetic phase (S-stage) of cells cycle was observed.

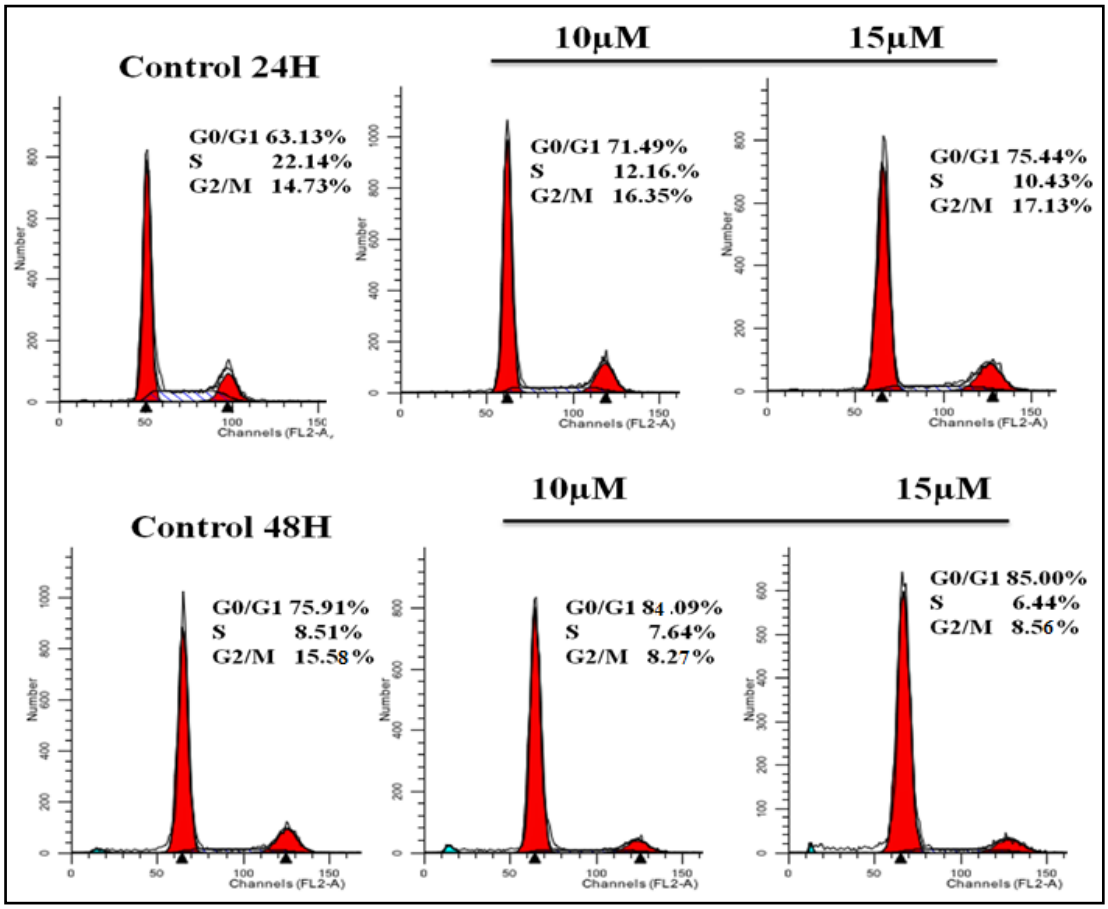

Figure 4.5 Effect of IJP-GNP on cell cycle progression in HCT 15. Cells were treated with IJP-GNP (10 µM/ml and 15 µM/ml) for 24 h and 48 h stained with PI and cell cycle analyzed by flow cytometry

4.9.11. Apoptosis induction

In order to evaluate the nuclear morphology of cells with the effect of IJP-GNP formulation, Hoechst 33258 staining was carried out using microscopy. Shrunken nucleus, peripherally clumped and fragmented chromatin was observed following the treatment with IJP-GNP formulation (Figure 4.6).

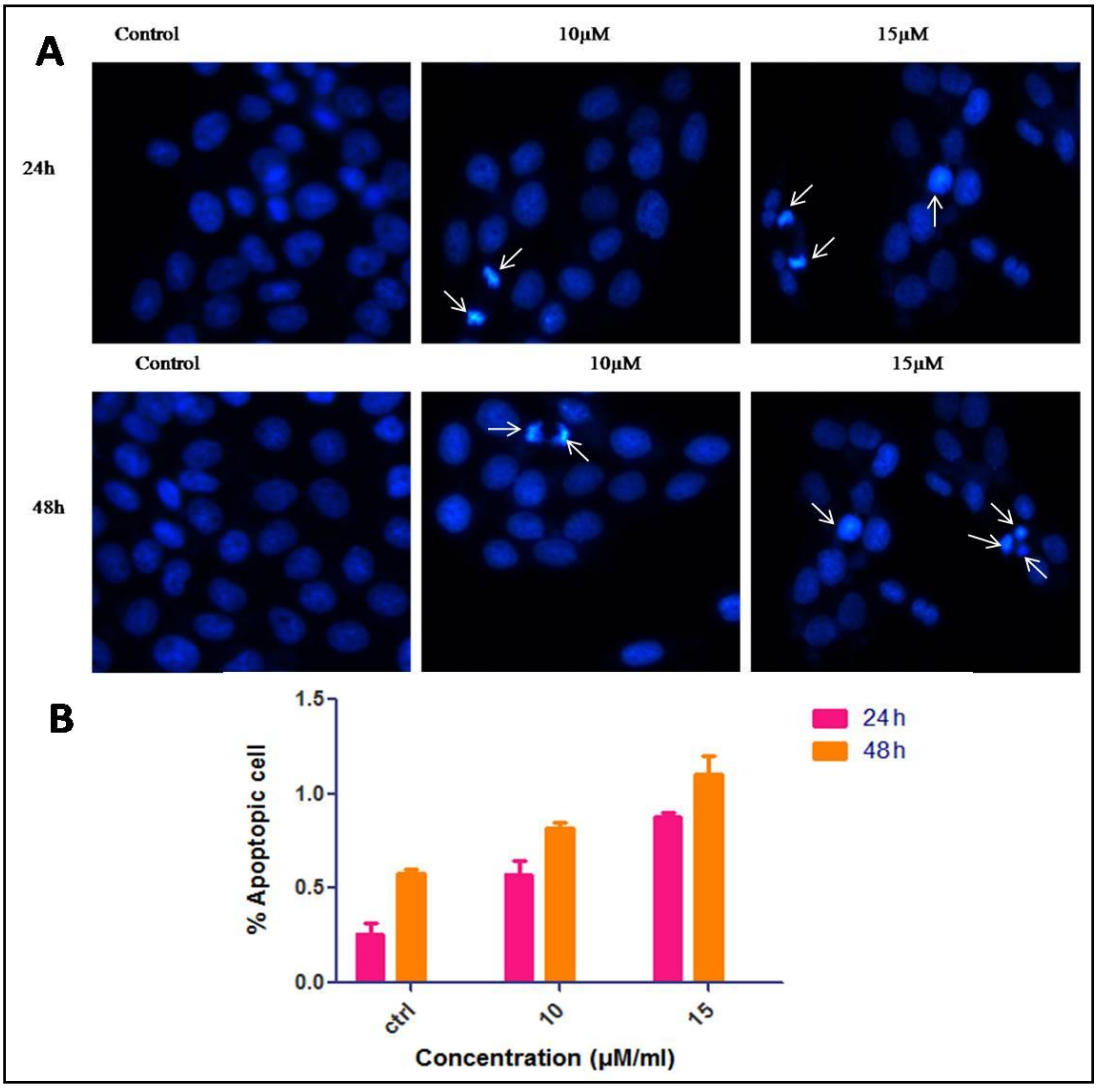

Figure 4.6 The treatment of HCT15 cells with IJP-GNP (10µM/ml and 15µM/ml for 24 h and 48 h) to indicate apoptotic cells with nuclear chromatin condensation and the formation of nuclear fragments and apoptotic bodies, (A) Pictorial representation (B) Graphical representation

4.9.12. AnnexinV-FITC and PI staining

In order to evaluate nuclear morphology to see the effect of IJP-GNP formulation, DAPI staining was done using microscopy in HCT15 cells. Shrunken nucleus, peripherally clumped and fragmented chromatin was seen. To further confirm our deliberations whether cell growth inhibition was coupled with physiological apoptosis, AnnexinV-FITC and PI dual staining was also carried out using flow cytometer. IJP-GNP displayed time as well as dose-dependent effects and increase of apoptotic cells (AnnexinV-FITC stained) and nonspecific necrotic (PI stained) population in the treatment when compared to untreated vehicle control, Figure 4.7.

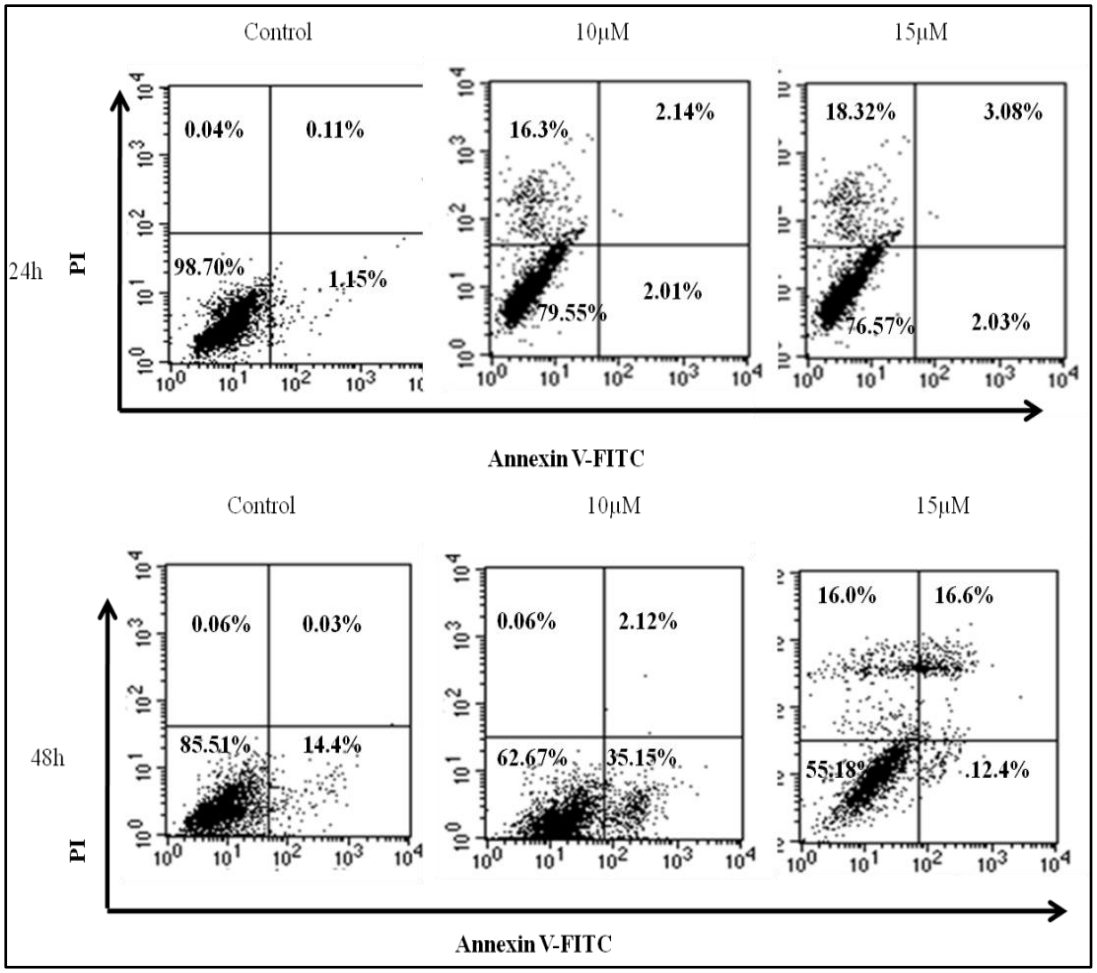

Figure 4.7 Effect of IJP-GNP on apoptosis in HCT 15 cells. Cells were treated with 10 µM/ml and 15 µM/ml concentrations of IJP-GNP for 24 h and 48 h. Apoptosis was analyzed by using AnnexinV-FITC/PI dual staining kit and flow cytometry

4.9.13. Activation of ROS

ROS plays a vital role in apoptosis induction under both physiological and pathological conditions. The HCT cells treated with IJP-GNP displayed a considerable increase in ROS intensity in a dose as well as time-dependent manner when contrasted with untreated cells (Figure 4.8).

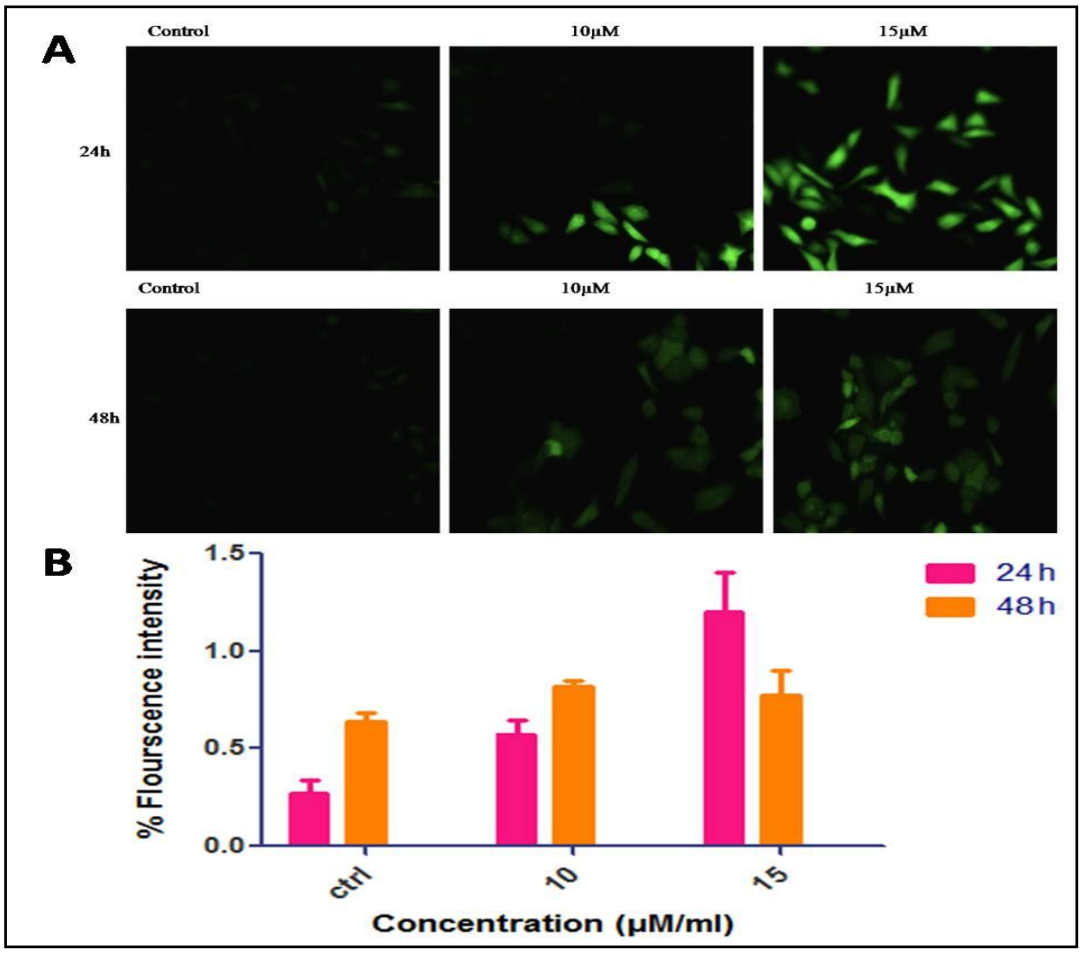

Figure 4.8 (A) Effect of sinapic acid on HCT 15 cells stained with DCFH-DA dye for 24 and 48 hrs. Generation of ROS levels during IJP-GNP treatment was measured spectrofluorimetrically by DCFH-DA staining. (B) % Fluorescence intensity of DCFH-DA dye in HCT 15 cells after exposure to IJP-GNP

4.9.14. *In-silico* analysis

The molecular characteristics and bioactivity of the compounds were determined by utilizing online data server Molinspiration and attained log P values along with other physiochemical properties, like molecular mass, the number of hydrogen bond acceptors and donors.

Table 4.5 *In-silico* determination of physicochemical pharmacokinetics for P-GNPS, IP6 by using online server Molinspiration

Compound	miLogP	Molecular weight	Hydrogen bond donor	Hydrogen bond acceptors
IJP-GNP	-0.51	196.97	0	0
IP6	-5.55	660.03	24	12

Table 4.6 *In-silico* determination of bioactivity score for IJP-GNPS and IP6 by using online server Molinspiration

Compound	GPCR ligand	Ion channel modulator	Kinase inhibitor	Nuclear receptor ligand	Enzyme inhibitor	Protease inhibitor
IJP-GNP	-3.87	-3.85	-3.87	-3.88	-3.85	-3.55
IP6	0.38	0.44	0.37	0.24	0.48	0.31

4.9.15. *In-silico* docking studies of IP6, P-GNP and IP-GNP with jacalin protein

The orientation and binding affinity of IP6, P-GNP and jacalin, in terms of the total docking score and binding residues with a docking score were 4098 and 2096 of IP6 and P-GNP respectively, when compared to the docking score of IJP-GNP complex, docking score which was 4422.

Table 4.7 Details of patch Dock score, inositol phosphate and gold NP with jacalin

Protein	Ligand	Score	-H Bond	Residues
1ku8	P-GNP	2096	LEU547	ILE108, ARG546, LEU547, GLY118, THR86, TYR73, SER575, SER597
1ku8	IP6	4098	ARG546	ILE108, ARG546, LEU547, GLY118, THR86, TYR73, ASN110, SER597
1ku8	IJP-GNP (Complex)	4422	LYS87(2) ASN643	LYS87, THR86, ASN110, ASN643, LYS87,PRO167,GLU67,MET86, ILE108

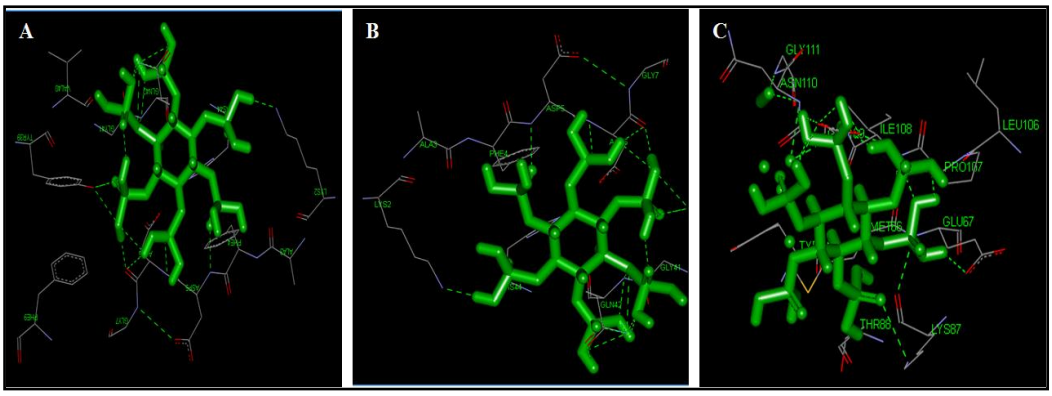

Figure 4.9 Representing the best conformation in the binding site of jacalin protein (A) IP6 (B) P-GNP (C) IJP-GNP

4.9.17. Hemodynamic changes

The IP6, IP-GNP and IJP-GNP affected diverse parameters of ECG when given to albino Wistar rats (Figure 4.10). Heart rate, P duration as well as QRS complex was seen higher in case of toxic control which was found to be normalized after IJP-GNP treatment. The lower frequency (LF) was found reduced in toxic control whereas raised significantly in the treatment groups. An analogous pattern was observed for higher frequency variables (HF) also (Table 4.8 and 4.9).

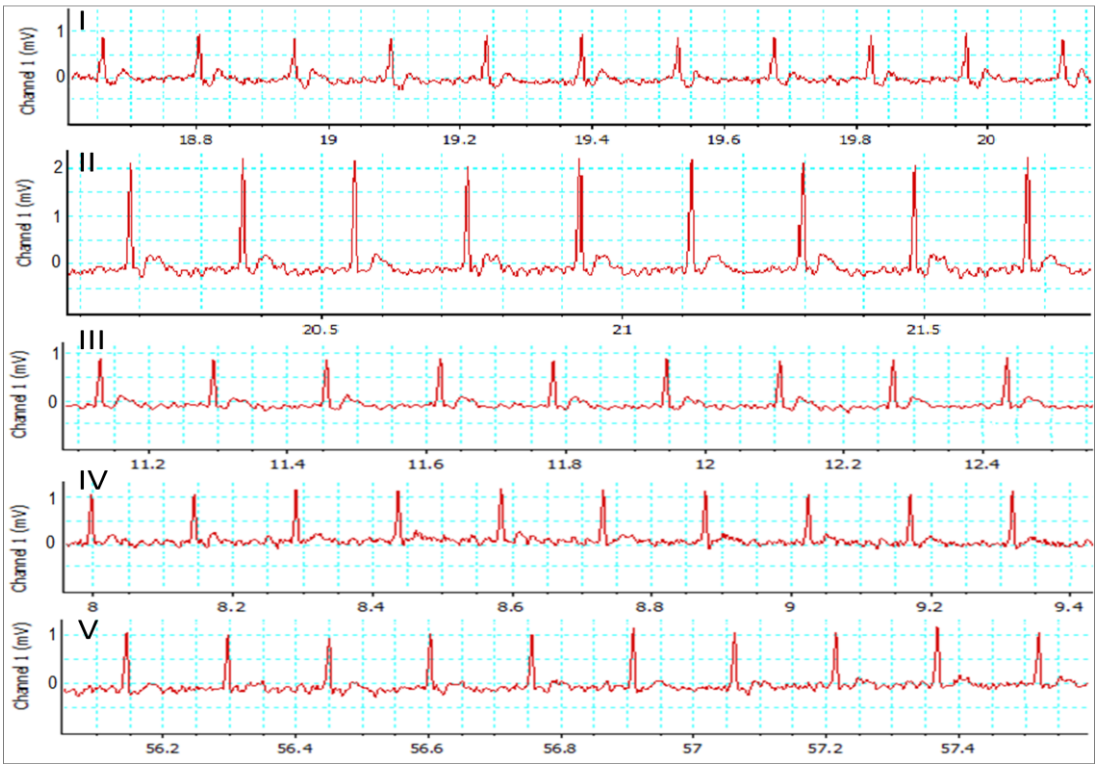

Figure 4.10 Representative ECG recordings of I- normal control, II- toxic control, III- standard, IV- IP-GNP and V- IJP-GNP, treated animals

Table 4.8 Effect of IP6, IP-GNP and IJP-GNP on ECG changes against DMH treatment to the animals, time domain

ECG Parameters	Normal control	Toxic control	Standard	IP-GNP	IJP-GNP
RR Interval(s)	0.18± 0.03	0.17± 0.01	0.17± 0.02	0.16± 0.01	0.17± 0.001
Heart Rate (BPM)	351.47± 27.66	382.47± 31.50	358.95± 27.71	358.48± 28.25	304.02± 15.04***
PR Interval(s)	0.04± 0.01	0.04± 0.02	0.04± 0.01	0.04± 0.01	0.04± 0.01
P Duration(s)	0.01± 0.001***	0.02± 0.001	0.01± 0.002***	0.01± 0.003***	0.01± 0.002***
QRS Interval(s)	0.01± 0.001***	0.02± 0.004	0.01± 0.004***	0.01± 0.002***	0.01± 0.007***
QT Interval(s)	0.05± 0.02	0.06± 0.01	0.06± 0.02	0.05± 0.03	0.05± 0.03
QTc(s)	0.13± 0.04	0.16± 0.04	0.13± 0.03	0.13± 0.04	0.10± 0.03
JT Interval(s)	0.04± 0.02	0.04± 0.02	0.03± 0.02	0.03± 0.02	0.02± 0.01
T peak Tend Interval(s)	0.02± 0.01	0.03± 0.01	0.02± 0.01	0.02± 0.01	0.02± 0.01
P Amplitude (mV)	0.09± 0.01	0.06± 0.02	0.05± 0.03	0.07± 0.01	0.03± 0.01**
Q Amplitude (mV)	0.01± 0.005***	0.04± 0.001	-0.05± 0.001***	-0.04± 0.003***	-0.16± 0.003***
R Amplitude (mV)	1.76±0.74	1.74± 0.04	0.92± 0.62	1.29± 0.58	0.55± 0.01**
S Amplitude (mV)	-0.18± 0.07***	-0.42± 0.03	-0.25± 0.01***	-0.07± 0.02***	-0.09± 0.03***
ST Height (mV)	0.01± 0.001	0.01± 0.008	0.003± 0.001	-0.02± 0.001***	-0.007± 0.005***
T Amplitude (mV)	0.19± 0.05***	0.46± 0.07	0.13± 0.02***	0.11± 0.02***	0.09± 0.02***

Values mentioned in mean±SD, n=8, comparisons were made with respect to toxic control using one-way ANOVA followed by Bonferroni multiple tests, *p<0.05, **p<0.01, ***p<0.001.

Table 4.9 Effect of IP6, IP-GNP and IJP-GNP on HRV changes against DMH treatment to the animals, frequency domain

HRV	Normal control	Toxic control	Standard	IP-GNP	IJP-GNP
Time Domain					
Average RR (ms)	173.71± 28.46	153.55± 27.39	170.97± 12.99	197.58± 14.23**	265.57± 7.10***
SDRR (ms)	7.48± 4.32**	15.92± 2.99	7.86± 2.16	7.17± 2.37***	7.02±3.96***
CVRR	0.06± 0.032**	0.02± 0.002	0.06± 0.01	0.06± 0.001*	0.06± 0.0001***
Frequency Domain					
LF (μs^2)	15.65± 8.86**	0.38±1.66	15.67± 3.01**	14.80± 6.45**	14.28±7.27**
HF (μs^2)	62.13± 13.95***	3.77±1.56	58.90± 11.86***	66.73± 9.36***	71.69± 16.67***
LF/HF(μs^2)	0.23± 0.04	0.18±0.06	0.27±0.03	0.21±0.08	0.20±0.09

Values mentioned in mean±SD, n=8, comparisons were made with respect to toxic control using one-way ANOVA followed by Bonferroni multiple tests, *p<0.05, **p<0.01, ***p<0.001.

4.9.18. Weight variation, pH, total acidity and ACF count

The toxic group animals displayed weight loss, decrease in pH along with increase in total acidity and formation of aberrant crypts when compared with control. Concomitant application of IP-GNP and IJP-GNP favorably regulated the weight and pH in the treated group animals. The total acidity along with ACF was also synchronized near to normal after IJP-GNP treatment (Table 4.10).

Table 4.10 Effect of IP6, IP-GNP and IJP-GNP on weight variation, pH, total acidity and ACF count against DMH induced colon carcinoma

Parameters	Normal control	Toxic control	Standard	IP-GNP	IJP-GNP
Weight variation (%)	18±2.31***	-6±0.02	13±1.34***	15±2.02***	16±3.11***
pH	7.23±0.52	6.5±0.41	6.86±0.44	6.99±0.32	7.42±0.51*
Total acidity (mEq/l)	118.34±12 .64	152.98± 23.64	121.24± 28.32	136.72± 18.93	111.31± 21.69*
Aberrant crypts (NoS)	17.61±2.8 9***	91.76± 3.63	58.19± 4.12***	23.42± 3.12***	18.14± 6.13***

Values mentioned in mean ±SD, n=8, comparisons were made with respect to toxic control using one-way ANOVA followed by Bonferroni multiple tests, *p<0.05, **p<0.01, ***p<0.001.

4.9.19. Antioxidant markers

DMH application significantly ($p<0.001$) dysregulated the level of protein carbonyl, MDA,GSH, SOD and catalase. IP-GNP and IJP-GNP treatment tried to restore the values towards normal (Table 4.11).

Table 4.11 Effect of IP6, IP-GNP and IJP-GNP on oxidative stress markers against DMH induced colon carcinoma

Parameters	Normal control	Toxic control	Standard	IP-GNP	IJP-GNP
Protein carbonyl (nM/ml)	0.64± 0.09***	2.24±0.07	1.43± 0.10***	0.91± 0.02***	0.67± 0.09***
TBARS (nM of MDA/µg of protein)	2.62± 0.06***	4.82±0.09	3.19± 0.02***	2.90± 0.08***	2.72± 0.10***
GSH*10^{-4} (µg %)	0.35± 0.03	0.29±0.01	0.31±0.02	0.43± 0.06***	0.46± 0.03***
SOD (unit of SOD/µg of protein)	1.84± 0.02***	1.66±0.03	1.69±0.02	1.74± 0.04***	1.82± 0.02***
Catalase(nM of H_2O_2 disappeared/ min/µg of protein)	0.62±0.07***	0.44±0.03	0.52±0.03*	0.59± 0.03***	0.63± 0.05***

Values mentioned in mean ±SD, n=8, comparisons were made with respect to toxic control using one-way ANOVA followed by Bonferroni multiple tests, *$p<0.05$, **$p<0.01$, ***$p<0.001$.

4.9.20. Morphological and histopathological evaluation

Toxic control animals displayed highest ACF count, abrupt crypts and loss of goblet cells, crypts and distorted lamina propria. Conversely, treatment with IP6, IP-GNP and IJP-GNP tried to restore the normal structure of colonic mucosa (Figure 4.11).

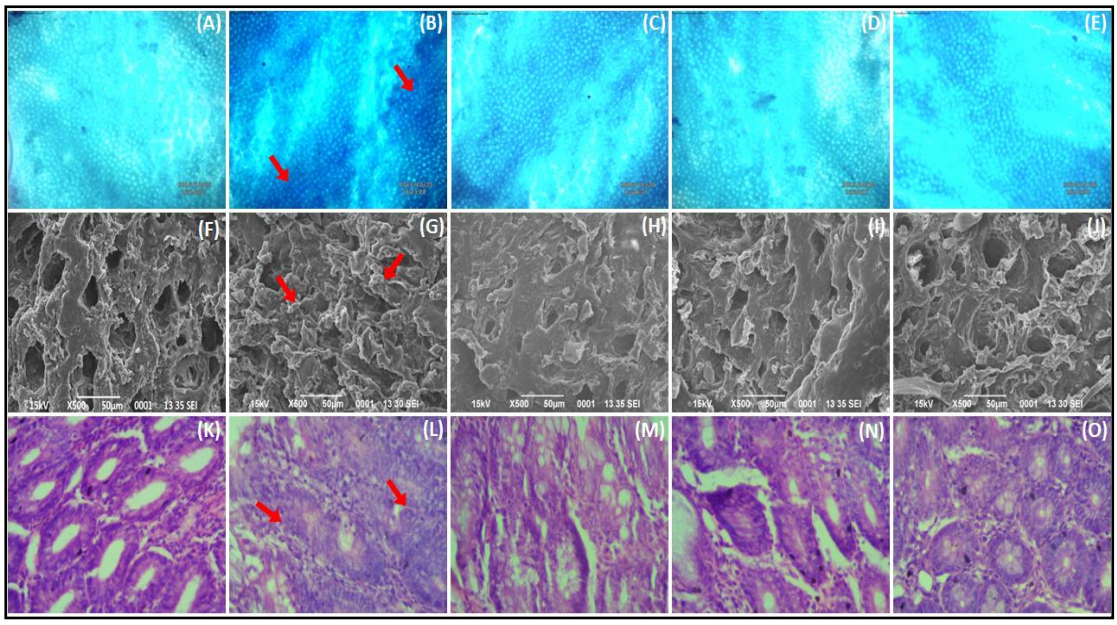

Figure 4.11 (A-E) Methylene blue stained colon tissues: A- normal control, B- toxic control, C- standard, D- IP-GNP and E- IJP-GNP, ➞ denotes aberrant crypts; (F-J) SEM (500X): F- normal control, G- toxic control, H- standard, I- IP-GNP and J- IJP-GNP, ➞ denotes aberrant crypts/ neoplastic lesions; (K-O) histopathological evaluation: K- normal control, L- toxic control, M- standard, N- IP-GNP and O- IJP-GNP, ➞ denotes aberration in colonic mucosa

4.9.21. Evaluation of altered gene expressions

Change in expressions of PI3K, Akt, and COX-2 genes was scrutinized through western blot and RT-PCR for protein and m-RNA levels respectively. Normal control was taken as the baseline (assumed with no up/ down regulation) and all comparisons were made with respect to it. The expressions of PI3K, Akt, and COX-2 proteins, as well as mRNA, showed a significant rise after DMH administration in the toxic control group. Treatment with IP6, IP-GNP and IJP-GNP helped to restore the expressions of above-mentioned genes. IJP-GNP revealed maximum restoration of protein as well as mRNA levels (Figure 4.12).

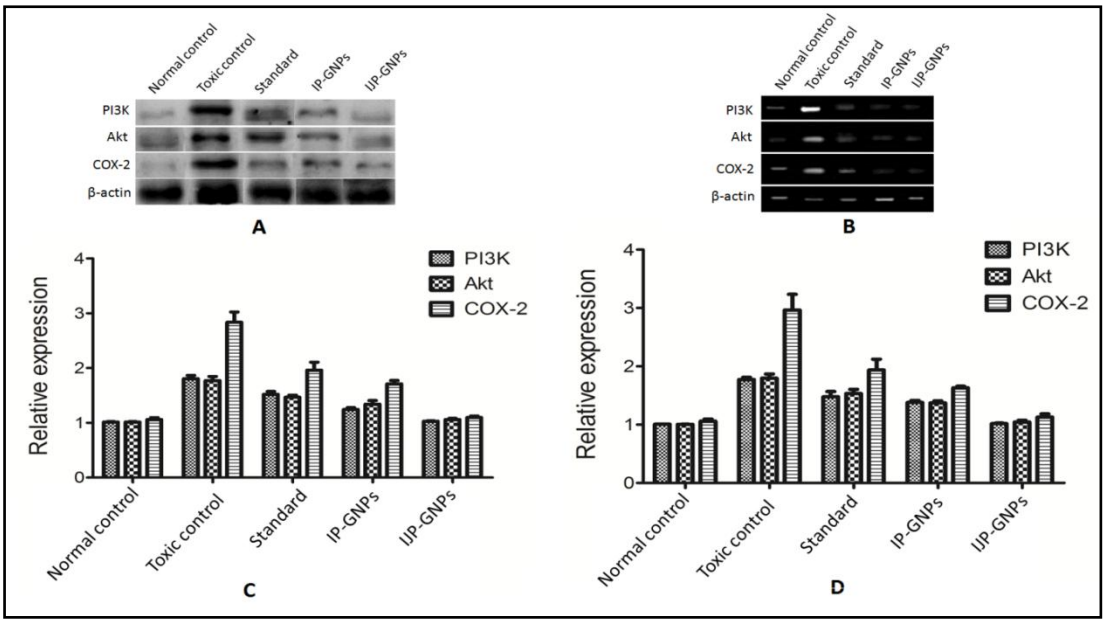

Figure 4.12 Effect of IP6, IP-GNP and IJP-GNP on DMH induced dysregulation of PI3K, Akt and COX-2. Quantitative analysis at the protein level (A and C) and at mRNA level (B and D). †p< 0.05, †† p < 0.01, ††† p < 0.001 (with respect to normal control) and *p< 0.05, ** p < 0.01, *** p < 0.001 (with respect to toxic control)

4.9.22. Serum metabolic profiling using ^{1}H NMR spectroscopy

The representative 1D ^{1}H CPMG NMR spectra of rat serum samples were obtained from different groups with the assigned resonances of relevant metabolites as shown in Figure 4.13. The major metabolites shown in the spectra were identified as per data reported in the literature and the Human Metabolome Database. The NMR spectra displayed signals from many metabolites including lipids/lipoproteins, polyunsaturated fatty acids (PUFAs) and amino acids (e.g. alanine, leucine, isoleucine, phenylalanine, valine, glutamine, lysine, histidine, tyrosine, glutamate etc.). Other recognized metabolites were glucose, creatine, creatinine, choline, acetate, pyruvate, citrate, ethanol, methanol and lactate. The multivariate data analysis was done to examine the DMH induced metabolic alterations and furthermore to reveal the effect of prepared formulations on these alterations, Figure 4.13 and 4.14.

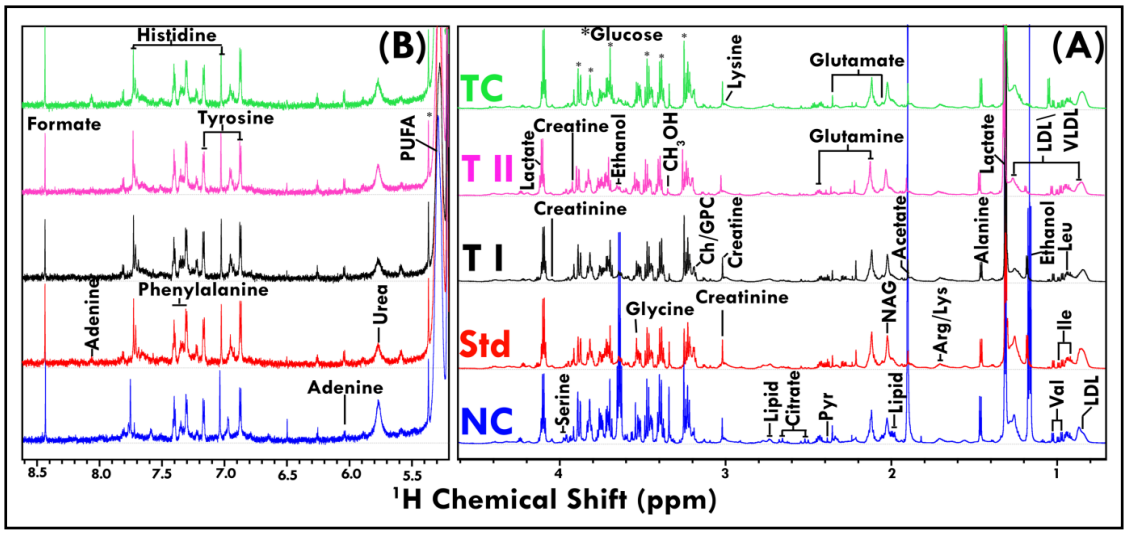

Figure 4.13 Stack plot of representative 1D 800-MHz ^{1}H CPMG NMR spectra (δ 0.7-4.6 and δ5.2-8.6) of rat serum of TC: Toxic control; TII: IJP-GNP; TI: IP-GNP; Std: IP6; NC: Normal control. The region of δ 5.2-8.6 (B) is magnified 8 times compared with the corresponding region of δ 0.7-4.6 (A) for the purpose of clarity. LDL/VLDL: Low/very-low-density lipoproteins; PUFA: polyunsaturated fatty acids; Ile: isoleucine; Leu: leucine; Val: Valine, Pyr: pyruvate; Ch: choline; GPC: glycerophosphocholine; Glucose resonances have been indicated using the symbol asterisk "*"; NAG: N-acetyl glycoprotein; OAG: O-acetyl glycoprotein; DMA: Dimethylamine

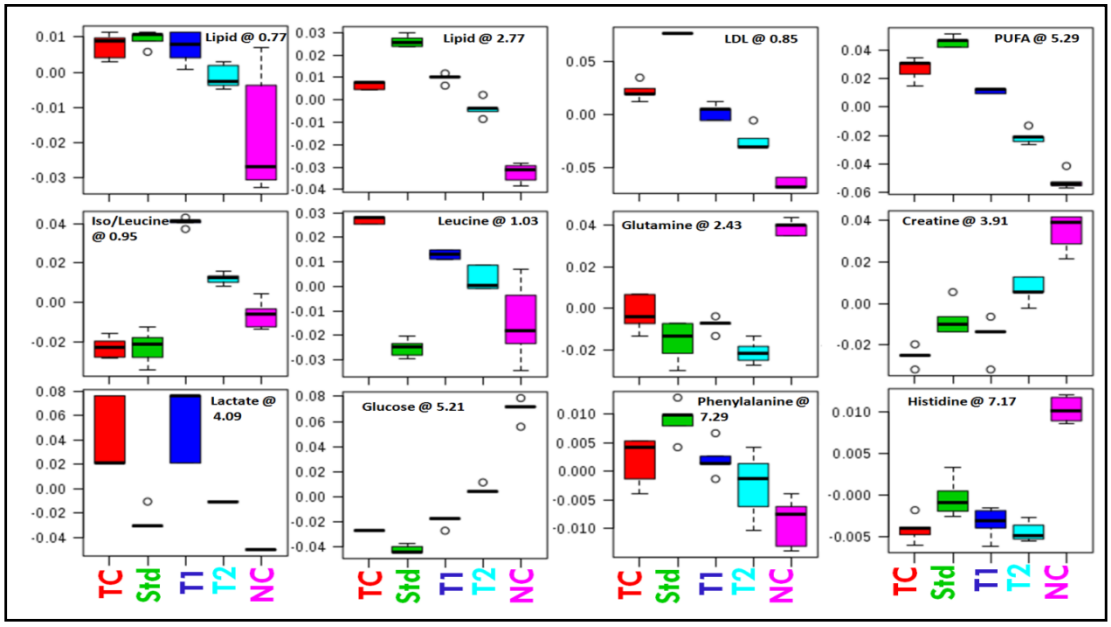

Figure 4.14 Representative box-cum-whisker plots showing quantitative variations of relative signal integrals for serum metabolites. Boxes denote interquartile ranges, horizontal line inside the box denote the median, and bottom and top boundaries of boxes are 25th and 75th percentiles, respectively. Lower and upper whiskers are 5th and 95th percentiles, respectively. TC: Toxic control; Std: IP6; T1: IP-GNP; T2: IJP-GNP; NC: Normal control

4.9.23. Metabolic changes

Unsupervised Principal Component Analysis (PCA) score plot was made for a primary overview of the data sets that demonstrated a clear trend of clustering in different groups and no outlier sample was seen(Figure 4.16). To obtain satisfactory classification and select metabolite markers, the pair-wise Partial Least Squares Discriminant Analysis (PLS-DA) analysis was performed further on NMR data matrices. The combined PLS-DA score plot for all the groups (Figure 4.15) and pair-wise PLS-DA score plots revealed that the DMH treated rats are significantly different from normal control (NC) group with a raised quality of fit and predictability (R^2 = 0.98, Q^2 = 0.94), which suggested significant metabolic changes in DMH treated rats when compared to NC. The metabolites which are responsible for discrimination of the two groups are shown in the loading plot in the prior latent variable of PLS-DA. The loading plots were colour-coded as per their absolute value of correlation coefficients (|r|), where a hot-coloured signal (red) designated more significant contribution to class separation than cold-coloured ones (blue). The significantly distinctive metabolites were determined according to values of variable importance on projection (VIP) scores, >1 and p<0.05. A number of metabolites were varied in the DMH treated group as compared to the normal control group. It was observed that DMH treated rats had higher levels of lipids, VLVL/LDL lipoprotein, PUFAs, lactate and pyruvate in their sera, on the contrary, they showed decreased levels of glucose and several amino acids when compared with the normal control group.

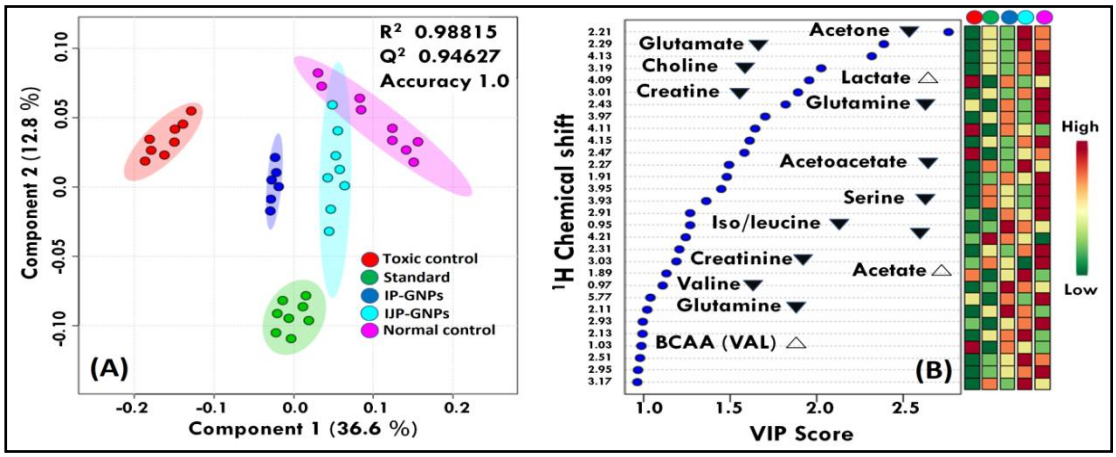

Figure 4.15 (A) PLS-DA score plot derived from 1D CPMG spectra of toxic control, standard, IP-GNP, IJP-GNP and normal control groups. (B) Variable importance in projection (VIP) plot demonstrating the metabolites responsible for the separation of various groups in the corresponding score plot shown in (A)

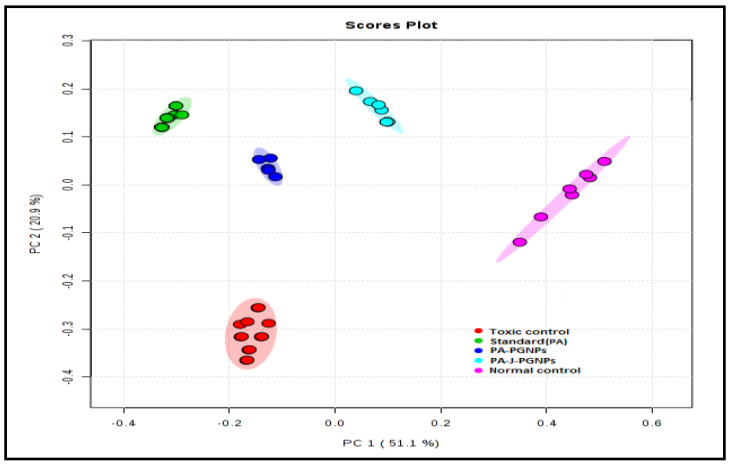

Figure 4.16 PCA score plot derived from 1D CPMG spectra of toxic control, standard, PA-PGNP, PA-J-PGNP and normal control groups

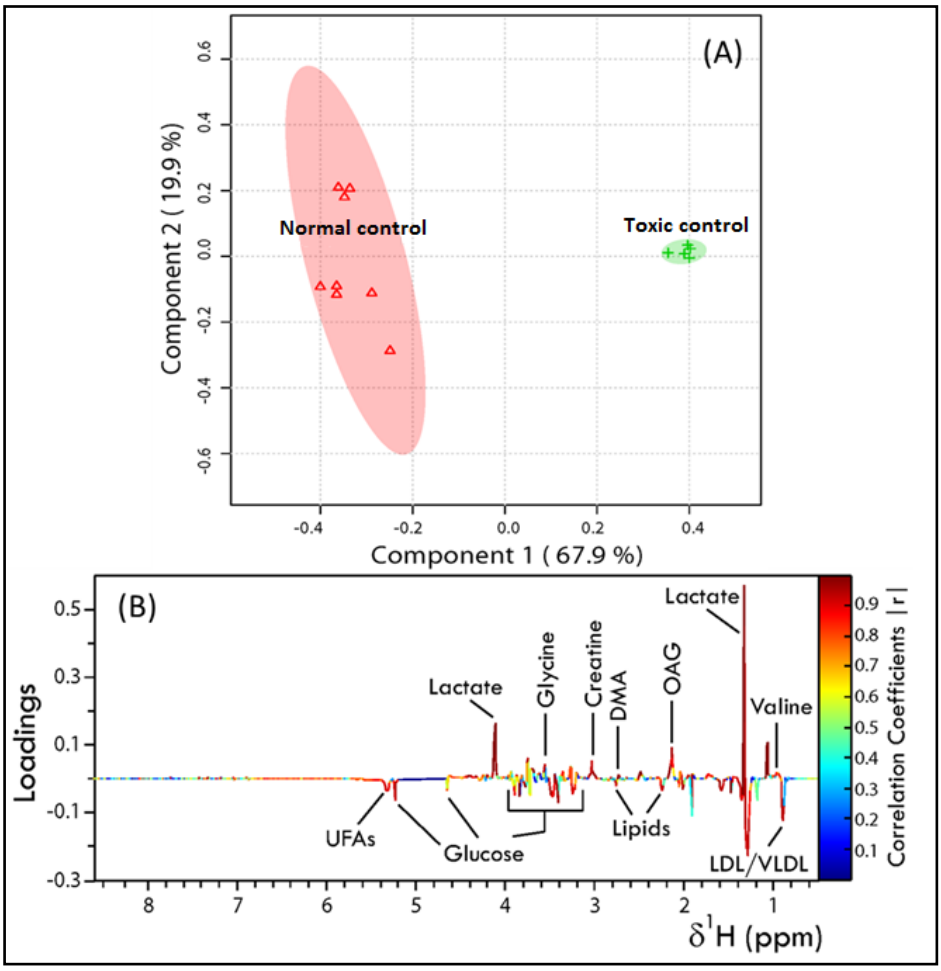

Figure 4.17 (A) PLS-DA score plot derived from 1D CPMG ^{1}H NMR spectra of serum samples obtained from normal control and DMH treated rats. **(B)** shows the corresponding colour-coded coefficient loading plot demonstrating the metabolites responsible for the discrimination of two groups. Peaks in the positive direction (>0) indicate the metabolites which are more abundant in the toxic control group and consequently, metabolites which are less abundant in the TC group are presented as peaks in the negative direction

The PLS-DA score plot shown in Figure 4.15 and 4.17 illustrates a marked discrimination between DMH treated rats and the group of rats which received the treatment with IP6 and formulation(s). Furthermore, it was found that the some of the metabolic alterations were observed in DMH treated group got ameliorated as an effect of IP-GNP and IJP-GNP treatment. Figure 4.14 displays the representative box-cum-whisker plots of the normalized integral area of a few metabolites which were modulated as a result of the action of IP-GNP and IJP-GNP treatment.

4.10. Discussions

IJP-GNP were produced by utilizing a green method of one-pot reduction of chloroauric acid by using pectin as reducing/ capping agent and jacalin as a surface modification agent. The inclusion of pectin as a reducing or capping agent was incited by virtue of it being a natural substance. Furthermore, pectin is a non-toxic agent and has the presence of carboxylate units that facilitates activation through jacalin. Jacalin is a lectin protein which has the ability to recognize as well as target tumour linked disaccharides which are largely expressed in almost all tumour cells. It contains functional groups like hydroxyl and amine that facilitate pectin activation [26, 55, 57]. In present studies, nanoparticles were selected for the purpose of drug attachment on to the pectin with gold as a core and jacalin and IP6 as the corona. Pectin assumed to facilitate interaction between the drug and the gold core. For this purpose, smaller nanoparticles may provide a much larger surface area, conversely, if bigger particles were utilized as the core they could have provided a higher volume but the lower surface area and hence gold nanoparticles proved to be a better choice. The change of colour from pale yellow to reddish purple confirmed the synthesis of P-GNP. The SPR of Au^{+} is responsible for the colour change phenomenon. When chloroauric acid was added to the pectin solution, –OH group of pectin would have bound to gold ions, probably through electron-rich oxygen atoms of –OH groups, as is anticipated to show interaction in an alkaline environment with electropositive metal cations. This would cause a reduction of Au^{+} ion to elemental gold. Moreover, pectin may also be involved in aggregation prevention through the layer formed on the gold nanoparticles, thereby acting as a reducing as well as capping agent [26, 55, 58]. The UV–visible spectra of formulations displayed absorption maxima at 520–530 nm which signified the formation of GNP [58]. Particle size increased with increasing concentration of chloroauric acid. According to previous researches, pectin functions

as a capping agent and also as a good stabilizer [55, 58]. Thus, when the concentration of chloroauric acid increased without increasing concentration of pectin, then less reducing and capping agent will be available which may contribute to increase in size of IJP-GNP. Consequently, the particle size of IJP-GNP can be controlled by regulating the concentration of chloroauric acid. The prepared metal particles were homogenous, as PDI values were < 0.5 for each concentration. Drug loading decreased with increasing concentration of chloroauric acid which may be attributed to the larger surface area of smaller particle size of metal nanoparticles that may allow attachment of more amounts of drug molecules. As a matter of fact, particle size below 100 nm may lead to nanotoxicity subsequent to internalization & non-biodegradability. Moreover, batch prepared with 3 mM (F3) of chloroauric acid showed optimum particle size and drug loading. FTIR analysis of IJP-GNP exhibited the shift in peaks of amines (1655.9 cm^{-1}, 1515.0 cm^{-1} and 1203.2 cm^{-1}) and hydroxyl (3417.5 cm^{-1}) of jacalin and IP6 respectively which may be due to their involvement in complex formation. Further, the spectra of IJP-GNP displayed all the characteristic peaks of IP6 and jacalin suggesting the surface decoration through corona of IP6 and jacalin. The absence of the peak of gold signified the complete coverage by this corona. Lesser drug release observed at acidic pH and higher in alkaline pH may be due to the fact that the pectin contains carboxyl groups in its structure which ionizes in neutral to alkaline pH. Besides, pectin degrades in the colonic microflora [59, 60]. Due to the ionization/ enzymatic degradation of pectin, the corona containing jacalin and IP6 would breakdown thereby releasing the drug in this particular pH. Morphological analysis of IJP-GNP through TEM revealed a corona surrounding the particulate surface which may be due to the formation of a layer of jacalin and IP6 around the P-GNP.

Cytotoxicity evaluation through MTT assay revealed that, in any case, IJP-GNP all the more adequately repressed HCT-15 cells when contrasted with other formulations and standard IP6. This superior inhibition effect may be attributed to the better cellular interaction due to the presence of jacalin protein, which has the property of recognition and attachment to the cancerous cells [13, 61, 62]. Thus IJP-GNP could have penetrated to cause maximum cell death. The inhibitory effect of IJP-GNP was found to be in accordance with earlier reports which projected IP6 as a potential antiangiogenic agent [63, 64]. The comparable IC50 value for IP6 has been accounted

by different analysts [65]. Besides, IP6 containing formulations did not indicate cytotoxicity against NCM460, which may be due to the use of naturally existing agents. Furthermore, it is the inherent property of IP6 that it affects only the cancerous cells and does not invade the normal cells of the body [24, 64]. This cytotoxicity information recommended that IJP-GNP was the most active formulation against HCT-15 in contrast with different formulations tested and also was safe for normal cells. As IJP-GNP was found most effective, thus, it was taken for further evaluations. As per colony forming assay, a huge reduction ($P < 0.05$) in the number of colonies formed under the different time intervals was seen when compared with untreated cells. This was attributed to the longer inhibition of the effect of IP6 loaded formulations. Further, it was indicated that IJP-GNP could cause cytotoxicity as well as inhibition. Cell cycle analysis displayed that mostly, IJP-GNP analysis is seen to induce G2/M arrest. In this perspective, we trust that the G1 arrest in cell cycle examination may recommend mitotic slippage into pseudo G1 followed by cellular termination. Low concentration of IJP-GNP (10 µM/ml) appeared to instigate G1 arrest. This effect of IJP-GNP may be attributed to the presence of IP6 as it is well known to show G1 arrest and apoptotic death of cancerous cells [66]. However, induction of cell cycle arrest in cancer cell lines constitutes one of the most prevalent strategies to stop or limit cancer spreading. Apoptosis induction studies revealed Shrunken nucleus, peripherally clumped and fragmented chromatin was seen following the treatment with IJP-GNP formulation, a typical characteristic of cells when undergoing apoptosis (Figure 4.7), which indicates the effective apoptosis due to the presence of IP6 [64, 66]. IJP-GNP displayed a time as well as dose-dependent increase of apoptotic cells (AnnexinV-FITC stained) and nonspecific necrotic (PI stained) population in the treatment when compared to untreated vehicle control, which is again indicating the call of apoptotic effect of IP6. Furthermore, accumulation of ROS is coupled with rise in oxidative stress and implicates the pathogenesis of several diseases together with cancers [67]. The results of the quantitative measurement of ROS revealed that 10 µM/ml of IJP-GNP induced 104.43% ($p<0.05$) enhancement in ROS production as compared to control. Moreover, ROS production was increased by 160.53% ($p<0.05$) at 15 µM/ml of IJP-GNP when compared to untreated cells. During apoptosis, ROS was produced by mitochondria which was responsible for raising the mitochondrial membrane permeability and lead to the apoptotic phenotype [68]. Our results clearly stated that

IJP-GNP triggered the cells death by ROS generation. As per *in-silico* analysis, molecules violating more than one of the Lipinski's rules may have problems with bioavailability. The combination of GPCR, ion channel modulator, kinase inhibitor, nuclear receptor ligands, protease inhibitor and enzyme inhibitor is assigned as druglikeness score that has been used to investigate the compounds potential to qualify as a drug. As a general rule, the larger the bioactivity score, the higher is the probability of the particular molecule to be active [69]. Therefore, a molecule having bioactivity score more than 0.00 is most likely to possess considerable biological activities, while values -0.50 to 0.00 are expected to be moderately active and if the score is less than -0.50 it is presumed to be inactive [70]. On this basis, the obtained values of druglikeness score showed that IJP-GNPS exhibited good druglikeness score (>0.50) when compared with the standard drug, IP6 (Table 4.5 and 4.6). The greater binding energy was observed in complex IJP-GNP as compared with single binding with IP6 as well as P-GNP with jacalin. The docking results revealed the interactive properties of IP-GNP complex with jacalin and suggested that it could inhibit tumour formation activity and supported further *in-vitro* studies, which proved that the IJP-GNP may inhibit the growth of colon cancer. This could be one of the mechanisms by which the complex of IJP-GNP exerts its chemopreventive or chemotherapeutic effects.

In-vivo studies displayed that, depreciated ECG and HRV are related with cancer patients. Higher HRV is linked with the low-level tumour markers and lower HRV is coupled with the autonomic dysfunction in advanced cases of cancer. A similar pattern of reduced HRV was apparent in the DMH treated animals, in time as well as frequency domain. Application of IP6, IP-GNP and IJP-GNP revealed considerable restoration of time and frequency domain paradigms towards normal values (Table 4.8 and 4.9) which may be due to the action of IP6. Oxygen radicals supplement all stages of the multistep process of cancer progression [71]. There is an established connection between colon cancer progression and serious oxidative stress. Previous studies have reported raised levels of lipid peroxide and protein carbonyl and reduced SOD, catalase and GSH in clinical stage IV of colon cancer [72]. Present studies, also inveterate the decrease in SOD, catalase and GSH levels in colon tissue of DMH treated animals which may be due to the initiation of colon cancer [73, 74]. IJP-GNP

displayed maximum restoration (Table 4.11) of these biochemical changes towards normal validating the maximized efficacy of IP6 in the form of IJP-GNP.

Cell deterioration and abnormal proliferation lead to abnormalities in the architecture of crypts known as aberrant crypts, which ultimately cause invasive cancers [75, 76]. The highest restoration was of ACF count by IJP-GNP (Figure 4.11) which may be because of targeted delivery into the affected cells due to the presence of jacalin. The histopathological analysis of normal colon tissue depicted three layers including mucosa, submucosa and muscularis. The intact architecture of colonic mucosa was seen in the normal control group describing all the three layers, in contrast to the toxic group animals which showed abrupt/ impaired arrangement of cells (Figure 4.11(L)). The IJP-GNP application showed maximum similarity with the normal control group which could again be a call out of targeting to the required site because of jacalin.

Earlier studies have reported the involvement of IP6 in the inhibition of PI3K/Akt [2, 77] and β- catenin and COX-2 [78] pathways. Consequently, we found it significant to analyze the efficacy of IP6 formulation(s) against DMH induced dysregulation of PI3K, Akt and COX-2. PI3K is a lipid kinase and a second messenger which translocates Akt to the plasma membrane, where it phosphorylates to activate PDK1 and PDK2. Variations in the PI3K-Akt signalling pathway have already been seen frequently in human cancers. The developments, as well as the progression of cancers, are the result of interruptions in the equilibrium of cell proliferation and cell apoptosis. Eventually, PI3K-Akt signalling is associated with both of these events and imparts a vital role in tumour growth as well as tumour treatment [2, 79]. DMH treatment revealed significant upregulation of PI3K and Akt at protein and mRNA levels. Application of IP-GNP and IJP-GNP conveyed favourable restoration. To further boost up the pondering, we examined the expression of COX-2. COX-2 is a well documented inflammatory marker involved in tumour progression [80]. DMH application prompted a significant upregulation of the COX-2 protein and mRNA expression, in toxic control. Concomitant application of the IP-GNP and IJP-GNP displayed significant restoration (Figure 4.12) which validated the inhibitory action of IP6 for aforesaid enzymes.

^{1}H NMR based metabolic profiling was carried out to explore the biochemical changes linked with colon cancer and to further examine how these changes get modulated in rats receiving the treatment with IP6 formulation(s). Increased levels of

lipoproteins and PUFAs in DMH treated animals entails rapid cellular regeneration and the high cancer cell lipid demand for cell membrane biosynthesis [81]. The lesser concentration of choline and its derivatives may be correlated with the rapid cellular regeneration in tumours. Serum creatine was lowered considerably in DMH treated rats and this can be associated with the increase in energy consumption due to rapid cell division. Raised levels of amino acids in DMH rats suggest an increased catabolism because of the rapid cell proliferation [82, 83]. Furthermore, a reduced level of glucose designated the increase in glucose metabolism through glycolysis to generate ATP instead of oxidative phosphorylation that enhances the glucose uptake in tumour cells to meet the energy requirement of fast proliferation. The higher glycolytic rates in tumour cells also result in the generation of huge quantities of lactate from pyruvate and thus supported our result of raised serum levels of lactate in toxic control rats. The observed lowering of levels of glucose and an increase in lactate levels are consistent with earlier researches dealing with human rectal cancer [84]. Dimethylamine, a product of choline metabolism, was also observed to be altered in the DMH treated rats demonstrating the interruption of choline metabolism. Furthermore, the raised serum levels of N- and O-acetyl glycoproteins imitate a nonspecific inflammatory response in DMH treated rats. The disturbed metabolic pathways discussed above lead us to infer the acceleration of cell proliferation in the process of tumour formation, hyperplasia in colonic mucosa and rise in inflammation in DMH taking rats. Almost all metabolic changes in DMH treated animals were returned back towards normal after IP6 formulation(s) applications, signifying that the formulation(s) has potential to normalize the DMH altered metabolic changes.

4.11. Conclusions

The formulations, P-GNP, IP-GNP and IJP-GNP were prepared and evaluated successfully. Formulations were screened for the anticancer studies on the basis of the cytotoxicity observed on HCT 15 cells in a dose and time-dependent manner. Amongst all, IJP-GNP was found to be the most potent formulation with the lowest IC50 value. IJP-GNP caused cell cycle arrest at the G0/G1 phase, induced ROS and subsequent apoptosis. The docking results showed that the interactive properties of IP-GNP complex with jacalin could inhibit the tumour formation activity and supported *in-vitro* studies, which proved that the IJP-GNP inhibited the growth of colon cancer. Furthermore, *in-vivo* studies suggested that IJP-GNP displayed

significant effect against progression of colon carcinogenesis by positively modulating the physiological markers, hemodynamic changes, oxidative stress, inflammatory markers and serum metabolomics. All in all, results confirmed that IP6 formulation(s) could constitute a promising tool for the anticipation of DMH induced neoplastic damage, dysregulation of proliferation markers and metabolic changes.

4.12. References

1. Arnold M, Sierra MS, Laversanne M, Soerjomataram I, Jemal A, Bray F. Global patterns and trends in colorectal cancer incidence and mortality. Gut. 2016:gutjnl-2015-310912.
2. Liu G, Song Y, Cui L, Wen Z, Lu X. Inositol hexaphosphate suppresses growth and induces apoptosis in HT-29 colorectal cancer cells in culture: PI3K/Akt pathway as a potential target. International journal of clinical and experimental pathology. 2015;8(2):1402.
3. Wang K, Liu P, Ye Y, Li J, Zhao W, Huang X. Fabrication of a novel laccase biosensor based on silica nanoparticles modified with phytic acid for sensitive detection of dopamine. Sensors and Actuators B: Chemical. 2014;197:292-9.
4. Saad N, Esa NM, Ithnin H, Shafie NH. Optimization of optimum condition for phytic acid extraction from rice bran. African Journal of Plant Science. 2011;5(3):168-75.
5. Shamsuddin AM. Metabolism and Cellular Functions of IP6. A Review. Anticancer Research. 1999;19(5):3733-6.
6. He L, Musick MD, Nicewarner SR, Salinas FG, Benkovic SJ, Natan MJ, et al. Colloidal Au-enhanced surface plasmon resonance for ultrasensitive detection of DNA hybridization. Journal of the American Chemical Society. 2000;122(38):9071-7.
7. Ghosh P, Han G, De M, Kim CK, Rotello VM. Gold nanoparticles in delivery applications. Adv Drug Deliv Rev. 2008;60(11):1307-15.
8. Barreto JA, O'Malley W, Kubeil M, Graham B, Stephan H, Spiccia L. Nanomaterials: applications in cancer imaging and therapy. Advanced Materials. 2011;23(12).
9. Nghiem THL, La TH, Vu XH, Chu VH, Nguyen TH, Le QH, et al. Synthesis, capping and binding of colloidal gold nanoparticles to proteins. Advances in Natural Sciences: Nanoscience and Nanotechnology. 2010;1(2):025009.
10. Medley CD, Bamrungsap S, Tan W, Smith JE. Aptamer-conjugated nanoparticles for cancer cell detection. Analytical chemistry. 2011;83(3):727-34.
11. Yang L, Mao H, Wang YA, Cao Z, Peng X, Wang X, et al. Single chain epidermal growth factor receptor antibody conjugated nanoparticles for in vivo tumour targeting and imaging. Small. 2009;5(2):235-43.
12. Hakomori S. Glycosylation defining cancer malignancy: new wine in an old bottle. Proceedings of the National Academy of Sciences. 2002;99(16):10231-3.
13. Danella Polli C, Pereira Ruas L, Chain Veronez L, Herrero Geraldino T, Rossetto de Morais F, Roque-Barreira MC, et al. Jacalin-activated macrophages exhibit an antitumour phenotype. BioMed Research International. 2016;2016.
14. Lis H, Sharon N. Lectins: carbohydrate-specific proteins that mediate cellular recognition. Chemical reviews. 1998;98(2):637-74.

15. Ruffet E, Paquet N, Frutiger S, Hughes GJ, Jaton J-C. Structural and electron-microscopic studies of jacalin from jackfruit (Artocarpus integrifolia) show that this lectin is a 65 kDa tetramer. Biochemical Journal. 1992;286(1):131-4.

16. Mody R, antaram Joshi S, Chaney W. Use of lectins as diagnostic and therapeutic tools for cancer. Journal of pharmacological and Toxicological Methods. 1995;33(1):1-10.

17. Sastry M, Banarjee P, Patanjali SR, Swamy M, Swarnalatha G, Surolia A. Analysis of saccharide binding to Artocarpus integrifolia lectin reveals specific recognition of T-antigen (beta-D-Gal (1----3) D-GalNAc). Journal of Biological Chemistry. 1986;261(25):11726-33.

18. Jeyaprakash AA, Rani PG, Reddy GB, Banumathi S, Betzel C, Sekar K, et al. Crystal structure of the jacalin–T-antigen complex and a comparative studies of lectin–T-antigen complexes. Journal of molecular biology. 2002;321(4):637-45.

19. Singh S, Kotla NG, Tomar S, Maddiboyina B, Webster TJ, Sharma D, et al. A nanomedicine-promising approach to provide an appropriate colon-targeted drug delivery system for 5-fluorouracil. International journal of nanomedicine. 2015;10:7175.

20. Liu J, Zhang L, Jia Y, Hu W, Zhang J, Jiang H. Preparation and evaluation of pectin-based colon-specific pulsatile capsule in vitro and in vivo. Archives of pharmacal research. 2012;35(11):1927-34.

21. Safwat MA, Soliman GM, Sayed D, Attia MA. Gold nanoparticles enhance 5-fluorouracil anticancer efficacy against colorectal cancer cells. International journal of pharmaceutics. 2016;513(1-2):648-58.

22. Liu X, Atwater M, Wang J, Huo Q. Extinction coefficient of gold nanoparticles with different sizes and different capping ligands. Colloids and Surfaces B: Biointerfaces. 2007;58(1):3-7.

23. Borker S, Patole M, Moghe A, Pokharkar V. Engineering of pectin-reduced gold nanoparticles for targeted delivery of an antiviral drug to macrophages: in vitro and in vivo assessment. Gold Bulletin. 2017;50(3):235-46.

24. Arya M, Tiwari P, Tripathi CB, Parashar P, Singh M, Sinha P, et al. Colloidal vesicular system of Inositol hexaphosphate to counteract DMBA induced dysregulation of markers pertaining to cellular proliferation/differentiation and inflammation of epidermal layer in mouse model. Mol Pharm. 2017;14(3):928-39.

25. Izadi Z, Divsalar A, Saboury AA, Sawyer L. β-lactoglobulin–pectin Nanoparticle-based Oral Drug Delivery System for Potential Treatment of Colon Cancer. Chemical biology & drug design. 2016;88(2):209-16.

26. Verma J, Kanoujia J, Parashar P, Tripathi CB, Saraf SA. Wound healing applications of sericin/chitosan-capped silver nanoparticles incorporated hydrogel. Drug delivery and translational research. 2017;7(1):77-88.

27. Kandzari SJ, Riggs D, Jackson B, Luchey A, Oliver C, Zaslau S. In vitro regulation of cell growth and angiogenesis by inositol hexaphosphate in bladder cancer. Current urology. 2012;6(4):199-204.

28. Kaleem S, Siddiqui S, Siddiqui HH, Hussain A, Arshad M, Akhtar J, et al. Eupalitin induces apoptosis in prostate carcinoma cells through ROS generation and increase of caspase-3 activity. Cell Biol Int. 2016;40(2):196-203.

29. Saini KS, Ajay A, Devender N, Bhattacharjee A, Das S, Dwivedi S, et al. Triazole analog 1-(1-benzyl-5-(4-chlorophenyl)-1H-1, 2, 3-triazol-4-yl)-2-(4-bromophenylamino)-1-(4-

chlorophenyl) ethanol induces reactive oxygen species and autophagy-dependent apoptosis in both in vitro and in vivo breast cancer models. Int J Biochem Cell Biol. 2015;65:275-87.

30. Hallstrom TC, Nevins JR. Balancing the decision of cell proliferation and cell fate. Cell Cycle. 2009;8(4):532-5.
31. Alam A, Shaikh S, S Ahmad S, A Ansari M, Shakil S, MD Rizvi S, et al. Molecular interaction of human brain acetylcholinesterase with a natural inhibitor Huperzine-B: An Enzoinformatics approach. CNS & Neurological Disorders-Drug Targets (Formerly Current Drug Targets-CNS & Neurological Disorders). 2014;13(3):487-90.
32. Chattopadhyay I, Biswas K, Bandyopadhyay U, Banerjee RK. Turmeric and curcumin: Biological actions and medicinal applications. Curr Sci. 2004;87:44-53.
33. Parvathy K, Negi P, Srinivas P. Curcumin–amino acid conjugates: synthesis, antioxidant and antimutagenic attributes. Food Chem. 2010;120(2):523-30.
34. Sirajuddin M, Ali S, McKee V, Ullah H. Synthesis, spectroscopic characterization and in vitro antimicrobial, anticancer and antileishmanial activities as well interaction with Salmon sperm DNA of newly synthesized carboxylic acid derivative, 4-(4-methoxy-2-nitrophenylamino)-4-oxobutanoic acid. Spectrochim Acta A Mol Biomol Spectrosc. 2015;138:569-78.
35. Chaudhary HT, Hasnain S. In-silico analysis; analysis of S-303 binding to CD-61 of platelets. The Professional Medical Journal. 2016;23(2).
36. Shukla K, Raj P, Kumar A, Kumar M, Kaithwas G. Effect of monotherapy and combination therapy of pantoprazole and aprepitant in gastric esophageal reflux disease in albino rats. The Scientific World Journal. 2014;2014.
37. Khinchi P, Saha S, Saraf SA, Kaithwas G. Combination therapy of gamma-aminobutyric acid derivative promotes proton pump inhibitor based healing of reflux esophagitis in animal model. Pharmacol Rep. 2014;66(1):165-8.
38. Kumar S, Singh M, Rawat JK, Gautam S, Saraf SA, Kaithwas G. Effect of rutin against gastric esophageal reflux in experimental animals. Toxicology mechanisms and methods. 2014;24(9):666-71.
39. Bird RP. Observation and quantification of aberrant crypts in the murine colon treated with a colon carcinogen: preliminary findings. Cancer Lett. 1987;37(2):147-51.
40. Gupta SK, Gautam S, Rawat JK, Singh M, Saraf SA, Kaithwas G. Efficacy of variable dosage of aspirin in combating methotrexate-induced intestinal toxicity. RSC Advances. 2015;5(13):9354-60.
41. Mishra RK, Sammi SR, Rawat JK, Roy S, Singh M, Gautam S, et al. Palonosetron attenuates 1, 2-dimethyl hydrazine induced preneoplastic colon damage through downregulating acetylcholinesterase expression and up-regulating synaptic acetylcholine concentration. RSC Advances. 2016;6(46):40527-38.
42. Singh M, Kanoujia J, Parashar P, Arya M, Tripathi CB, Sinha V, et al. Augmented bioavailability of felodipine through an α-linolenic acid-based microemulsion. Drug delivery and translational research. 2017:1-22.
43. Guleria A, Pratap A, Dubey D, Rawat A, Chaurasia S, Sukesh E, et al. NMR based serum metabolomics reveals a distinctive signature in patients with Lupus Nephritis. Scientific reports. 2016;6.

44. Beckonert O, Keun HC, Ebbels TM, Bundy J, Holmes E, Lindon JC, et al. Metabolic profiling, metabolomic and metabonomic procedures for NMR spectroscopy of urine, plasma, serum and tissue extracts. Nature protocols. 2007;2(11):2692-703.

45. Chenomx NMR Suite v8.1, Chenomx Inc. [Internet]. 2016. Available from: www.chenomx.com.

46. Nicholson JK, Foxall PJ, Spraul M, Farrant RD, Lindon JC. 750 MHz 1H and 1H-13C NMR spectroscopy of human blood plasma. Analytical chemistry. 1995;67(5):793-811.

47. Guleria A, Bajpai NK, Rawat A, Khetrapal C, Prasad N, Kumar D. Metabolite characterisation in peritoneal dialysis effluent using high-resolution 1H and 1H–13C NMR spectroscopy. Magnetic Resonance in Chemistry. 2014;52(9):475-9.

48. Ulrich E, Akutsu H, Doreleijers J, Harano Y, Ioannidis Y, Lin J, et al. BioMagResBank Nucleic Acids Res. 2008, 36 (suppl 1). D402-D408.

49. Wishart DS, Tzur D, Knox C, Eisner R, Guo AC, Young N, et al. HMDB: the human metabolome database. Nucleic acids research. 2007;35(suppl_1):D521-D6.

50. Xia J, Sinelnikov IV, Han B, Wishart DS. MetaboAnalyst 3.0—making metabolomics more meaningful. Nucleic acids research. 2015;43(W1):W251-W7.

51. Xia J, Psychogios N, Young N, Wishart DS. MetaboAnalyst: a web server for metabolomic data analysis and interpretation. Nucleic acids research. 2009;37(suppl_2):W652-W60.

52. Worley B, Powers R. Multivariate analysis in metabolomics. Current Metabolomics. 2013;1(1):92-107.

53. Guolin H, Jeffrey S, Kai Z, Xiaolan H. Application of ionic liquids in the microwave-assisted extraction of pectin from lemon peels. Journal of analytical methods in chemistry. 2012;2012.

54. Koperuncholan M. Bioreduction of chloroauric acid (HAuCl4) for the synthesis of gold nanoparticles (GNP): A special empathies of pharmacological activity. International Journal of Phytopharmacy. 2015;5(4):72-80.

55. Marangoni VS, Paino IM, Zucolotto V. Synthesis and characterization of jacalin-gold nanoparticles conjugates as specific markers for cancer cells. Colloids and Surfaces B: Biointerfaces. 2013;112:380-6.

56. Daneluti ALM, Matos JdR. Studies of thermal behavior of phytic acid. Brazilian Journal of Pharmaceutical Sciences. 2013;49(2):275-83.

57. Madhusudhan A, Reddy GB, Venkatesham M, Veerabhadram G, Kumar DA, Natarajan S, et al. Efficient pH dependent drug delivery to target cancer cells by gold nanoparticles capped with carboxymethyl chitosan. International journal of molecular sciences. 2014;15(5):8216-34.

58. Suganya KU, Govindaraju K, Kumar VG, Karthick V, Parthasarathy K. Pectin mediated gold nanoparticles induces apoptosis in mammary adenocarcinoma cell lines. International journal of biological macromolecules. 2016;93:1030-40.

59. Liu L, Fishman ML, Kost J, Hicks KB. Pectin-based systems for colon-specific drug delivery via oral route. Biomaterials. 2003;24(19):3333-43.

60. Dongowski G, Lorenz A, Anger H. Degradation of pectins with different degrees of esterification by Bacteroides thetaiotaomicron isolated from human gut flora. Applied and environmental microbiology. 2000;66(4):1321-7.

61. Mody R, Antaram Joshi S, Chaney W. Use of lectins as diagnostic and therapeutic tools for cancer. J Pharmacol Toxicol Methods. 1995;33(1):1-10.

62. Sastry M, Banarjee P, Patanjali SR, Swamy M, Swarnalatha G, Surolia A. Analysis of saccharide binding to Artocarpus integrifolia lectin reveals specific recognition of T-antigen (beta-D-Gal (1----3) D-GalNAc). J Biol Chem. 1986;261(25):11726-33.

63. Liu G, Song Y, Cui L, Wen Z, Lu X. Inositol hexaphosphate suppresses growth and induces apoptosis in HT-29 colorectal cancer cells in culture: PI3K/Akt pathway as a potential target. Int J Clin Exp Pathol. 2015;8(2):1402.

64. Shamsuddin AM. Metabolism and Cellular Functions of IP6. A Review. Anticancer Res. 1999;19(5):3733-6.

65. Khazaei S, Hamid RA, Esa NM, Ramachandran V, Aalam GTF, Etemad A, et al. Promotion of HepG2 cell apoptosis by flower of Allium atroviolaceum and the mechanism of action. BMC Complement Altern Med. 2017;17(1):104.

66. Singh RP, Agarwal C, Agarwal R. Inositol hexaphosphate inhibits growth, and induces G1 arrest and apoptotic death of prostate carcinoma DU145 cells: modulation of CDKI-CDK-cyclin and pRb-related protein-E2F complexes. Carcinogenesis. 2003;24(3):555-63.

67. Thannickal VJ, Fanburg BL. Reactive oxygen species in cell signaling. Am J Physiol Lung Cell Mol Physiol. 2000;279(6):L1005-L28.

68. Gu C, Wilson MS, Jessen HJ, Saiardi A, Shears SB. Inositol pyrophosphate profiling of two HCT116 cell lines uncovers variation in InsP8 levels. PLoS One. 2016;11(10):e0165286.

69. Khan S, Kumar S, Maqsood A. Virtual Screening of Molecular Properties and Bioactivity Score of Boswellic Acid Derivatives in Search of Potent Anti-Inflammatory Lead Molecule. International Journal of Interdisciplinary and Multidisciplinary Studies. 2013;1(1):8-12.

70. Verma A. Lead finding from Phyllanthus debelis with hepatoprotective potentials. Asian Pacific Journal of Tropical Biomedicine. 2012;2(3):S1735-S7.

71. Skrzydlewska E, Stankiewicz A, Sulkowska M, Sulkowski S, Kasacka I. Antioxidant status and lipid peroxidation in colorectal cancer. Journal of toxicology and environmental health Part A. 2001;64(3):213-22.

72. Skrzydlewska E, Sulkowski S, Koda M, Zalewski B, Kanczuga-Koda L, Sulkowska M. Lipid peroxidation and antioxidant status in colorectal cancer. World journal of gastroenterology: WJG. 2005;11(3):403.

73. Raj P, Singh M, Rawat JK, Gautam S, Saraf SA, Kaithwas G. Effect of enteral administration of α-linolenic acid and linoleic acid against methotrexate induced intestinal toxicity in albino rats. RSC Advances. 2014;4(104):60397-403.

74. Kaithwas G, Majumdar DK. In vitro antioxidant and in vivo antidiabetic, antihyperlipidemic activity of linseed oil against streptozotocin-induced toxicity in albino rats. European Journal of Lipid Science and Technology. 2012;114(11):1237-45.

75. Khare S, Chaudhary K, Bissonnette M, Carroll R. Aberrant crypt foci in colon cancer epidemiology. Cancer Epidemiology: Modifiable Factors. 2009:373-86.

76. Wargovich MJ, Brown VR, Morris J. Aberrant crypt foci: the case for inclusion as a biomarker for colon cancer. Cancers. 2010;2(3):1705-16.

77. Vucenik I, Stains J. Cancer preventive and therapeutic properties of IP6: efficacy and mechanisms. Periodicum biologorum. 2010;112(4):451-8.

78. Shafie NH, Mohd Esa N, Ithnin H, Md Akim A, Saad N, Pandurangan AK. Preventive inositol hexaphosphate extracted from rice bran inhibits colorectal cancer through involvement of Wnt/β-catenin and COX-2 pathways. BioMed research international. 2013;2013.

79. Osaki M, Oshimura Ma, Ito H. PI3K-Akt pathway: its functions and alterations in human cancer. Apoptosis. 2004;9(6):667-76.

80. Edelman MJ, Hodgson L, Wang X, Kratzke RA, Vokes EE. Cyclooxygenase-2 (COX-2) as a predictive marker for the use of COX-2 inhibitors in advanced non–small-cell lung cancer. Journal of Clinical Oncology. 2012;30(16):2019.

81. Chan ECY, Koh PK, Mal M, Cheah PY, Eu KW, Backshall A, et al. Metabolic profiling of human colorectal cancer using high-resolution magic angle spinning nuclear magnetic resonance (HR-MAS NMR) spectroscopy and gas chromatography mass spectrometry (GC/MS). Journal of proteome research. 2008;8(1):352-61.

82. Leichtle AB, Nuoffer J-M, Ceglarek U, Kase J, Conrad T, Witzigmann H, et al. Serum amino acid profiles and their alterations in colorectal cancer. Metabolomics. 2012;8(4):643-53.

83. Koh TJ, Dockray GJ, Varro A, Cahill RJ, Dangler CA, Fox JG, et al. Overexpression of glycine-extended gastrin in transgenic mice results in increased colonic proliferation. Journal of Clinical Investigation. 1999;103(8):1119-26.

84. Wang L, Chen J, Chen L, Deng P, Xiang P, Li M, et al. 1 H-NMR based metabonomic profiling of human esophageal cancer tissue. Molecular cancer. 2013(1):12-25.

Chapter 5

Summary and conclusion

Summary

Many efforts are being made to triumph over cancer amongst which, the use of natural constituents as chemopreventive, as well as chemotherapeutic agents, have shown a rise, because of their safety, availability and general acceptance. Inositol hexaphosphate (IP6) is as such a natural bioactive constituent of cereals, legumes etc. Various researchers have already proved that the intake of IP6 containing legumes is connected with the lowering of cancer incidences. Instead, this potent bioactive carbohydrate is not very popular in cancer therapy due to its shortcoming of fast chelation and elimination from the body, within an hour of administration. Present studies focus on the development of a suitable dosage form(s) of IP6 that may enhance its residence time, thereby increasing its chemopreventive as well as chemotherapeutic effect.

The size of nano-material is the property that makes them ideal for increasing residence time, surface area, higher drug loading, rapid commencement of therapeutic action etc. Anticancer drugs in nanoformulations display superior therapeutic index as a result of improved pharmacokinetics, distribution and accumulation of drug at the tumour site. The nano-sized system exhibited more permeability into the tumour site, as tumour sites have a leaky vasculature. Consequently, nano drug delivery systems can be successful tools for anticancer therapy. Thus, the preparation and evaluation of IP6 containing nanoformulations were explored in this research work.

Experimental section was divided into two parts: part I deals with the preparation and evaluation of IP6 loaded niosomal suspension and part II deals with the preparation and evaluation of IP6 loaded gold nanoparticles.

Identification of drug sample was performed through melting point and FTIR analysis. Melting point was found to be in the range of 22-25°C. FTIR analysis displayed the characteristic peak at 3430.3 cm^{-1} which relates to OH stretching, peaks near 1662.1 cm^{-1} was probably due to the carboxyl group and at 1061.5 cm^{-1} allocated the phosphate radical or hydrogen phosphate radical. The results were similar as reported earlier, indicating the purity of the drug sample. The standard curve of the drug was prepared by using UV-visible spectroscopy method as reported by Haug and Lantzsch. Standard solution of IP6 (100 μg/mL) was prepared and scanned in the range of 400-600 nm using distilled water as the blank. The λmax of the drug was

found to be 520 nm. Straight fit equation (y = -0.030x + 1.041) thus obtained was utilized for further quantification of IP6 in various samples.

In part I of the experiment, the IP6 loaded niosomal suspension was optimized, developed and characterized for intended topical drug delivery against skin cancer. A 2^3 (two-level, three-factor) full factorial experimental design was utilized for statistical optimization of the formulation variables, in the preparation of IP6 niosomes. For the purpose, three independent variables (cholesterol: surfactant ratio, sonication time and dicetylphosphate (DCP) concentration) and two dependent variables (particle size and encapsulation efficiency) were taken. Nine batches of different combinations were developed and evaluated.

Unilamellar niosomal vesicles were prepared from surfactant (Span 80), cholesterol and DCP, by utilizing thin film hydration method. Prepared niosomal vesicles were analysed for particle size, polydispersity index (PDI), zeta potential, encapsulation efficiency, *in-vitro* drug release, morphology and stability testing.

Particles size range was observed between 268.9±3.8 nm to 965.5±5.2 nm and the PDI value ranged from 0.212±0.18 to 0.431±0.15. The vesicles with diameter ≤ 600 nm may penetrate into deeper layers of skin and consequently raise the possibility of systemic absorption. Since a topical effect was required, therefore, the IP6 loaded niosomal formulations which showed particle size of more than 600 nm were considered further for the studies.

IP6 was efficiently incorporated into niosomal vesicles with encapsulation efficiency ranging from 11.3±2.9 to 82.9±2.6%. It was seen that the encapsulation efficiency moved parallel with particle size. Greater encapsulation was observed in larger vesicles and vice-versa. Zeta potential values were found to be in the range of -6±0.21 to -36±0.36. Batches which did not contain DCP revealed lower values and those which contained it, displayed higher values of charge, as DCP is a negative charge inducing agent. The *in-vitro* drug release of optimized formulation, at the end of 24 h was found to be 97.61±1.39%. The release kinetics of formulation was best explained by Higuchi's equation, as the plot showed the maximum linearity (R^2= 0.9627) followed by zero order (R^2 = 0.8107) kinetics. To observe the morphology of niosomes, various microscopic studies were performed and were found to be spherical in shape. IP6 loaded niosomes were tested for stability testing. Results of stability

studies showed that prepared niosomal formulation was stable till 180 days at room temperature. All the parameters were found stable during the analysis and significant degradation was not observed during storage at the temperature of 30°C±2°C and 60%±5% relative humidity. After analyzing the above mentioned pharmaceutical parameters, niosomes were further dispersed in a suspension to make them suitable for topical application.

The suspension was prepared through emulsification and analysed for pH, viscosity, texture, *in-vitro* skin permeation, irritation, *in-vitro* cell proliferation/ cytotoxicity against human cancer cell lines and *in-vivo* studies. On visual inspection, the developed niosomal suspension revealed good homogeneity. pH of the suspension was found to be 6.9±0.002 (similar to skin pH range) and its viscosity was seen to be 9650±50.0 cp with spindle number 3. Regarding the texture parameters, firmness was found to 19 g, spreadability value was 1.5 mJ and extrudability was found to be 55.6 mJ. Physicochemical parameters revealed that IP6 loaded niosomal suspension could be applied topically by application of a small amount of shear. *In-vitro* skin permeation studies were done with Swiss albino mice skin in which niosomal and plain IP6 suspensions were compared. Observation detailed that none/ negligible quantity of IP6 was left unabsorbed on the skin surface after 24 h, in the case of both, plain IP6 suspension as well as niosomal suspension of IP6. The cumulative amount of IP6 permeated from plain IP6 suspension was higher than that of niosomal suspension. The lower flux of niosomal suspension displayed prolonged drug release behaviour. Hen's Egg Test on the Chorioallantoic Membrane (HET-CAM) was used to examine the skin irritancy of the developed formulations. The irritation score was observed to be in the range of 0 to 0.42±0.03, which confirmed the formulation to be non-irritant. Studies revealed that the formulation was well tolerated. The cytotoxicity studies displayed significant changes in the tested cell lines and lead to inhibition of cell proliferation and apoptosis after the application of the niosomal formulation. IP6 pure displayed IC50 value at the concentration of 1.39 mM , whereas niosomal suspension displayed a value of 0.96 mM, i.e., niosomal suspension loaded with IP6 was significantly ($p<0.05$) more effective than pure IP6. IP6 in niosomal suspension displayed superior inhibition which may be attributed to the fact that niosomes in suspension displayed better interaction with lipid layer of the cell and hence micronized drug particles could have penetrated easily to lead to the maximum

percentage of cell death. Inhibitory effect of the niosomal suspension was seen to be in concordance with previous reports which projected that IP6 is a potential antineoplastic agent. Thus, it was considered worthwhile to evaluate the *in-vivo* efficacy of prepared formulations against DMBA induced dysregulation of markers pertaining to cellular proliferation/ differentiation and inflammation.

A short-term *in-vivo* study was performed taking Swiss albino mice as the model. 7,12-Dimethylbenzanthracene (DMBA, carcinogen) applied to induce dysregulation of proliferation markers (ODC, PCNA, COX-2 and cyclin D1) and the effect of formulation for inhibition of the dysregulation was estimated through western blotting (for protein levels) and RT-PCR (for m-RNA levels). Results revealed that IP6 loaded niosomal formulation marginalized the deleterious effect of DMBA and displayed favourable regulation towards the normal, when compared with IP6 alone and IP6 plain suspension. During the histopathological studies, the control group animals showed no alterations in the epidermal thickness. Significant hyperplasia was seen in DMBA treated skin with the increase in time. IP6 niosomal suspension displayed a better reduction in skin thickness when compared with the standard.

For part II of the experimental section, pectin encrusted gold nanoparticles containing IP6 were prepared with and without jacalin, by using reduction followed by incubation method. The inclusion of pectin as a reducing or capping agent was incited by virtue of it being a natural and nontoxic agent containing carboxylate unit which facilitated activation through jacalin. Jacalin is a lectin protein which has the ability to recognize and target tumour linked disaccharides which are over-expressed in almost all tumour cells and contain functional groups like hydroxyl and amine that facilitate pectin activation. By varying concentration of chloroauric acid (1, 2 and 3 mM), three different batches of formulations were prepared and characterised for particle size, PDI and drug loading. Particle sizes of prepared IP6-jacalin-pectin-gold nanoparticles (IJP-GNP) were found to be 67.4±2.38 nm, 128.29±3.12 nm and 283±4.94 nm respectively. Particle size increased with increasing concentration of chloroauric acid. Pectin may perform the dual function of a capping agent and may prove to be a good stabilizer. Thus, when the concentration of chloroauric acid increased without increasing concentration of pectin, then lesser reducing and capping agent may have been available which lead to an increase in size of nanoparticles. Thus, it was concluded that the particle size can be controlled by regulating the concentration of

chloroauric acid. The formulation showed PDI values of 0.24, 0.29 and 0.32 respectively. The prepared metal particles were homogenous, as revealed by PDI values were < 0.5 for each concentration. Percentage drug loaded was found to be 81.63±1.21%, 78.86±1.98% and 76.1±2.69 % respectively. Drug loading decreased with increasing concentration of chloroauric acid which may be attributed to the larger surface area of smaller metal nanoparticles which would allow attachment of an increased number of drug molecules.

Formulation made with 3mM of chloroauric acid displayed required characteristics and was taken up for further analysis. Formulation was analysed for FTIR, morphology, *in-vitro* cell line studies to estimate their potential against human colon cancer cells (HCT 15) and *in-vivo* studies in Wistar rat model. FTIR spectroscopy of pectin, chloroauric acid, IP6, jacalin and IJP-GNP was performed. All the excipients showed their characteristic peaks. In case of pectin, the peaks were observed at 2935.8 cm^{-1} and 1746.8 cm^{-1} which correspond to C-H and C=O bond vibrations. For chloroauric acid, the peaks at 1631.4 cm^{-1} and 3389.8 cm^{-1} corresponds to C-O and -OH stretches respectively. Peaks near 1654.4 cm^{-1} showed the main vibrational bands of amide groups of jacalin and the bands near 1378.8 cm^{-1} displayed vibrational mode of the COOH and C-O groups of aspartic acid, glutamic acid like amino acids, present in jacalin. Peak near 3430.3 cm^{-1} in case of IP6 relates to OH stretching. IJP-GNP revealed the shift in peaks of hydroxyl and carbonyl groups and also displayed all the characteristic peaks of IP6 and jacalin. It also exhibited the shift in peaks of amines (1655.9 cm^{-1}, 1515.0 cm^{-1} and 1203.2 cm^{-1}) and hydroxyl (3417.5 cm^{-1}) of jacalin and IP6 respectively which may be due to their involvement in complex formation. Further, the spectra of IJP-GNP displayed all the characteristic peaks of IP6 and jacalin suggesting the corona of IP6 and jacalin. The absence of the peak of gold signified the complete coverage by this corona. *In-vitro* drug release was observed to be significantly low in acidic pH, which increased after changing the pH of media to 6.8 and was found to be even higher with media containing cecal content of pH 7.4. Lesser drug release at acidic pH and higher in alkaline pH indicated that the pectin contains carboxyl groups in its structure which ionize in neutral to alkaline pH. Besides, pectin degrades in the colonic microflora. Due to the ionization/ enzymatic degradation of pectin, the corona containing jacalin and IP6 would breakdown thereby releasing the drug in this particular pH. Morphological evaluation of P-GNP through

TEM displayed spherical shape, while IJP-GNP revealed a corona surrounding the surface.

Synthesized formulations (P-GNP, IP-GNP and IJP-GNP) were evaluated for their anti-cancer activity along with IP6 (as standard) against the development of HCT-15, in a dose as well as time-dependent way by MTT assay. IJP-GNP was found to be the most effective formulation in the arrangement with the least IC50 value at the concentration of 15 µM/ml at 24 h treatment and sub IC50 value at 10 µM/ml at 48 h against standard medication IC50 value at 30 µM/ml at 24 h and sub IC50 value at 15 µM/ml at 48 h against colon cancer cells. This superior inhibition effect may be attributed to the better cellular interaction due to the presence of jacalin protein, which has the property of recognition and attachment to the cancerous cells. IP6 containing formulations did not indicate cytotoxicity against human normal colon cells (NCM460) which may be attributed to the use of natural agents. Since IJP-GNP was found to be more effective, thus it was taken up for further evaluations. In colony forming assay, the number of colonies diminished with respect to increment in the time of treatment with IJP-GNP formulation (192 colonies). The untreated HCT 15 cells were found to create an extreme of 210 colonies after 24 h. This signified a longer inhibitory effect of IP6 loaded formulations, as envisaged. Cell cycle analysis displayed the percentage of HCT cells in the G0/G1 stage for IJP-GNP. Low concentration of IJP-GNP (10 µM/ml) also displayed an induction of G1 arrest, confirming the effect of IP6 as earlier reported. Apoptosis assay was utilized in order to evaluate nuclear morphology in response to the IJP-GNP formulation. Shrunken nucleus, peripherally clumped and fragmented chromatin was observed following the treatment with the IJP-GNP formulation, indicating effective apoptosis due to the presence of IP6. In order to evaluate nuclear morphology in response to IJP-GNP treatment, DAPI staining through microscopy was performed. To further confirm our deliberations regarding cell growth inhibition associated with physiological apoptosis, AnnexinV-FITC and PI dual staining was also carried out using flow cytometer. IJP-GNP displayed time as well as dose-dependent increase of apoptotic cells and nonspecific necrotic population. The results of the quantitative measurement of ROS revealed that 10 µM/ml of IJP-GNP induced 104.43% ($p<0.05$) enhancement in ROS production as compared to control. Moreover, ROS production was increased by 160.53% ($p<0.05$) at 15 µM/ml concentration of IJP-GNP when compared to

untreated cells. Results clearly stated that IJP-GNP triggered the cells death by ROS generation. *In-vitro* studies were also correlated with the *in-silico* approach to study inter-molecular interactions between IP6, P-GNP and jacalin protein. The molecular properties and bioactivity of the leading compounds were determined by using online data server Molinspiration. The obtained values of druglikeness score showed that IJP-GNP exhibited good druglikeness score (>0.50). IP6, as well as P-GNP with jacalin protein, displayed a docking score of 4098 and 2096 respectively, as compared to the docking score of IJP-GNP complex, which displayed a docking score of 4422. Greater binding energy and binding sites were seen in complex IJP-GNP when compared with single binding of IP6, as well as P-GNP with jacalin. The docking results showed that interactive properties of IP-GNP complex with jacalin could inhibit the tumour formation activity and supported *in-vitro* studies.

During *in-vivo* studies, dimethylhydrazine (DMH) was administered subcutaneously to induce colon cancer. Animals were scrutinized for their electrocardiogram (ECG) and heart rate variability (HRV) paradigms and blood was collected through the retro-orbital plexus. The blood serum, colon tissue and colon content were collected and stored for further analysis. Colon content was estimated for pH and total acidity. Colon tissue was examined for aberrant crypt foci (ACF), morphological evaluation by SEM and histopathology, biochemical changes, western blotting and RT-PCR. Blood serum was utilized for serum metabolomics assay.

IP6, IP-GNP and IJP-GNP affected diverse parameters of ECG when given to albino Wistar rats. Depreciated ECG and HRV values were reflected in the DMH treated animals, in time as well as frequency domain. Treatment with formulations revealed significant restoration towards normal values which may be ascribed to the action of IP6. The toxic group animals displayed weight loss, decrease in pH along with an increase in total acidity and formation of aberrant crypts when compared with control. Concomitant application of IP-GNP and IJP-GNP favourably regulated the weight and pH of the treated group animals. The total acidity along with ACF was also synchronized near to normal after IJP-GNP treatment. DMH application significantly altered the biochemical parameters (protein carbonyl, malondialdehyde (MDA), GSH, SOD and catalase) in the toxic control group which were found to be significantly normalised with IP-GNP and IJP-GNP treatments.

Toxic control animals showed highest ACF count, abrupt crypts and loss of goblet cells, crypts and distorted lamina propria. Treatment with developed formulations tried to restore the normal structure of colonic mucosa. Maximum restoration of ACF count was observed by IJP-GNP, which may be attributed to the targeted delivery into the affected cells due to the presence of jacalin. The histopathological analysis displayed intact architecture of colonic mucosa in the normal control, in contrast to the toxic group animals which showed abrupt/ impaired arrangement of cells. The IJP-GNP treated groups showed maximum similarity with the normal control group which could again be a call out of targeting the required site because of jacalin.

Change in expressions of PI3K, Akt and COX-2 genes were scrutinized. Normal control was taken as the baseline (assumed with no up/ down regulation) and all comparisons were made with respect to it. Treatment with IP6, IP-GNP and IJP-GNP helped to restore the expressions of above-mentioned genes which validate the inhibitory action of IP6 for aforesaid enzymes. IJP-GNP revealed maximum restoration of protein as well as mRNA levels.

^{1}H NMR based metabolic profiling was performed to explore the biochemical changes associated with colon cancer and to further see how these changes get modulated in the rats receiving the treatment with IP6 formulation(s). Increased levels of lipoproteins, PUFAs and amino acids were seen in DMH treated animals implying rapid cellular regeneration and catabolism due to the rapid cell proliferation. The lower concentration of choline, its derivatives and serum creatine were observed which can be correlated with the cellular regeneration of tumours and increased energy consumption due to rapid cell division. Further a decreased level of glucose was also observed which indicated the increase in glucose metabolism through glycolysis to generate ATP instead of oxidative phosphorylation which enhances glucose uptake in tumour cells to meet the energy requirement of quick proliferation. All in all, the disturbed metabolic pathways as observed, lead to infer the acceleration of cell proliferation in the process of tumour formation, hyperplasia in colonic mucosa and an increase in inflammation in DMH treated rats. Almost all metabolic changes in DMH treated animals returned back towards normal after IP6 formulation(s) treatment, suggesting that the formulation(s) has potential to normalise the DMH altered metabolic changes.

Conclusion

The nanoformulations containing IP6 were developed and optimized successfully. The niosomal suspension and gold nanoparticles of IP6 were evaluated for numerous physicochemical parameters, *in-vitro* and *in-vivo* performances which exhibited the development of a consistent, stable as well as an effective delivery system for cancer therapy.

IP6 niosomal suspension was found to be non-irritant, aesthetic and had desirable properties for the topical application. Formulation proved to possess anticancer activity and induced apoptosis in SK-MEL-2 cancer cell lines. The DMBA altered expression of ODC, PCNA, COX-2 and Cyclin D1 was significantly prevented by concomitant application of niosomal formulations.

The gold nanoparticles (P-GNP, IP-GNP and IJP-GNP) were screened for the anticancer studies on the basis of the cytotoxicity observed on HCT 15 cells in a dose and time-dependent manner. Amongst all, IJP-GNP was found to be the most potent formulation with lowest IC50 value. IJP-GNP caused cell cycle arrest at the G0/G1 phase, induced ROS and subsequent apoptosis. The docking results showed that the interactive properties of IP-GNP complex with jacalin that could inhibit the tumour formation activity and supported *in-vitro* studies, which proved that the IJP-GNP inhibited the growth of colon cancer. Furthermore, *in-vivo* studies suggested that IJP-GNP displayed significant effect against progression of colon carcinogenesis by positively modulating the physiological markers, oxidative stress, inflammatory markers and hemodynamic changes.

Taken together, all these findings suggested an effective anticancer effect of the IP6 loaded formulations that raise the hope of future drug delivery strategy targeted to the numerous cancer treatments. Further studies may be performed for successive scale-up of such formulations having drugs of natural origin, from bench to bedside.

Research papers

1) **Malti Arya**, Prakash Tiwari, Chandra B. Tripathi, Poonam Parashar, Mahendra Singh, Priyam Sinha, Narayan P. Yadav, Gaurav Kaithwas, Krishna P. Gupta, Shubhini A. Saraf. Novel niosomal lotion of Inositol hexaphosphate against inflammation/ hyperplasia in epidermal layer of Swiss albino mice. Molecular Pharmaceutics. 2017;14(3):928-939. **(Impact factor- 4.556)**

2) **Malti Arya**, Krishna P Gupta, Shubhini A Saraf. Quantification using ultraviolet spectroscopy method and in vitro stability study of nanovesicular system containing Phytic acid. Asian Journal of Pharmaceutical and Clinical Research. 2018;11(8):374-377. **(Impact factor- 0.49)**

3) **Malti Arya**, Pooja Singh, Chandra B Tripathi, Poonam Parashar, Mahendra Singh, Jovita Kanoujia, Anupam Guleria, Gaurav Kaithwas, Krishna P Gupta, Shubhini A Saraf. Pectin encrusted gold nanocomposites containing Phytic acid and jacalin: 1,2-dimethylhydrazine induced colon carcinogenesis in Wistar rats, PI3K/Akt, COX-2 and serum metabolomics as potential targets. Drug delivery and translational research. (under communication) **(Impact factor- 3.395)**

4) **Malti Arya**, Nidhi Mishra, Pooja Singh, Chandra B Tripathi, Poonam Parashar, Mahendra Singh, Gaurav Kaithwas, Krishna P Gupta, Shubhini A Saraf. *In-vitro* & *in-silico* molecular interaction of multiphase nanoparticles containing inositol hexaphosphate and jacalin: therapeutic potential against colon cancer cells (HCT 15). Phytomedicine (under communication) **(Impact factor-3.610)**

5) Pooja Singh, **Malti Arya**, Jovita Kanoujia, Mahendra Singh, Kishna P. Gupta, Shubhini A Saraf. Effect of Silymarin nanolipoidal carriers on 7,12-dimethylbenz anthracene (DMBA) induced cellular proliferation in mice model. RSC Advances. 2016;6:84965-84977. **(Impact factor- 2.936)**

6) Pooja Singh, Mahendra Singh, Jovita Kanoujia**, Malti Arya,** Shailendra K. Saraf, Shubhini A Saraf, Process Optimization and Photostability of Silymarin Nanostructured Lipid Carriers: Effect on UV Irradiated rat Skin and SK-MEL 2 cell line, Drug Delivery and Translational Research, 2016;6(5):597-609. **(Impact factor- 3.395)**

7) Chandra Bhushan Tripathi, Poonam Parashar, **Malti Arya**, Mahendra Singh, Jovita Kanoujia, Gaurav Kaithwas, and Shubhini A Saraf. Development of α-Linolenic Acid Potentiated Nanoemulsion for Targeted Delivery of Doxorubicin in DMBA Induced Mammary Gland Carcinoma: in vitro and in vivo Evaluation. Drug Delivery and Translational Research, 2018;1-22. **(Impact factor- 3.395)**

8) Poonam Parashar, Chandra Bhushan Tripathi, **Malti Arya**, Jovita Kanoujia, Mahendra Singh, Abhishek Yadav, Shubhini A Saraf. Biotinylated Naringenin Intensified Anticancer Effect of Gefitinib in Urethane-Induced Lung Cancer in Rats: Favorable Modulation of Apoptotic Regulators and Serum Metabolomics. Artificial cell, nanomedicine and biotechnology, 2018 (accepted manuscript) DOI: 10.1080/21691401.2018.1505738. **(Impact factor- 3.026)**

9) Poonam Parashar, Chandra Bhushan Tripathi, **Malti Arya**, Jovita Kanoujia, Mahendra Singh, Abhishek Yadav, Shubhini A Saraf. A Facile Approach for Fabricating CD44 Targeted Delivery of Hyaluronic Acid Functionalized PCL Nanoparticles in Urethane-Induced Lung Cancer: Bcl-2, MMP-9, Caspase-9 and BAX as Potential Markers. 2018 (accepted manuscript). Drug delivery and translational research. 2017:1-22. **(Impact factor- 3.395)**

10) Mahendra Singh, Jovita Kanoujia, Poonam Parashar, **Malti Arya**, Chandra B. Tripathi, Vivek Sinha, Shailendra K. Saraf, Shubhini A. Saraf. Augmented bioavailability of felodipine through an α-linolenic acid-based microemulsion. Drug delivery and translational research. 2017:1-22. **(Impact factor- 3.395)**

11) Mahendra Singh, Jovita Kanoujia, Poonam Parashar, **Malti Arya**, Chandra B. Tripathi, Vivek Sinha, Shailendra K. Saraf, Shubhini A. Saraf:, Assessment of improved buccal permeation and bioavailability of felodipine microemulsion-based cross-linked polycarbophil gel, Drug Delivery and Translational Research. DOI: 10.1007/s13346-018-0489-5. **(Impact factor- 3.395)**

12) Mahendra Singh, Jovita kanoujia, Pooja Singh, Poonam Parashar, **Malti Arya,** Chandra Bhusan Tripathi, Vivek Sinha, Shubhini A. saraf, Development of an a-linolenic acid containing soft nanocarrier for oral delivery part II: buccoadhesive gel, RSC Advances. 2016;6:101602-101612 **(Impact factor- 2.936)**

13) Jovita Kanoujia, Mahendra Singh, Pooja Singh, Poonam Parashar, Chandra Bhusan Tripathi, **Malti Arya,** Shubhini A. Saraf**,** Genipin crosslinked soy-whey based bioactive material for atorvastatin loaded nanoparticles: Preparation, characterization and in vivo antihyperlipidemic study. RSC Advances. 2016;6:93275-93287. **(Impact factor- 2.936)**

14) Mahendra Singh, Jovita Kanoujia, Pooja Singh, Chandra B. Tripathi, **Malti Arya**, Poonam Parashar, Vivek R. Sinha, Shubhini A. Saraf, Development of ana-linolenic acid containing soft nanocarrier for oral delivery: in vitro and in vivo evaluation, RSC Advances, 2016;6:77590–77602. **(Impact factor- 2.936)**

15) Samipta Singh, Mahendra Singh, Chandra Bhushan Tripathi, **Malti Arya**, Shubhini A Saraf, "Development and Evaluation of Ultra-Small

Nanostructured Lipid Carriers: Novel Topical Delivery System for Athlete's Foot" Drug delivery and translational research, 2016; 6(1): 38-47. **(Impact factor- 3.395)**

16) Chandra B. Tripathi, Neha Gupta, Pranesh Kumar, Ashok Kumar Singh, Vinit Raj, Poonam Parashar, Mahendra Singh, Jovita Kanoujia, **Malti Arya,** Shubhini A. Saraf**,** Sudipta Saha. ω-3 Fatty Acid Synergized Novel Nanoemulsifying System for Rosuvastatin Delivery: In Vitro and In Vivo Evaluation. AAPS PharmSciTech. 2017:1-14. **(Impact factor- 2.451)**

17) Md. Meraj Anjum, Jovita Kanoujia, Poonam Parashar, **Malti Arya**, Alok Kumar Yadav, Shubhini A. Saraf, Evaluation of a Polymer-Lipid-Polymer type of System Utilising Hybrid Nanoparticles for Dapsone as a Novel Antiacne Agent. Current Drug Therapy. 2016; 11(2):86-100.

18) Mahendra Singh, Nidhi Gangwar, Poonam Parashar, Chandra Bhushan Tripathi, **Malti Arya**, Shubhini A Saraf and Sudipta Saha. Topical Delivery of Fluconazole via Microemulsion Incorporated Hydrogel for the Management of Fungal Dermatophytosis. Current Drug Therapy. 2016; 11(2): 129-141.

19) Anubhav Anand, **Malti Arya**, Gyanendra Singh, Gaurav Kaithwas, Shubhini A. Saraf. Design and development of Resveratrol NLCs and their role in Synaptic Transmission of Acetylcholine in C. elegans Model. Current Drug Therapy. 2017; 134-148.

20) Md. Faheem Haider, Jovita Kanoujia, Chandra BhushanTripathi, **Malti Arya**, Gaurav Kaithwas, Shubhini A. Saraf. Pioglitazone loaded niosomes as vesicular carriers for anti-diabetic activity: Optimization by central composite design. Journal of Pharmaceutical Sciences and Pharmacology, 2015; 2: 11–20.

Conferences and workshops

1) **Oral** presentation at National Conference on the topic "Being in nature helps in reducing stress" in "Tourists and Green Spaces: Healthier Lifestyle Approaches from nature", held at B.B.A. University, Lucknow, dated 15th & 16th July 2017.

2) Presented **scientific poster** in International Conference on Updates in Cancer Prevention and Research (ICUCPR-2017) & Satellite Conference on Translational Research: Trends and Implications (IPCBBAU-2017). February 14th-16th & 20th, 2017.

3) Presented **scientific poster** entitled "Nano-niosomes of Phytic Acid as novel carriers for cancer prevention: In vitro and in vivo studies" in 4th Nano Today Conference- 2015, **Dubai**. December 6th -10th, 2015.

4) **Oral** presentation on the topic "Formulation and Evaluation of Herbal Antibacterial Cream for Treatment of Acne" in 3rd Lucknow Science Congress LUSCON-2015 on "Hope for Society through Drug Research", held at B.B.A. University, Lucknow, U.P., India. October 31st - November 2nd, 2015.

5) Presented **scientific poster** entitled "Advanced drug delivery of natural agents for chemoprevention" in 2nd National Seminar on "Profession of Pharmacy: Challenges & Opportunities", held at I.P.S.R., Lucknow, U.P., India. 18th October, 2015.

6) Presented **scientific poster** entitled "Development and Characterizations of Layer by Layer Mucoadhesive Microcapsule of Omeprazole" at International Pharmaceutical Conference-2015 on "Nanoformulations and Translational Research: Small Getting Bigger", held at B.B.A. University, Lucknow, U.P., India. February 2nd – 3rd, 2015

7) Presented **scientific poster** entitled "Development and Characterization of Targeted Green Nanotechnology Based Delivery System(s) for Cancer Therapy" at 2nd Lucknow Science Congress on "Leveraging Science and Innovation for Development", held at B.B.A. University, Lucknow, U.P., India. March 27th – 28th, 2014.

8) Presented **scientific poster** entitled "Application of Taguchi design in preparation, optimization and characterization of Methotrexate Nanostructured Lipid Carriers" at IHPA GOLDCON- 2104 on "Restructuring Pharmacy Curricula: Need of Health Sector", held at B.B.A. University, Lucknow, U.P., India. March 1st – 2nd, 2014.

9) Presented **scientific poster** entitled "Formulation and Evaluation of Nanoemulsion of Miconazole Nitrate for Treatment of Topical Fungal Infection" at International Conference on Pharmaceutical Sciences on Present Trends and Future Prospects in Pharmaceutical Sciences , held at Shri Guru

Ram Rai Institute of Technology and Science, Dehradun, Uttarakhand, India. February 14th – 15th, 2014.

10) Presented **scientific poster** entitled "Formulation and Evaluation of NLCs based Gel containing Methotrexate for Treatment of Rheumatoid Arthritis" at 65th Indian Pharmaceutical Congress on "Pharma Vision 2020", held at Amity University, Noida, Delhi NCR, U.P., India. December 20th – 22nd, 2013.

11) Attended a sixteen days workshop of DBT course in Biotechnology on the topic "Techniques in Molecular Biology", held at S.G.P.G.I.M.S., Lucknow, U.P., India. September 15th to September 30th, 2015.

12) Attended seven days Workshop on NMR/MRI: From molecules to human behaviour. Sponsored by Department of Science and Technology (DST), India. Held at BBAU, Lucknow, U.P., India. June 21st to 27th, 2015.

CSIR-INDIAN INSTITUTE OF TOXICOLOGY RESEARCH

Post Box 80, M. G. Marg, Lucknow – 226001

Institutional Animal Ethics Committee

Registration No. 54/99/CPCSEA, Dated: 11.03.1999

Dated: 03/ 02/2015

Dr.D.C.Purohit,
Secretary,
Institutional Animal Ethics Committee.

Dear Dr. K P Gupta

The Institutional Animal Ethics Committee of CSIR- IITR met on 16 Jan. 2015 and discussed/reviewed the project 'Development and characterization of targated green nano technology based delivery system for cancer therapy- short term studies on the nano formulation for their antitumor efficacy in vivo' and approved the submitted project.

Decision of IAEC is given below for your information and necessary action accordingly.

Reference No: IITR/IAEC/04/2015, for future correspondence.

Comment : Chairman of IAEC and experts including CPCSEA nominee approved Mice, no. 84, in the study.

Decision: Approved.

D.C.Purohit

To,

Dr K P Gupta ,
IITR, Lucknow

विद्ययामृतमश्नुते

S. D. College of Pharmacy & Vocational Studies

(Approved By AICTE, PCI, New Delhi & Affiliated to U.P. Technical University, Lucknow)

Bhopa Road,
Muzaffarnagar-251 001 (U.P.)

Office : 0131-2604546
Fax : 0131-2604546
E-mail : sdcop@rediffmail.com
Web : sdcopmzn.com

Ref. No. : SDCOP&VS/AH/CPCSEA/01/0028 Dated 06/05/2014

INSTITUTIONAL ANIMAL ETHICAL COMMITTEE (IAEC)

REG. No. 876/ac/05/CPCSEA Dated 13/09/2004 UNDER THE RULE 13 OF THE "BREEDING OF AND EXPERIMENTS ONANIMALS (CONTROL AND SUPERVISION) RULE 1998"

DATE: 06/05/2014

Approval No.: SDCOP&VS/AH/CPCSEA/01/0028

CERTIFICATE

This is to certify that Mr./Ms./Mrs. **Chandra Bhushan Tripathi/Poonam Parashar/Malti** student of M.Pharm / Ph.D. are permitted to carry out experiments for dissertation / thesis work entitled **"Development and assessment of anticancer potential of nanoparticulate system(s) of anticancer drug(s) in various cancer"** as per the details mentioned and after the observing the usual formalities laid down by IAEC as per the provisions made by CPCSEA.

MEMBER SECRETARY

CHAIRMAN

Plagiarism report of thesis

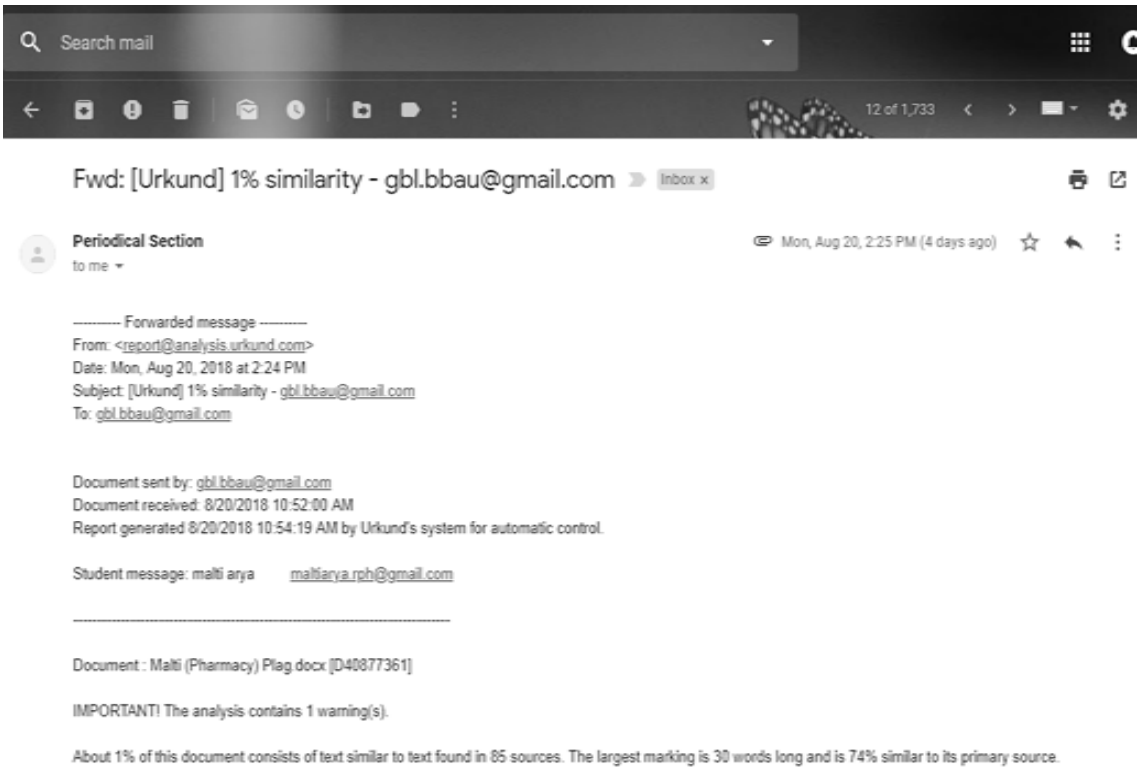

Search mail

12 of 1,733

Fwd: [Urkund] 1% similarity - gbl.bbau@gmail.com Inbox ×

Periodical Section Mon, Aug 20, 2:25 PM (4 days ago)
to me

---------- Forwarded message ----------
From: <report@analysis.urkund.com>
Date: Mon, Aug 20, 2018 at 2:24 PM
Subject: [Urkund] 1% similarity - gbl.bbau@gmail.com
To: gbl.bbau@gmail.com

Document sent by: gbl.bbau@gmail.com
Document received: 8/20/2018 10:52:00 AM
Report generated 8/20/2018 10:54:19 AM by Urkund's system for automatic control.

Student message: malti arya maltiarya.rph@gmail.com

Document : Malti (Pharmacy) Plag docx [D40877361]

IMPORTANT! The analysis contains 1 warning(s).

About 1% of this document consists of text similar to text found in 85 sources. The largest marking is 30 words long and is 74% similar to its primary source.

Brief curriculum vitae

Name: Malti

Date of birth: 01-09-1987

Education: B. Pharm (2011) from Rajiv Academy for Pharmacy, Mathura. Gautam Buddh Technical University, Lucknow, U.P. (India), First division.

M. Pharm (Pharmaceutics, 2013) from Babu Banarasi Das University, Lucknow, U.P. (India)**,** First division with honours.

M.Pharm project: Formulation and evaluation of nanostructured lipid carriers (NLCs) based topical gel containing methotrexate for treatment of rheumatoid arthritis.

PhD project: Development and Characterization of Targeted Green Nanotechnology Based Delivery System(s) for Cancer Therapy, under guidance of Prof. (Dr.) Shubhini A. Saraf (Head, Dept. of Pharmaceutical Sciences, Babasaheb Bhimrao Ambedkar University Lucknow, U.P. India) and in co-guidance of Dr. Krishna Prabha Gupta (Ex-Senior Principal Scientist, Carcinogenesis Division, CSIR-Indian Institute of Toxicology Research, M.G.Marg, Lucknow, U.P. India).

Fellowships:

- Rajiv Gandhi National Fellowship for Ph.D., 2014-15. Code number: F1-17.1/2014-15/RGNF-2014-15-SC-UTT-70422/ (SA-III/Website) dated on 26-Feb-2015, from UGC, Government of India.
- Graduate pharmacy aptitude test (GPAT), 2011, fellowship for post graduation, roll no. 2011117.
- Foundation for Academic Excellence and Access (FAEA), 2007, fellowship for graduation, confirmation code– 207810034.

Research Publications:

1. Eighteen (18) international/ national research articles
2. Thirteen (13) oral/ poster presentation in national/ international seminars/ conferences
3. Five (05) workshops/ conferences attended

Research area: Formulation development, lipoidal & colloidal drug delivery, green nanotechnology, carcinogenesis.

Address: 52A/ 173A Chack Meera Patti, Allahabad, Uttar Pradesh, India- 211011

(Malti)

molecular pharmaceutics

Article

pubs.acs.org/molecularpharmaceutics

Colloidal Vesicular System of Inositol Hexaphosphate to Counteract DMBA Induced Dysregulation of Markers Pertaining to Cellular Proliferation/Differentiation and Inflammation of Epidermal Layer in Mouse Model

Malti Arya,[#] Prakash Tiwari,[†] Chandra Bhushan Tripathi,[#] Poonam Parashar,[#] Mahendra Singh,[#] Priyam Sinha,[§] Narayan P. Yadav,[§] Gaurav Kaithwas,[#] Krishna P. Gupta,[†] and Shubhini A. Saraf*[,#]

[#]Department of Pharmaceutical Sciences, Babasaheb Bhimrao Ambedkar University, Vidya Vihar, Raebareli Road, Lucknow-226025, U.P., India

[†]Environmental Carcinogenesis Division, CSIR-Indian Institute of Toxicology Research, Post Box No. 80, Mahatma Gandhi Marg, Lucknow-226001, U.P., India

[§]CSIR-Central Institute of Medicinal and Aromatic Plants, PO CIMAP, Lucknow-226015, U. P., India

Supporting Information

ABSTRACT: Cancer is a global health problem and chemoprevention is a promising approach for reducing cancer burden. Inositol hexaphosphate (IP6), a natural bioactive constituent of cereals, legumes, etc., has momentous potential as an antiangiogenic agent, that specifically affects malignant cells. The shortcoming is its quick absorption on oral/topical administration. Niosomes are flexible carriers for topical drug delivery. The central venture of current research was to optimize and characterize niosomal delivery system of IP6 for treatment of skin cancer. Thin film hydration method was utilized to prepare IP6 niosomes, and these were dispersed as a suspension in a suitable base. Developed formulations were analyzed for various physicochemical and pharmacological parameters such as particle size, encapsulation efficiency, morphology, drug release, texture analysis, irritability, cell line studies, Western blotting, RT-PCR, and histopathology. IP6 niosomal suspension and IP6 in acetone displayed IC_{50} value at the concentration of 0.96 mM (0.63 mg/mL) and 1.39 mM (0.92 mg/mL), respectively. IP6 niosomal suspension showed significantly higher ($p < 0.05$) activity and showed cytotoxic effect in SK-MEL-2 cancer cell line. Crucial events of cellular proliferation and differentiation, like expression of ornithine decarboxylase (ODC), proliferating cell nuclear antigen (PCNA), cycloxygenase-2 (COX-2) and Cyclin D1 were initiated from the fourth hour through application of 7,12-dimethylbenzanthracene (DMBA) on albino mice. The DMBA altered expression of aforesaid enzymes was significantly ($P < 0.001$) prevented by concomitant application of niosomal formulations. Results of cell line study, Western blotting, RT-PCR, and histopathology suggested that IP6 niosomal suspension could constitute a promising approach for prevention of cellular proliferation as well as DMBA induced dysregulation of cellular proliferation/differentiation and inflammation.

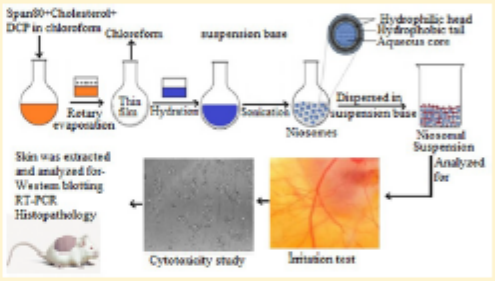

KEYWORDS: *skin cancer, phytic acid, niosomes, suspension, SK-MEL-2 cell line, histopathology, Western blotting, RT-PCR*

INTRODUCTION

Cancer remains a life threatening disease, and various efforts to contain the same have hitherto proved almost futile.[1] On an average, 3−8% increase in skin cancer per year has been recorded, with >1 million new cases every year.[2] Globally, people still rely on herbal medicines as first line treatment, owing to their perception of safety and general acceptance for cancer prevention as well as treatment. The wide investigation has identified numerous dietary, botanical, and natural compounds that have chemopreventive properties.[3,4]

Inositol hexaphosphate (IP6), commonly known as phytic acid, is a natural bioactive constituent of grains, legumes, and cereal products.[5,6] Chemically, IP6 is a simple carbohydrate with six phosphates attached to each carbon (inositol-1,2,3,4,5,6-hexaphosphate) and a principal storage of phosphorus in several plant tissues.[7,8] It possesses various health benefits such as lowering of serum cholesterol, strong antioxidant properties, etc. It has also been revealed to have significant potential as an antiangiogenic agent that only affects malignant

Received: December 21, 2016
Revised: February 2, 2017
Accepted: February 7, 2017
Published: February 7, 2017

DOI: 10.1021/acs.molpharmaceut.6b01147
Mol. Pharmaceutics XXXX, XXX, XXX−XXX

ASIAN JOURNAL OF PHARMACEUTICAL AND CLINICAL RESEARCH

INNOVARE ACADEMIC SCIENCES
Knowledge to Innovation

Vol 11, Issue 8, 2018

Online - 2455-3891
Print - 0974-2441

Research Article

QUANTIFICATION USING ULTRAVIOLET SPECTROSCOPY METHOD AND *IN VITRO* STABILITY STUDY OF NANOVESICULAR SYSTEM CONTAINING PHYTIC ACID

MALTI ARYA, KRISHNA P GUPTA, SHUBHINI A SARAF*

Department of Pharmaceutical Sciences, School of Biosciences and Biotechnology, Babasaheb Bhimrao Ambedkar University, Vidya Vihar, Raebareli Road, Lucknow – 226 025, Uttar Pradesh, India. Email: shubhini.saraf@gmail.com

Received: 12 April 2018, Revised and Accepted: 08 May 2018

ABSTRACT

Objective: The quantification of drug and stability of nanoparticulate delivery systems is one of the major apprehensions in biomedical applications. The present research work was attempted to quantify phytic acid by utilizing ultraviolet (UV) spectroscopy method and to evaluate the stability of nanovesicular (niosomes) system containing phytic acid.

Methods: Niosomes containing phytic acid were developed by thin-film hydration method. Nanoformulation was subjected to stability testing as per the International Council for Harmonisation (ICH) guidelines. The formulation was stored at 30°C±2°C and 65%±5% RH, samples were withdrawn at 15th, 30th, 60th, 90th, 120th, and 180th day of analysis and examined for the integrity of vesicular/particle size, polydispersity index, zeta potential, and percent encapsulation efficiency.

Results: Prepared nanoformulation displayed a straight line (y=mx+c) equation of y=−0.0309x+1.0413. Optimized batch of niosomes, which was prepared including dicetylphosphate showed zeta potential value of −36±0.36. Stability study showed that prepared niosomal formulation was stable up to 180 days at room temperature.

Conclusion: Findings of the current research work suggested that UV spectroscopy method can be effectively used for the quantification of phytic acid and niosomal formulation of phytic acid. The formulation was found to be stable as per the ICH guidelines for stability testing.

Keywords: Phytic acid, Niosomes, Quantification, Stability testing.

 DOI: http://dx.doi.org/10.22159/ajpcr.2018.v11i8.26671

INTRODUCTION

Phytic acid is a natural constituent present in almost all the cereals and legumes. It is extensively being studied to assess its effects on health and is shown to have chelation ability with minerals. It possesses various benefits on the human body such as lowering serum cholesterol, inhibitor for renal stone development, strong antioxidant, and antiangiogenic properties. It is confirmed by numerous researches that antioxidant scavenge free radicals, thus ultimately help in the cancer prevention. So far, molecular mechanism of action of phytic acid for chemoprevention is not very clear [1-3]. Previous *in vitro* and *in vivo* reports proved its anticancerous properties against prostate, colon, lung, metastatic, and mammary cancers [4].

Investigation and quantification are important elements in the formulation development of any drug. An appropriate method must exist for the quantification of the drug molecule in formulation for analysis of entrapment efficiency, dissolution studies, biological samples, etc. [5]. Ultraviolet (UV) spectroscopy is simplest and commonly used technique for such study. However, the UV region lies from 200 to 400 nm and visible region ranges from 400 to 800 nm. Phytic acid does not come under the UV region. Here comes the play of colorimetric analysis. Thus, phytic acid needs chromophores to be added for its quantification through UV spectroscopy.

Nanotechnology is meant for the development of nanomedicines that deliver drugs in a sustained or controlled mode and enhances residence time of drug [6]. Nanomedicine emerged as a new epoch with growth in the application of nanotechnology in the field of diagnosis and therapy. Nanoparticles are widely being used as pharmaceutical nanocarriers, and these include metallic, polymeric, vesicular, and lipidic nanoparticles [7,8]. Non-ionic surfactant vesicles (niosomes) are of intervening importance as a delivery system [9,10]. Niosomes are flexible carrier which is pertinent for systemic as well as topical applications [10]. These may be uni- or multi-lamellar spheroids in structures [11,12]. Niosomes are formed through self-assembly of non-ionic surfactant monomers which are proficient in entrapping a variety of drugs (both hydrophilic and lipophilic) [12,13]. They generally exhibit a longer storage time and may also act as targeting agents [7,14].

Drug delivery systems play a key role in therapy development. The extension of the pharmaceutical industry and dosage form development is well-recognized [15]. Development of pharmaceutical products for global use necessitates that the prepared dosage form must be stable for longer duration along with persistent pharmacological potential [16]. Nanotechnologies being actively involved in the area remain linked with the development of effectual and stable dosage form [17]. To test the stability of newly developed dosage form is performed to show the evidence how properties change with the influence of time, temperature, and humidity or how long product may be used, thus to establish shelf lives [18, 19].

Phytic acid has momentous prospective to act as an antiangiogenic agent. Instead of having a great potential, it is grossly underutilized due to a flaw of rapid absorption and excretion from the body as it forms insoluble chelates when it comes in contact with biological ions. It is thus required to develop some novel drug delivery systems of phytic acid that can reduce its flaw, thereby increasing its anticancer effect. For the development of a novel delivery system, it is required to quantify it effectively through proper method for precise characterization. Hence, the endeavor of the current work was to quantify phytic acid and develop and characterize a niosomal delivery system of it.

RSC Advances

PAPER

Cite this: *RSC Adv.*, 2016, **6**, 84965

Design of topical nanostructured lipid carrier of silymarin and its effect on 7,12-dimethylbenz[*a*] anthracene (DMBA) induced cellular differentiation in mouse skin†

Pooja Singh,[a] Malti Arya,[a] Jovita Kanoujia,[a] Mahendra Singh,[a] Krishna P. Gupta[b] and Shubhini A. Saraf*[a]

Received 10th August 2016
Accepted 27th August 2016

DOI: 10.1039/c6ra20231d

www.rsc.org/advances

Stable and novel silymarin bearing nanostructured lipid carriers (NLC) were prepared using a hot high pressure homogenization process. Silymarin NLC were physicochemically characterized *via* particle size, zeta potential, transmission electron microscope (TEM), entrapment efficiency (EE), *in vitro* release studies and optimized through experimental design. Stability data confirmed a stable dosage form. The anti proliferative activity of silymarin NLC was studied in 7,12-dimethylbenz[*a*]anthracene (DMBA) induced cellular progression/differentiation in an albino mice model using western blot and reverse transcription polymerase chain reaction (RT-PCR) analysis. In order to see the molecular changes with cellular proliferative controls such asornithine decarboxylase (ODC), proliferating cell nuclear antigen (PCNA), cyclooxygenase-2 (COX-2) and cyclin D1 at protein and messenger ribonucleic acid (mRNA) level were studied. The proliferation markers such as ODC, COX-2, cyclin D1 displayed reduced levels. In conclusion, silymarin NLC possessed activities against progression and proliferation, which were associated with enhanced solubility and stability of silymarin and greater permeation into the affected cells. Silymarin NLC could therefore be useful for chemo preventive use in skin cancer, as a topical formulation.

1. Introduction

Many pharmaceutical agents have a long history of use as herbal remedies, including opium, aspirin, digitalis, and quinine. At least 7000 medicinal compounds in the modern pharmacopoeia are derived from plants.[1] It is known that natural actives have potential therapeutic value, but limitations related to their poor solubility, bioavailability, toxicity and stability sometimes restrict their use as drugs. Nanotechnology promotes the development of herbal medicine as dosage forms and also assists in bioavailability enhancement of herbal drugs. It also offers several advantages for delivery of phytochemicals: for instance, enhanced solubility, stability, permeability and reduced toxicity amid the targeted site of action.[2,3] Lipid nanocarriers limit the use of toxic non-polar solvents that are habitually used to enhance the solubility and formulation parameters,[4,5] with the added advantage of unique small size and controlled release of drugs.[6–8] Tumours have distinctive features which make them different from normal tissues. Nanocarriers can be used to specifically target the bigger pores, lower pH and higher temperature of tumours. This situation promotes the delivery and retention of drug-loaded nanoparticles in tumour tissue. This phenomenon is known as the enhanced permeability and retention (EPR) effect. The hydrophobic surfaces of nanomaterials are highly susceptible to opsonization and clearance.[9–13] However, better penetration of the introduced nano systems through cellular membranes is an additional benefit that contributes to enhancing the bioactivity of drugs encapsulated in nanocarriers.[14–17]

Silymarin, a standardized extract of milk thistle seeds, contains a mixture of flavonolignans.[18] It has demonstrated *in vitro* and *in vivo* anti-cancer effects against prostate cancer, adenocarcinoma, breast cancer, ectocervical cancer, colon cancer, and lung cancer.[19–21] Silymarin prevents both photocarcinogenesis and skin tumour promotion by antioxidant action.[22,23] It inhibits mitogenic and cell survival signalling and induces apoptosis.[24–27] It is well established in the literature that inflammation is linked to carcinogenesis and acts as a driving force in premalignant and malignant transformation of cells.[28] It has been observed that cyclooxygenase-2 (COX-2) is upregulated after UV exposure to skin cells and is involved in the

[a]*Department of Pharmaceutical Sciences, Babasaheb Bhimrao Ambedkar University, Vidya Vihar, Raebareli Road, Lucknow 226025, India. E-mail: shubhini.saraf@gmail.com; Tel: +91 522 2998129*

[b]*Environmental Carcinogenesis Division, CSIR-Indian Institute of Toxicology Research, Mahatma Gandhi Marg, Lucknow 226001, India*

† Electronic supplementary information (ESI) available. See DOI: 10.1039/c6ra20231d

Drug Deliv. and Transl. Res.
DOI 10.1007/s13346-016-0317-8

ORIGINAL ARTICLE

Process optimization and photostability of silymarin nanostructured lipid carriers: effect on UV-irradiated rat skin and SK-MEL 2 cell line

Pooja Singh[1] · Mahendra Singh[1] · Jovita Kanoujia[1] · Malti Arya[1] · Shailendra K. Saraf[1,2] · Shubhini A. Saraf[1]

Abstract The objective of the present work was to formulate a novel stable delivery system which would not only overcome the solubility issue of silymarin, but also help to increase the therapeutic value by better permeation, anticancer action and reduced toxicity. This was envisaged through the recent developments in nanotechnology, combined with the activity of the phytoconstituent silymarin. A 2^3 full factorial design based on three independent variables was used for process optimization of nanostructured lipid carriers (NLC). Developed formulations were evaluated on the basis of particle size, morphology, in vitro drug release, photostability and cell line studies. Optimized silymarin-NLC was incorporated into carbopol gel and further assessed for rheological parameters. Stable behaviour in presence of light was proven by photostability testing of formulation. Permeability parameters were significantly higher in NLC as compared to marketed phytosome formulation. The NLC based gel described in this study showed faster onset, and prolonged activity up to 24 h and better action against edema as compared to marketed formulation. In case of anticancer activity of silymarin-NLC against SK-MEL 2 cell lines, silymarin-NLC proved to possess anticancer activity in a dose-dependent manner (10–80 μM) and induced apoptosis at 80 μM in SK-MEL 2 cancer cells. This work documents for the first time that silymarin can be formulated into nanostructured lipoidal carrier system for enhanced permeation, greater stability as well as anticancer activity for skin.

Keywords Lipoidal carrier · Skin cancer · Apoptosis · NLC · Factorial design

Introduction

Nanotechnology promises superior treatment and management of chronic diseases such as cancer. Several advantages, such as low skin irritation, increased protection of encapsulated drug and increased penetrability through the skin are offered [1–3]. Solid lipid nanoparticles (SLN) were developed as an alternative colloidal carrier system to emulsion, liposomes and polymeric nanoparticles [4]. SLNs had the drawback of drug leakage after long-term storage, and drug expulsion due to an ongoing crystallization process of the lipid towards a perfect crystal [1, 2]. Nanostructured lipoidal carriers (NLC) were developed to overcome potential limitations associated with SLNs and are the second generation nanoparticles composed of solid and liquid lipid matrix. NLC composed of diverse oils with solid lipid, can produce imperfections in their lattice structure and create separation in the fatty acid chain packing, making more space for the drug [2, 3]. Liquid lipids are better solubilizers for drugs as compared to solid lipids [9]. Miglyol 812 (a mixture of triglycerides), was selected as the lipid of choice based on composition of the epidermis which is mainly triglycerides (25 %), by virtue of its low viscosity, and because of its ability of lowering prostaglandin E2, which is a pro-inflammatory mediator. Compritol 888 ATO (glyceryl dibehenate) was taken as the solid lipid, which is suitable for production of lipid nanoparticles [10–13]. There are numerous methods to produce lipid nanoparticles such as micro emulsion method, solvent

Electronic supplementary material The online version of this article (doi:10.1007/s13346-016-0317-8) contains supplementary material, which is available to authorized users.

✉ Shubhini A. Saraf
shubhini.saraf@gmail.com

[1] Babasaheb Bhimrao Ambedkar University, Lucknow, UP, India

[2] BBDNIIT, Lucknow, India

Published online: 18 July 2016